

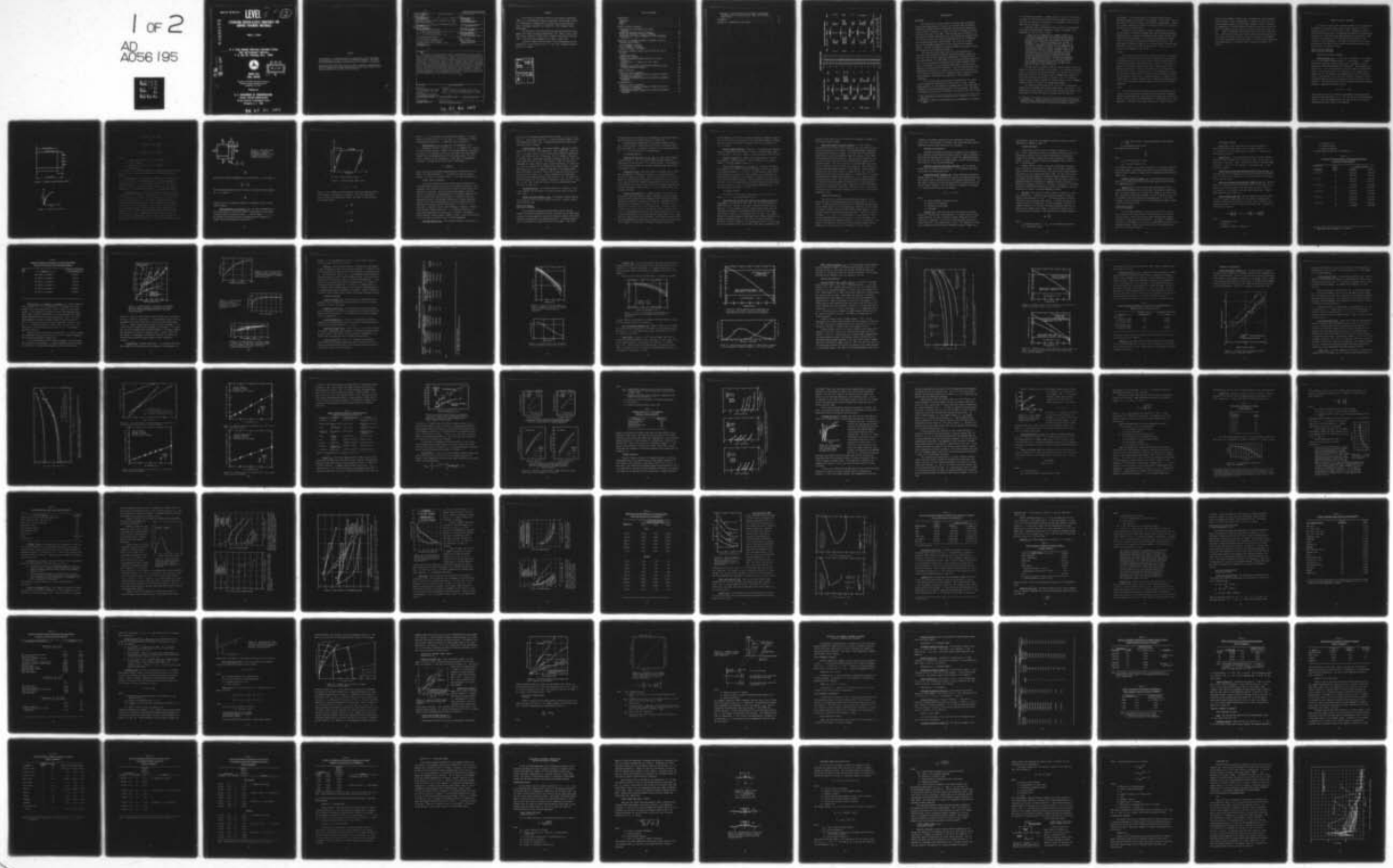
AD-A056 195 ARMY ENGINEER WATERWAYS EXPERIMENT STATION VICKSBURG MISS F/G 1/5  
LITERATURE REVIEW - ELASTIC CONSTANTS FOR AIRPORT PAVEMENT MATE--ETC(U)  
MAR 78 J L GREEN DOT-FA73WAI-377

UNCLASSIFIED

FAA-RD-76-138

NL

1 of 2  
AD  
A056 195



Report No. FAA-RD-76-138

# LEVEL

I  
II  
R  
⑫

AD A 056195

## LITERATURE REVIEW-ELASTIC CONSTANTS FOR AIRPORT PAVEMENT MATERIALS

James L. Green

U. S. Army Engineer Waterways Experiment Station  
Soils and Pavements Laboratory  
P. O. Box 631, Vicksburg, Miss. 39180

AD No. |  
DDC FILE COPY



MARCH 1978  
FINAL REPORT

DDC  
REF ID: A65195  
JUL 12 1978  
E

Document is available to the public through the  
National Technical Information Service,  
Springfield, Va. 22151

Prepared for

U. S. DEPARTMENT OF TRANSPORTATION  
FEDERAL AVIATION ADMINISTRATION  
Systems Research & Development Service  
Washington, D. C. 20591

78 07 03 062

#### NOTICES

This document is disseminated under the sponsorship of the Department of Transportation in the interest of information exchange. The United States Government assumes no liability for its contents or use thereof.

The United States Government does not endorse products or manufacturers. Trade or manufacturers' names appear herein solely because they are considered essential to the object of this report.

Technical Report Documentation Page

1. Report No. FAA-RD-76-138	2. Government Accession No.	3. Recipient's Catalog No.	
4. Title and Subtitle <b>LITERATURE REVIEW - ELASTIC CONSTANTS FOR AIRPORT PAVEMENT MATERIALS</b>		5. Report Date March 1978	
6. Author(s) James L. Green		7. Performing Organization Code	
8. Performing Organization Report No. 1211410		9. Work Unit No. (TRAINS)	
10. Contract or Grant No. DOT-FAT3WAI-377		11. Type of Report and Period Covered Final Report	
12. Sponsoring Agency Name and Address U. S. Department of Transportation Federal Aviation Administration Systems Research and Development Service Washington, D. C.		13. Sponsoring Agency Code ARD 430	
14. Supplementary Notes			
15. Abstract <p>A literature review was made to support an ongoing study to develop a method for evaluating airport pavements based on the layered elastic theory and using constants as determined from vibratory test results. The review covered the definitions and relations between elastic constants, methods used by various researchers for measuring elastic constants, and values of elastic constants found (or used) by various researchers. The review also included a study to determine the sensitivity of pavement responses to arbitrarily assigned values of elastic constants and an examination of the relationships between vibrator test results and elastic constants. The latter subject included a special preliminary examination of the relationship between the results from tests with the WES 16-kip vibrator and elastic constants. A summary discussion was given of the findings from the literature review and the special preliminary examination. Finally recommendations were made to facilitate further planning and implementation of the ongoing study mentioned.</p>			
16. Key Words Elasticity Flexible pavement performance and evaluation (Airfields) Pavements Rigid pavement performance and evaluation (Airfields)	17. Distribution Statement Vibration response tests Vibrators	18. Distribution Statement Document is available to the public through the National Technical Information Service, Springfield, Va. 22151.	
19. Security Classif. (of this report) Unclassified	20. Security Classif. (of this page) Unclassified	21. No. of Pages 138	22. Price

Form DOT F 1700.7 (8-72)

Reproduction of completed page authorized

78 07 03 062  
438100

act

## PREFACE

This study was conducted by the Soils and Pavements Laboratory (S&PL), U. S. Army Engineer Waterways Experiment Station (WES), for the U. S. Department of Transportation, Federal Aviation Administration, under Inter-Agency Agreement No. FA73WAI-377, "New Pavement Design Methodology."

The literature review reported herein was made during June 1975-January 1976 under the general supervision of Mr. James P. Sale, Chief, S&PL, and Mr. Alfred H. Joseph, Chief, Pavement Investigation Division (PID). This report was prepared by Mr. James L. Green, PID.

Director of WES during the conduct of the investigation and the preparation of this report was COL G. H. Hilt, CE. Technical Director was Mr. F. R. Brown.

ACCESSION NO.	
NTIC	White Section <input checked="" type="checkbox"/>
DDC	Buff Section <input type="checkbox"/>
UNANNOUNCED	<input type="checkbox"/>
JUSTIFICATION	
BY	
DISTRIBUTION/AVAILABILITY CODES	
Dist.	AVAIL. and/or SPECIAL
A	

## TABLE OF CONTENTS

INTRODUCTION . . . . .	5
BACKGROUND . . . . .	5
PURPOSE . . . . .	7
SCOPE . . . . .	7
REVIEW OF ELASTIC CONSTANTS . . . . .	9
DEFINITIONS AND RELATIONSHIPS OF ELASTIC CONSTANTS . . . . .	9
METHODS FOR MEASURING ELASTIC CONSTANTS . . . . .	15
VALUES AND VARIATIONS OF ELASTIC CONSTANTS . . . . .	21
RELATIONSHIPS OF ELASTIC CONSTANTS TO OTHER PARAMETERS IN SOILS . . . . .	64
SENSITIVITY OF PAVEMENT RESPONSES TO CHANGES IN ELASTIC CONSTANTS AND THICKNESS . . . . .	74
RIGID PAVEMENTS (PACKARD <sup>4</sup> ) . . . . .	74
RIGID PAVEMENTS (PICHUMANI <sup>5</sup> ) . . . . .	74
FLEXIBLE PAVEMENTS (PICHUMANI <sup>5</sup> ) . . . . .	78
RELATIONSHIPS BETWEEN VIBRATORY TEST RESULTS AND ELASTIC CONSTANTS . . . . .	85
MATHEMATICAL MODELS . . . . .	85
VIBRATOR WAVE PATTERNS . . . . .	91
COMMENTS ON RELATING VIBRATOR RESULTS AND ELASTIC CONSTANTS . . . . .	95
EXTRAPOLATION OF G FROM LOW TO HIGH STRESS LEVELS . . . . .	97
PRELIMINARY RELATIONSHIP ESTABLISHED BETWEEN WES 16-KIP VIBRATOR AND ELASTIC MODULUS . . . . .	99
SUMMARY DISCUSSION . . . . .	105
REVIEW OF ELASTIC CONSTANTS . . . . .	105
SENSITIVITY OF PAVEMENT RESPONSES TO CHANGES IN ELASTIC CONSTANTS AND THICKNESS . . . . .	122
RELATIONSHIPS BETWEEN VIBRATORY TEST RESULTS AND MATERIAL PARAMETERS . . . . .	123
RECOMMENDATIONS . . . . .	127
REVIEW OF ELASTIC CONSTANTS . . . . .	127
SENSITIVITY OF PAVEMENT RESPONSES TO CHANGES IN ELASTIC CONSTANTS AND THICKNESS . . . . .	130
RELATIONSHIPS BETWEEN VIBRATORY TEST RESULTS AND MATERIAL PARAMETERS . . . . .	131

BREAKDOWN OF ONGOING STUDY FOR DEVELOPMENT OF EVALUATION PROCEDURE BASED ON LAYERED ELASTIC THEORY AND VIBRATORY TEST RESULTS . . . . .	132
REFERENCES . . . . .	133
APPENDIX A: ABBREVIATIONS AND SYMBOLS . . . . .	137

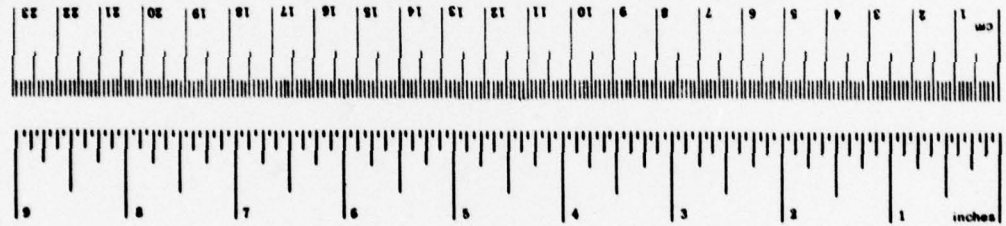
**Approximate Conversions to Metric Measures**

Symbol	When You Know	Multiply by	To Find	Symbol	When You Know	Multiply by	To Find
<b>LENGTH</b>							
inches	12.5	centimeters	millimeters	mm	0.04	inches	mm
feet	.30	centimeters	centimeters	cm	0.4	feet	cm
yards	0.9	meters	meters	m	3.3	yards	m
miles	1.6	kilometers	kilometers	km	1.1	miles	km
<b>AREA</b>							
square inches	6.5	square centimeters	square centimeters	cm²	0.16	square inches	cm²
square feet	0.09	square meters	square meters	m²	1.2	square yards	m²
square yards	0.3	square kilometers	square kilometers	km²	0.4	square miles	km²
square miles	2.5	hectares	hectares (10,000 m²)	ha	2.5	acres	ha
acres	0.4						
<b>MASS (weight)</b>							
ounces	28	grams	grams	g	0.035	ounces	g
pounds	0.45	kilograms	kilograms	kg	2.2	pounds	kg
short tons	0.9	tonnes	tonnes (1000 kg)	t	1.1	short tons	t
(2000 lb)							
<b>VOLUME</b>							
teaspoons	5	milliliters	milliliters	ml	0.03	fluid ounces	ml
tablespoons	15	milliliters	milliliters	ml	2.1	pints	ml
fluid ounces	.30	liters	liters	l	1.06	quarts	l
cups	0.24	liters	liters	l	0.26	gallons	l
pints	0.47	liters	liters	l	26	cubic feet	l
quarts	0.95	liters	liters	l	1.3	cubic yards	l
gallons	3.8	cubic meters	cubic meters	m³			
cubic feet	0.03	cubic meters	cubic meters	m³			
cubic yards	0.76						
<b>TEMPERATURE (exact)</b>							
Fahrenheit	5/9 (after subtracting 32)	Celsius temperature	Celsius temperature	°C			
Temperature							

1 in = 2.54 centimeters. For other exact conversions and more detail and tables, see NBS Special Publication 286, "Units of Weights and Measures," Pt. Ia (1925), SC Catalog No. C13.10.286.

mm = millimeter; cm = centimeter; m = meter; km = kilometer; ha = hectare; g = gram; kg = kilogram; t = tonne (1000 kg); ml = milliliter; l = liter; m³ = cubic meter; in = inch; ft = foot; yd = yard; mi = mile; cu in = cubic inch; cu ft = cubic foot; cu yd = cubic yard; °F = Fahrenheit; °C = Celsius; °R = Rankine; °K = Kelvin.

**METRIC CONVERSION FACTORS**



## INTRODUCTION

### BACKGROUND

The nondestructive nature, speed of testing, ease of operation, accuracy and repeatability of results, and the fact that moving-wheel loads can be simulated have made vibratory testing devices popular for airport pavement evaluation. At least four types of portable vibratory testing devices are in use today. These devices are the Dynaflect, the Road Rater, a vibrator developed by the Civil Engineering Research Facility of the Air Force, and a vibrator developed by the U. S. Army Engineer Waterways Experiment Station (WES\*). The first two of these devices are available commercially and the other two are research devices. The WES testing device is made available to any public agency that requests it for evaluation purposes.

The vibrators listed above (and others not mentioned) are associated with different procedures that permit pavement evaluation, but none of the vibratory procedure combinations is considered to be fully satisfactory. In a WES study<sup>1</sup> for the Federal Aviation Administration (FAA), a procedure was developed using the WES 16-kip\*\* vibrator that is considered to be a significant improvement in nondestructive methods of evaluating airport pavements. This procedure was based on an experimental correlation of vibratory test results with allowable aircraft loads as computed using the conventional direct sampling evaluation procedures. Improvement and upgrading of this procedure is continuing.

It is probable that the procedure referenced above will serve airport evaluation requirements for several years to come. However, being empirical, it can be applied confidently only to the same kinds of pavements and aircraft loading from which it was developed. New kinds of pavements and aircraft of the future could severely test the efficacy

---

\* For convenience, necessary abbreviations and symbols are listed on page A1.

\*\* A table of factors for converting units of measurement is presented on page 4.

of the evaluation procedure. Clearly, there is a need for more analytical means of designing and evaluating airport pavements than now exist. That need has long been recognized and a considerable effort has been made, and is being made, to fill it.

Currently, WES is conducting a study for FAA to satisfy commitments under FAA-ER-430-002b, Amendment 1, dated 10 September 1974, paragraph 3.4, which states, in part:

Phase B of the nondestructive pavement evaluation is concerned with development of the nondestructive evaluation method compatible with the selected rational design procedure for flexible and rigid pavements described in paragraph 3.3\*. A theoretical analysis will be made to determine if the vibratory load-deflection data can be converted to appropriate modulus or other parameters for use with the rational procedure. The end product is the load-carrying capacity of airport pavements based on the nondestructive test and rational procedure. Results of the analysis will be verified by experimental results using all available data at the Waterways Experiment Station and any additional data obtained by the associated experiments described in the previous paragraphs on the climatological effects. A tentative nondestructive evaluation methodology developed in Phase B for both flexible and rigid pavement is to be made available by the end of fiscal year 1976.

The WES study in progress is based on layered elastic theory and results of tests with the WES 16-kip vibrator. The evaluation procedure, which is a reverse of the design procedure, will consist of first determining the values of the required elastic constants from vibrator results and then using those values as inputs to one of the existing layered elastic computer programs for pavement design, such as CHEVRON, BISTRO, or AFPAV, to predict the pavement performance.

The vibrator test results will be in the form of deflections measured at the pavement surface under known loads. The success of the whole endeavor rests heavily on the accuracy and ease with which it will be possible to extract the elastic constants from the deflection

---

\* Paragraph 3.3: "These procedures will be selected or adopted from various rational design methods such as finite element, layered elastic theory, finite difference, and layered viscoelastic theory."

measurements. A reasonable degree of confidence exists that an acceptable degree of accuracy will be obtained. Several models that relate elastic constants to vibrator test results are available. However, one of these, developed by Weiss,<sup>2,3</sup> is unique in that it is the only one based on a nonlinear theory.

Because of the importance of elastic constants per se to the ongoing study, a corollary literature search was considered essential regarding elastic constants (how measured, what values obtained, what causes variation in values, etc.) to support and enhance the larger study. Accordingly, the study reported herein was devoted to the development of empirical equations for deriving elastic constants from measurements made with the WES 16-kip vibrator. This report also includes a brief summary of that effort.

#### PURPOSE

The purpose of this study was to conduct a review of literature in support of an ongoing study to develop a method for evaluating airport pavements based on the layered elastic theory and using elastic constants as determined from vibratory test results. This report is expected to provide a convenient reference in facilitating efforts to develop such a method. The specific objectives of the study were: (a) review the elastic constants known to be of significance in applying the layered elastic theory to the evaluation of airport pavements; (b) determine the sensitivity of pavement responses to changes in assigned values of elastic constants; and (c) make a preliminary examination of the relationships between vibratory test results and elastic constants.

#### SCOPE

The review of elastic constants consisted of defining the pertinent elastic constants and stating their relationships, examining methods for measuring them, reporting specific values and variations or values of the constants, and indicating their relationships with other parameters. The sensitivity study consisted of a review of work by

Packard<sup>4</sup> and Pichumani<sup>5</sup> in which they, independently, used the layered elastic theory to study the magnitudes of changes that occurred in predicted pavement responses with arbitrary changes in elastic constants. The examination of the relationships between vibratory test results and material parameters mainly comprised a review of existing models, but also included a preliminary relationship between the results from tests with the WES 16-kip vibrator and elastic moduli developed especially for this study. The report includes a summary discussion and recommendations to be considered in planning studies to develop airport evaluation methodology based on the layered elastic theory and vibratory test devices.

## REVIEW OF ELASTIC CONSTANTS

The review of those elastic constants known to be of significance in applying the layered elastic theory to the evaluation of airport pavements consists of (a) defining the elastic constants and stating relationships between them, (b) examining test methods for measuring the constants, (c) indicating values and variations of the constants found by several researchers, and (d) showing the relationships of the constants to other parameters. The names and symbols for the elastic constants and the units in which they are expressed are given as they were used by the references cited.

### DEFINITIONS AND RELATIONSHIPS OF ELASTIC CONSTANTS

#### QUASI-STATIC ELASTIC CONSTANTS

Elastic Modulus, E. In the study of materials, it is common to plot the relationships between stress,  $\sigma$ , and strain,  $\epsilon$ . Figure 1 illustrates a material under uniaxial stress, and Figure 2 shows a generalized stress-strain graph for the material. Each material has a unique curve. For a certain distance from the origin, the experimental values of stress versus strain lie essentially on a straight line, except that for some materials the straight part of the curve hardly exists. Nevertheless, up to some point, such as A (Figure 2), the relationship between stress and strain may be said to be linear for all materials. This generalization is known as Hooke's law and for uniaxial loading is expressed in equation form as

$$\sigma = E\epsilon \quad \text{or} \quad \epsilon = \frac{\sigma}{E}$$

which means that stress is directly proportional to strain where the constant of proportionality is  $E$ . For the case of a three-dimensional state of stress, the generalized Hooke's law, valid for an isotropic homogeneous material, leads to the equations:

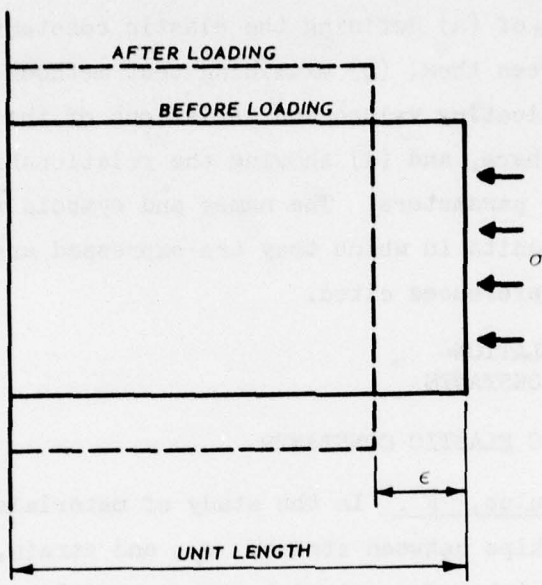


Figure 1. Material under uniaxial stress

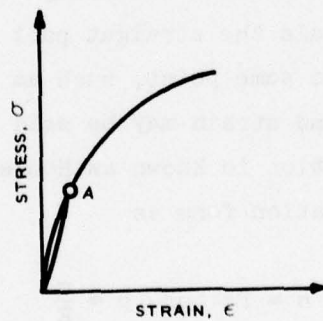


Figure 2. Stress versus strain

$$\epsilon_x = \frac{1}{E} [\sigma_x - v(\sigma_y + \sigma_z)]$$

$$\epsilon_y = \frac{1}{E} [\sigma_y - v(\sigma_x + \sigma_z)]$$

$$\epsilon_z = \frac{1}{E} [\sigma_z - v(\sigma_x + \sigma_y)]$$

where

$\epsilon$  = normal strain in the x, y, or z direction

E = elastic modulus

$\sigma$  = normal stress in the x, y, or z direction

v = Poisson's ratio

The constant E, the elastic modulus, is a definite property of a material. It also is called the coefficient of elasticity and Young's modulus.

Unconfined clay is one material for which a stress-strain curve is far from linear. For such a material, it is often expedient to employ variations of E to characterize the material. The most commonly used are  $E_i$ , the initial tangent modulus;  $E_t$ , the tangent modulus;  $E_s$ , the secant modulus; and  $E_h$ , the hysteresis modulus.

Poisson's Ratio, v. The elastic modulus reflects a property of a material in the direction of an applied force. At right angles to a force applied to an element, Figure 3 shows the lateral expansion or contraction that takes place. The lateral deformations per unit of length are termed lateral strains. Lateral strains bear a constant relationship to the longitudinal or axial strains caused by an axial force, provided a material remains elastic and is homogeneous and isotropic. For the two-dimensional element (Figure 3), the positive normal stress is  $\sigma_x/E$ . However, the positive normal stress,  $\sigma_y$ , also produces a strain normal to the y-z plane that is opposite in direction to the strain produced by  $\sigma_x$ . This lateral strain is equal to

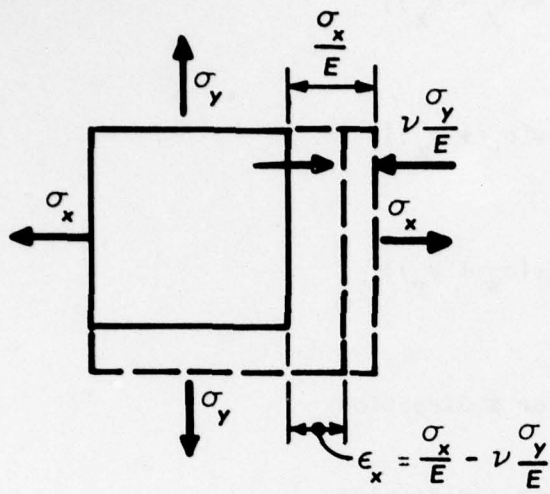


Figure 3. Two-dimensional homogeneous isotropic rectangular element of unit thickness subjected to a biaxial state of stress

$$\nu \frac{\sigma_y}{E}$$

and the total lateral deformation in the  $x$  direction,  $\epsilon_x$ , is equal to

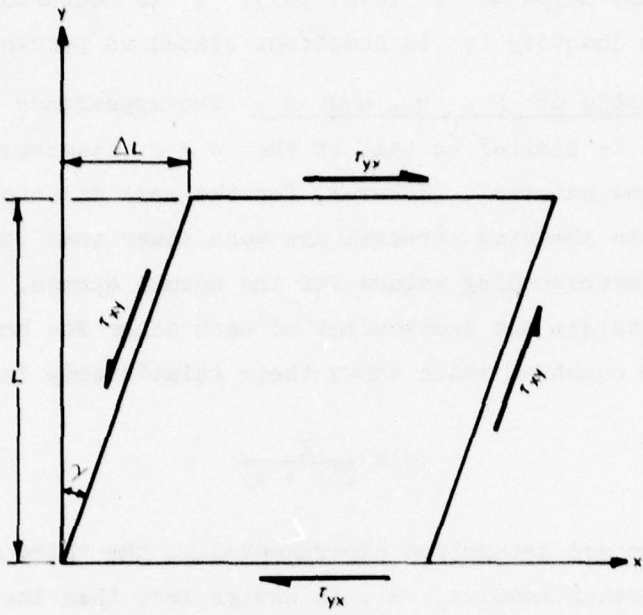
$$\frac{\sigma_x}{E} - \nu \frac{\sigma_y}{E}$$

For the three-dimensional state of stress, the lateral strain produced by  $\sigma_z$  is equal to

$$\nu \frac{\sigma_z}{E}$$

Poisson's ratio is a definite property of a material, just as is the elastic modulus.

Shearing Modulus of Elasticity, G. For small deformations in the elastic range of a material, Figure 4 illustrates the linear relationship between the shearing stress,  $\tau$ , and the angle,  $\gamma$ . If  $\gamma$  is defined as the shearing strain, mathematically the extension of Hooke's law for shearing stress and strain is



$$\frac{\Delta L}{L} = \tan \gamma = \gamma \text{ (RADIANS), FOR SMALL STRAINS}$$

Figure 4. Material under shear stress

$$\tau = G\gamma \quad \text{or} \quad \gamma = \frac{\tau}{G}$$

where  $G$  is a constant of proportionality called the shearing modulus of elasticity or the modulus of rigidity. For a three-dimensional state of stress, the generalized Hooke's law leads to three equations for shearing strain:

$$\gamma_{xy} = \frac{\tau_{xy}}{G}$$

$$\gamma_{yz} = \frac{\tau_{yz}}{G}$$

$$\gamma_{zx} = \frac{\tau_{zx}}{G}$$

Like  $E$ ,  $G$  is a constant for a given elastic material. It is measured in the same units as  $E$  (e.g. psi);  $\gamma$  is measured in radians, a dimensionless quantity ( $\gamma$  is sometimes stated as percent).

Relationship of  $E$ ,  $v$ , and  $G$ . The appearance of the  $\tau - \gamma$  diagrams is similar to that of the  $\sigma - \epsilon$  diagrams for a tension test for the same material. However, for the same material, the numerical values of the shearing stresses are much lower than (approximately one half) the corresponding values for the normal stress. The three elastic constants are not independent of each other for homogeneous materials. The equation which shows their relationship is

$$G = \frac{E}{2(1 + v)}$$

Thus, if any two are determined experimentally, the third may be computed. The shearing modulus,  $G$ , is always less than the elastic modulus,  $E$ , since the Poisson's ratio,  $v$ , is a positive quantity.

#### DYNAMIC ELASTIC CONSTANTS

The airport pavement evaluation method under consideration is concerned with in-place states of stress in pavements subjected to moving wheel loads; therefore, the material properties under dynamic loading must be considered. The stress-strain relationships indicated earlier for quasi-static loading apply also for dynamic loading in the case of linear elastic materials; however, it should be noted that quantitative values of the dynamic response are frequency dependent. Poisson's ratio and shearing modulus of elasticity usually have the same basic definitions, and the relationship,  $G = E/2(1 + v)$ , for quasi-static conditions is also used for dynamic conditions. However, for repetitive loading conditions,  $G$  is commonly determined for a given strain amplitude and a given cycle of loading. The dynamic elastic modulus, however, takes a number of forms. Those forms referred to in this study are defined in the following paragraphs.

Resilient Modulus,  $M_R$ . The resilient modulus of elasticity is

the ratio of the repeatedly applied deviator stress,  $\sigma_o$  ( $\sigma_o = \sigma_1 - \sigma_3$  where  $\sigma_1$  equals axial stress and  $\sigma_3$  equals confining stress), to the recoverable axial strain.  $M_R$  is usually determined at a given stress level and cycle of loading.

Complex Modulus,  $E^*$ . The complex modulus,  $E^*$ , is a complex number,  $E^* = E_1 + iE_2$ , whose magnitude,  $|E^*| = \sqrt{E_1^2 + E_2^2}$ , gives the ratio of the axial stress to axial strain during a uniaxial compression test. The laboratory test to determine  $|E^*|$  is similar to that used to determine  $M_R$ , except that sinusoidal loading is used for  $|E^*|$  and pulse loading is used for  $M_R$ . The values of  $|E^*|$  are used interchangeably for elastic moduli values by some researchers. If values for  $E_1$ , the real component of the complex modulus where strain is in phase with stress, and  $E_2$ , the imaginary component of the complex modulus where the modulus of strain is 90 deg out of phase with the stress, are desired, the "loss angle,"  $\theta_L$ , must be measured in the laboratory. The strain vector lags behind the stress vector by  $\theta_L$ , the tangent of which is known as the "loss tangent," defined by  $\tan \theta_L = E_2/E_1$ . Knowing  $\theta_L$  and  $|E^*|$  allows the solution of the two simultaneous equations for  $E_1$  and  $E_2$ .

Stiffness Modulus. The stiffness modulus is a modulus of elasticity computed from the results of repetitive load tests on thin circular slabs.

Dynamic Stiffness Modulus, DSM. The dynamic stiffness modulus is the ratio of load to deflection when the load is a specific steady-state vibratory load.

#### METHODS FOR MEASURING ELASTIC CONSTANTS

The following paragraphs reference and/or briefly describe several test methods for measuring elastic constants for portland cement concrete (PCC) and asphaltic concrete (AC) wearing surfaces, treated and untreated base materials, and subgrade materials. A detailed description of test methods is beyond the scope of this report. The tests

discussed usually are performed in the laboratory, with one exception, the wave velocity test, which normally is a field test.

Each paragraph is headed by a test reference (ASTM,<sup>6</sup> CRD-C,<sup>7</sup> etc.) or name reference (Massachusetts Institute of Technology (MIT), Glynn and Kirwan, etc.) followed by a symbol for the constant measured (E, v, etc.) by the reference, in parentheses.

#### PCC WEARING SURFACES

ASTM C469-65<sup>6</sup> and CRD-C 21<sup>7</sup> (E and v). Quasi-static methods for determining v and E of PCC are ASTM Designation C469-65 for compression testing and CRD-C 21 for flexure testing. There apparently is no established procedure for directly determining the quasi-static shear modulus of PCC.

ASTM C597-71<sup>6</sup> (E). This test method is sometimes used to determine the modulus of elasticity of concrete. It involves the pulse velocity of compressional waves. However, the procedure is not recommended for establishing the compliance of the modulus of elasticity of field concrete with that assumed in design because the pulse velocity is not influenced by minute cracks in a concrete pavement, and the test procedure may assign a higher value of E to a cracked pavement than actually justified.

MIT and WES (Dynamic E). A dynamic modulus of elasticity for PCC has been determined under a single concentrated load by a machine developed by MIT and modified by Lundeen at WES.<sup>8</sup> The device yielded satisfactory results for compressive testing, but improvements to the apparatus were recommended for flexural testing. The impact load is produced by driving a piston with nitrogen under 1,000-psi pressure. A constant-slope loading pulse is produced that peaks in approximately 1 msec. Instrumentation consists of a 30,000-lb capacity load cell and an oscilloscope modified to provide only one trigger sweep or to be used with a d-c amplifier and an x-y recorder. The strains are measured with SR-4 strain gages and are recorded on a dual-trace oscilloscope equipped with a camera. For the test, a cylindrical specimen encased in a

flexible membrane is placed in a triaxial compression chamber, subjected to a constant lateral fluid pressure, and then loaded axially to failure. The size of the test specimen is limited to 1-1/2 in. in diameter by 3 in. in height.

Murillo Engineering<sup>9</sup> (E). Values of E at rupture were observed by Murillo Engineering from results of tests on concrete beams loaded at three points. The test is similar to that described in CRD-C 21-58.<sup>7</sup>

Barkan<sup>10</sup> (Dynamic E). Barkan used a sound generator to excite longitudinal or transverse waves of various frequencies in concrete samples to determine dynamic values of E.

CRD-C 18-59<sup>7</sup> (Dynamic E, G, and v). Procedures for measuring frequencies of concrete prisms and cylinders of PCC for the purpose of calculating dynamic E, G, and v are described in CRD-C 18-59. As with the pulse velocity test, the procedure is not recommended for establishing the compliance of the modulus of elasticity of field concrete with that assumed in design. Also, specimens of the same concrete that vary in size and shape may yield different computed modulus values. In this procedure, E and G are determined independently and v is calculated using the formula  $v = E/(2G - 1)$ .

#### AC WEARING SURFACES

No references were found to quasi-static E, v, or G or dynamic v or G testing procedures for AC.

Washington State University<sup>11</sup> (WSU) and the Asphalt Institute<sup>12</sup> (AI) ( $|E^*|$ ). Both WSU and AI used  $|E^*|$  for the elastic modulus of asphalt concrete. Neither of the above references describes the test apparatus or test procedure in detail; however, WSU reveals that test specimens are compacted to average densities (density of test track under study) in molds 4 in. in diameter and 8 in. high. The complex modulus is the axially applied sinusoidal stress function divided by the resulting sinusoidal strain. In the series of tests described in Reference 11, three frequencies of stress application (1, 4, and 16 cps) and three temperatures (40, 70, and 100°F) were used in combination with

a single stress level (35 psi) to describe the response of asphalt concrete under dynamic loading.

Glynn and Kirwan<sup>13</sup> (Stiffness Modulus). In their study of environmental factors and flexible pavements, Glynn and Kirwan initially tried to determine resilient moduli of bituminous mixtures using beam specimens with third-point loading. They found that the concentrated loads induced localized displacements and that testing of short beams was complicated by shear deflection. They developed a device for testing thin circular slabs, the results from which allow computation of stiffness modulus. The device consists of a loading frame that incorporates a flexible pressure pad and pulse generator. The pressure pad area was made approximately equal to a tire imprint. Pulsed loading is produced by a rotor valve fitted to a compressed air line. The slab diameter was three times the pad diameter. A testing rate of 25 cpm was used along with a maximum applied pressure of 5 psi. Higher pressures produced excessive creep. The authors noted that the Texas Transportation Institute earlier developed a similar device of which they were not aware at the time of their study. They found the stiffness modulus of dense AC to be between 75,000 and 125,000 psi at 20°C. In their calculations, Poisson's ratio was estimated to be 0.35 or 0.45 for several independent tests.

#### TREATED BASE MATERIALS

The method for testing treated base materials depends on the amount and type of treating agent used in the base material. For example, if a granular base course material is treated with enough cement, it will behave similar to PCC and beam-shaped specimens could be tested in flexure. However, materials stabilized with small amounts of lime or salt may require small cylindrical test specimens. Therefore, tests to determine E, v, and G of treated materials may either be similar to those described earlier for PCC and AC or to those described later for untreated bases and subgrade materials, i.e. soils, depending on the nature of the material. Most treated bases probably resemble wearing surfaces more closely than they do subgrades, and their elastic

constants are probably influenced by mix proportions, temperature, stress level, and frequency of loading to the same extent that those of comparable wearing surface materials are influenced.

#### UNTREATED BASE MATERIALS

Untreated base materials usually are crushed rock or granular soil. Methods for measuring quasi-static values of elastic constants in untreated base materials are the same as those for subgrade materials. Three types of tests used to determine dynamic values of elastic moduli are discussed in the following paragraphs.

Repetitive Triaxial Compression Test (M<sub>R</sub>). This is the most common test for dynamic elastic modulus. It is described later under test methods for subgrade materials.

Dorman and Klomp<sup>14</sup> (Dynamic E). These researchers determined dynamic values of E by measuring the velocity of transverse waves that were radiated from a vibratory load on the untreated base material. In this type of testing, electronic sensing devices are placed on the surface at various distances from the vibrator to determine a wavelength. E is then calculated from the relationship

$$E = q \times d \times f(\lambda)^2$$

where

q = factor dependent on Poisson's ratio

d = density of the material

f = frequency of wavelength

$\lambda$  = wavelength

Hardin<sup>15</sup> (G). Hardin has done extensive work with the shear modulus of soils and base course materials. For shear testing of base course materials, he used a torsional resonant column device at the University of Kentucky. A torsionally vibrating table produces torsional vibration of the sample about its axis. The frequency of vibration is measured, and the resonant frequency is used to compute the

shear modulus. Theory for the resonant column test results is found in "The Nature of Damping in Sands."<sup>16</sup>

#### SUBGRADE MATERIALS

Quasi-static tests from which the elastic constants of  $E$ ,  $v$ , and  $G$  can be determined for soils are probably routine for most soils laboratories; however, there are some difficulties in determining  $v$  because of the problem of measuring the small magnitude of lateral strains involved. Standard triaxial tests generally are used for  $E$  and  $v$  determinations.

Dynamic testing of soils is less well established than quasi-static testing but is becoming more common in the fields of road and airport design and evaluation because test results more nearly simulate the behavior of soils under moving wheel loads. At least seven laboratories are presently engaged in research of dynamic testing of soils: the Asphalt Institute Laboratory in College Park, Maryland; Construction Engineering Research Laboratory in Champaign, Illinois; University of Kentucky in Lexington; University of California in Berkeley; Cold Regions Research and Engineering Laboratory in Hanover, New Hampshire; WES; and University of Illinois in Urbana-Champaign, Illinois.

WES (MR). The test for resilient modulus is similar to a standard triaxial test. Definitions and procedures suggested by WES are found in Technical Report S-75-10.<sup>17</sup> The deviator stress is applied repetitively and at several stress levels. A constant lateral stress (chamber pressure) is maintained. The test equipment is similar to a standard triaxial cell, the major difference being that there must be some external loading source capable of providing a variable load of fixed cycle and load duration. The expression for resilient modulus is

$$M_R = \frac{\sigma_d}{\epsilon_R}$$

where

$$\begin{aligned}\sigma_d &= \text{deviator stress} = \sigma_1 - \sigma_3, \text{ or the repeated axial stress} \\ \sigma_1 &= \text{total axial stress}\end{aligned}$$

$\sigma_3$  = total radial stress (continuing pressure in the triaxial test)

$\epsilon_R$  = recoverable axial strain

Resilient Poisson's ratio is

$$\frac{\epsilon_L}{\epsilon_R}$$

where

$\epsilon_L$  = resilient lateral strain

$\epsilon_R$  = resilient axial strain

No published results of laboratory determination of resilient Poisson's ratios were found. Load versus time curves for the resilient modulus tests can take a variety of shapes, that is, haversine, sawtooth, haver square, etc.

Dorman and Klomp<sup>14</sup> (Dynamic E). Dorman and Klomp used their wave velocity method to determine an in-place dynamic elastic modulus for subgrade materials.

Hardin<sup>18</sup> (G). In his work with the shear modulus of soils, Hardin obtained dynamic values by applying a torsional load about the axis of a hollow cylinder of soil that was confined in a pressure chamber. The system could apply a maximum torque of 60 kg-cm, and the rate of loading for the tests varied from approximately 0.2 to 450 kg-cm per hour. Tests were conducted for strain amplitudes as small as about 0.00001 to as large as 0.005.

#### VALUES AND VARIATIONS OF ELASTIC CONSTANTS

The following paragraphs provide values of elastic constants and/or describe their variation with several factors, for PCC and AC wearing surfaces, treated and untreated base materials and subgrade materials, as found by several researchers. The elastic constant(s) discussed in a paragraph is (are) shown in parentheses at the end of the paragraph heading. Quantitative data are given in the same units as used by the referenced authors.

## PCC WEARING SURFACES

Popov<sup>19</sup> (E). Popov indicated that the elastic modulus of concrete varies with water-cement ratio. He gave a value of  $E = 2,000,000$  psi for 7-1/2-gal/sack concrete and  $E = 3,000,000$  psi for 6-gal/sack concrete.

Barkan<sup>10</sup> (E). In electroacoustic testing of concrete, Barkan showed how Young's modulus (E) varies with the age (7 and 28 days) and composition of concrete. Table 1 shows that in five of six cases aging increased E from 6.7 to 26.2 percent. In the sixth case, E was reduced 8.2 percent.

Yoder<sup>20</sup> and the Portland Cement Association<sup>4</sup> (PCA) (E and v). Both Yoder and the PCA suggested that the elastic modulus and Poisson's ratio of concrete can be assumed to be 4,000,000 psi and 0.15, respectively, for most cases.

Materials Research and Development<sup>21</sup> (MRD) (E and v). MRD used ASTM Test Procedure C469-65 in evaluating three PCC test sites at San Francisco International Airport and determined the elastic moduli of the concrete to be 3,440,000, 3,560,000, and 3,600,000 psi. They assumed Poisson's ratio to be 0.15.

Murillo Engineering<sup>9</sup> (E). Murillo Engineering used the results of tests on concrete beams loaded at three points to determine the modulus of elasticity at rupture for six test sites at Houston Intercontinental Airport. Table 2 presents the results, and E values computed used the equation

$$E = \frac{P\ell^3}{48I\Delta} \left[ 1 + (2.4 + 1.5v) \left( \frac{h}{\ell} \right)^2 - 0.84 \left( \frac{h}{\ell} \right)^2 \right]$$

where

P = maximum load, lb

$\ell$  = span, in.

I = moment of inertia of beam, in.<sup>4</sup>

$\Delta$  = deflection, in.

$v$  = Poisson's ratio

$h$  = depth of beam, in.

E values range from 362,663 to 1,289,642 psi.

Table 1

Variation of Young's Modulus with Age and Composition  
of Concrete (After Barkan<sup>10</sup>)

Composition of Concrete*	Age of Concrete days	Young's Modulus	
		tons/m <sup>2</sup>	psi
1:2.55:2.55	7	3,600,000	4,600,000
	28	3,810,000	4,910,000
1:3.0:3.0	7	3,020,000	3,890,000
	28	3,810,000	4,910,000
1:1.93:3.23	7	3,530,000	4,550,000
	28	4,110,000	5,300,000
1:2.64:4.05	7	4,320,000	5,570,000
	28	3,960,000	5,110,000
1:3.76:3.0	7	3,100,000	4,000,000
	28	3,670,000	4,730,000
1:4.65:6.18	7	2,950,000	3,800,000
	28	3,310,000	4,270,000

\* Cement:sand:coarse aggregate (by volume).

Table 2  
Summary of Flexural Strength of Concrete Beams (After  
Murillo<sup>9</sup>) at Houston Intercontinental Airport

Beam No.	Location	Modulus of Elasticity at Rupture, psi
1	Sta 15+12.5, Taxiway A	362,663
2	Sta 60+37.5, Taxiway B	642,534
3	Sta 83+12.5, Taxiway B	601,780
4	Sta 89+37.5, Runway 14-32	762,248
5	Sta 88+37.5, Taxiway K	1,289,642
6	Sta 70+12.5, Taxiway K	683,308

Neville<sup>22</sup> (E , v , Dynamic E , Dynamic v). Neville suggested that the higher the E of the aggregate is, the higher will be the modulus of the resulting concrete. Figure 5 shows the relationship between E and compressive strength for four gravel aggregate mixes and a similar (single) relationship for several expanded clay (light-weight) aggregate mixes of different proportions. The E of light-weight aggregate concrete is usually between 40 and 80 percent of the E of ordinary concrete of the same compressive strength. Since the E of lightweight aggregate differs little from the E of the cement paste, mix proportions do not affect the E of lightweight aggregate concrete.

Neville further stated that the quasi-static v of both ordinary and lightweight concrete varies from 0.11 to 0.21. Dynamic determination yields average values of about 0.24.

In the determination of the natural frequency of concrete beams for the purpose of calculating E , Neville suggested that since during the vibration of the specimen a negligible stress is applied, the

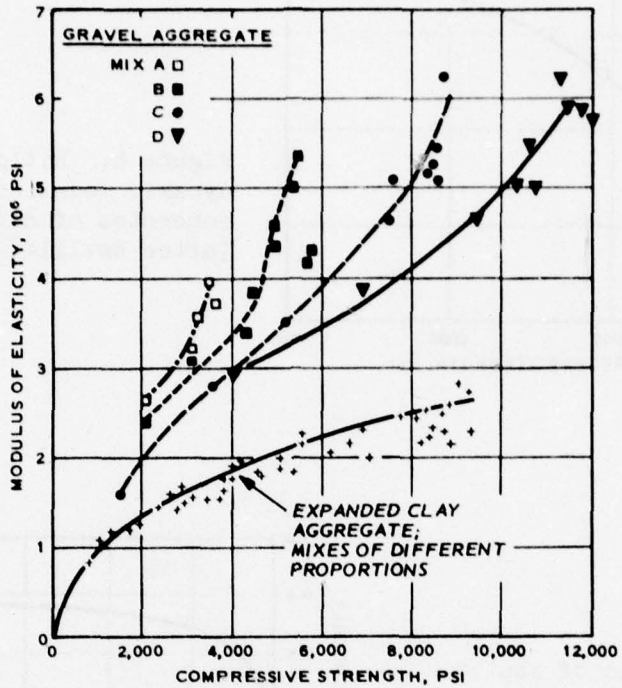


Figure 5. Static modulus of elasticity of concretes made with gravel aggregate and expanded clay aggregate and tested at different ages up to one year (after Neville<sup>22</sup>)

dynamic  $E$  refers to almost purely elastic effects and is unaffected by creep. Therefore, the dynamic  $E$  is approximately equal to the  $E_i$  determined in the static test and is, therefore, appreciably higher than  $E_s$ . Figure 6 shows that the ratio of static to dynamic  $E$  increases with an increase in the strength of the concrete. For a given mix, the ratio increases also with age (Figure 7). The static modulus was determined at 1000 psi in Figures 6 and 7. Figure 8 shows that the dynamic  $E$  determined by transverse vibration of cylinders increases almost linearly with an increase in their compressive strength.

Orchard<sup>23</sup> ( $v$ ). Orchard stated that  $v$  of concrete varies with the richness of the mix (proportion of cement to total aggregate, by

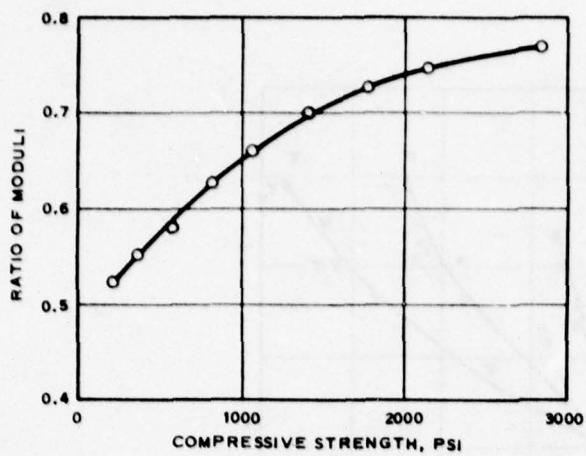


Figure 6. Ratio of static and dynamic moduli of elasticity of concretes of different strengths (after Neville<sup>22</sup>)

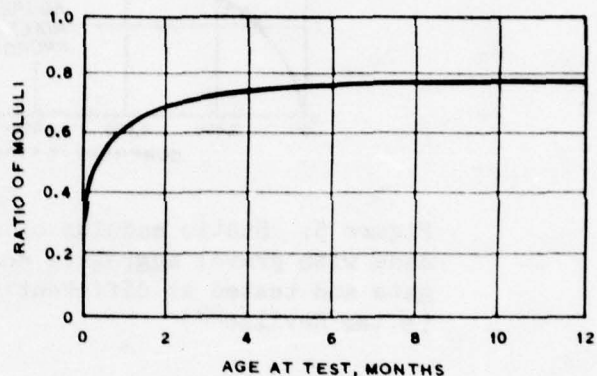


Figure 7. Ratio of static and dynamic moduli of elasticity of concrete at different ages (after Neville<sup>22</sup>)

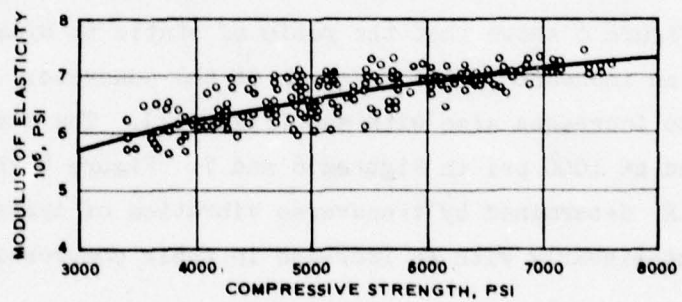


Figure 8. Relation between the dynamic modulus of elasticity, determined by transverse vibration of cylinders, and their compressive strength (after Neville<sup>22</sup>)

weight). It is approximately 0.20 for a 1 to 4-1/2 mix, 0.10 for a 1 to 6 mix, and 0.08 for a 1 to 9 mix.

WES<sup>8</sup> (E). Table 3 presents results of quasi-static and dynamic (single concentrated load) tests by WES to determine E values for low- and high-strength concrete at three different levels of confining stress,  $\sigma_3$ . The quasi-static values,  $E_{cs}$ , were determined using a standard triaxial compression device, and the dynamic values,  $E_{cd}$ , were determined using the MIT device. These test results show that the E values under the test conditions varied by a maximum factor of 1.4 when the confining pressure changed from 0 to 500 psi, by a maximum factor of 1.7 between low- and high-strength concrete, and by a maximum factor of 1.2 between quasi-static and dynamic test methods. Dynamic testing consistently yielded higher elastic modulus values than did static testing.

#### AC WEARING SURFACES

Glynn and Kirwan<sup>13</sup> (E). These researchers suggested that the modulus of AC is influenced by mix proportions as well as temperature but made no study of this point.

Morgan and Scala<sup>24</sup> (E). From observations of tests performed under rolling wheels in which they examined the strain gage output, Morgan and Scala decided that E is influenced by stress level, loading rate, and temperature.

Other Researchers (E). Several other researchers also have suggested that temperature, stress level, loading rate, and mix proportions have significant influence on E in AC.

Klomp and Niesman<sup>25</sup> (E). Figure 9 shows a relationship developed for modulus, temperature, and frequency of loading by Klomp and Niesman. Modulus decreases very rapidly with an increase in temperature, less rapidly with a decrease in rate of loading (vehicle speed).

Izatt et al.<sup>26</sup> (E). Izatt et al. developed a relationship between elastic modulus and temperature, which reveals that for the range in temperatures that exists in an AC wearing surface the modulus can vary by a factor of ten (Figure 10).

Table 3  
Summary of Triaxial Test Results (After Lundeen<sup>8</sup>)

Confining Pressure ( $\sigma_3$ ) psi	Low-Strength Concrete			High-Strength Concrete		
	Dynamic Modulus of Elasticity, $E_{cd}$ , * psi	Static Modulus of Elasticity, $E_{cs}$ , ** psi	$E_{cd}/E_{cs}$	Dynamic Modulus of Elasticity, $E_{cd}$ , psi	Static Modulus of Elasticity, $E_{cs}$ , psi	$E_{cd}/E_{cs}$
0	1,950,000	1,650,000	1.18	3,000,000	2,810,000	1.07
250	2,120,000	2,080,000	1.02	3,590,000	3,030,000	1.18
500	2,560,000	2,370,000	1.08	3,430,000	3,330,000	1.03

\* Determined using MIT device.  
 \*\* Determined using standard triaxial device.

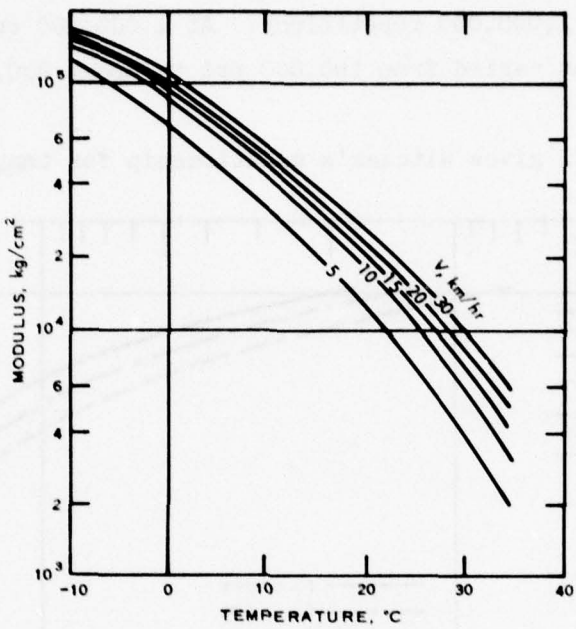


Figure 9. Asphalt concrete modulus related to temperature and rate of loading (vehicle speed) (after Klomp and Niesman<sup>25</sup>)

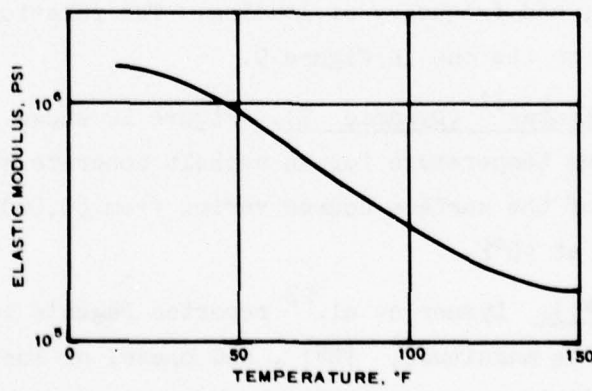


Figure 10. Variation of elastic modulus of AC with temperature (after Izatt et al.<sup>26</sup>)

Witezak<sup>27</sup> (E). For a hot environment, Witezak selected limiting design modulus values of from 200,000 psi at 100 strain repetitions to 100,000 psi at 1,000,000 repetitions. At 1,000,000 repetitions, the limiting modulus varied from 100,000 psi to about 230,000 psi for cold climates.

Figure 11 gives Witezak's relationship for temperature, asphalt

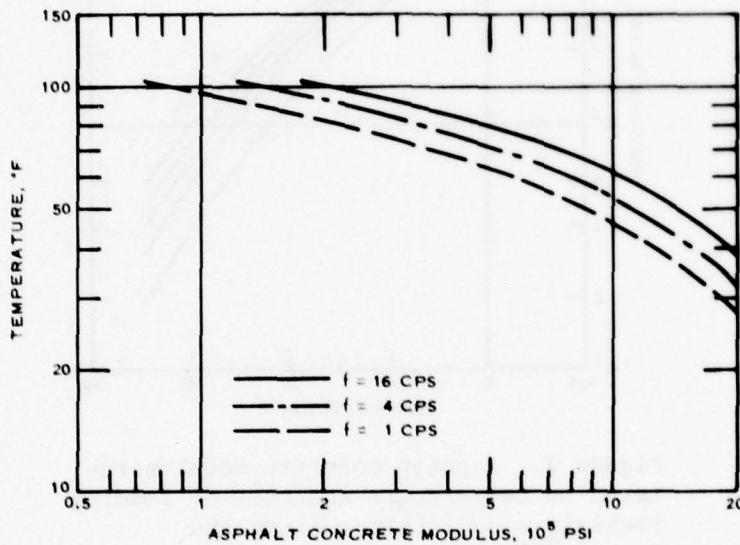


Figure 11. Effect of temperature and frequency upon typical asphalt concrete dynamic modulus (after Witezak<sup>27</sup>)

concrete modulus, and frequency of loading. The relationship is qualitatively similar to the one in Figure 9.

Cook and Krukar<sup>11</sup> (Dynamic E). Figure 12 shows a plot of dynamic modulus versus temperature for an asphalt concrete surface course. The dynamic E of the surface course varies from 60,000 psi at 100°F to 1,300,000 psi at 40°F.

Pagen (|E\*|). Lysmer et al.<sup>28</sup> reported Pagen's 1965 work relating the absolute magnitude,  $|E^*|$ , and phase, or loss, angle,  $\phi_L$ , of the complex modulus to the frequency of loading, for a typical AC at 77°F. Figure 13 gives this relationship. The absolute value,  $|E^*|$ , increases from 0 at 0 frequency to approximately 700,000 psi at a frequency of 100 rad/sec (15.9 Hz).

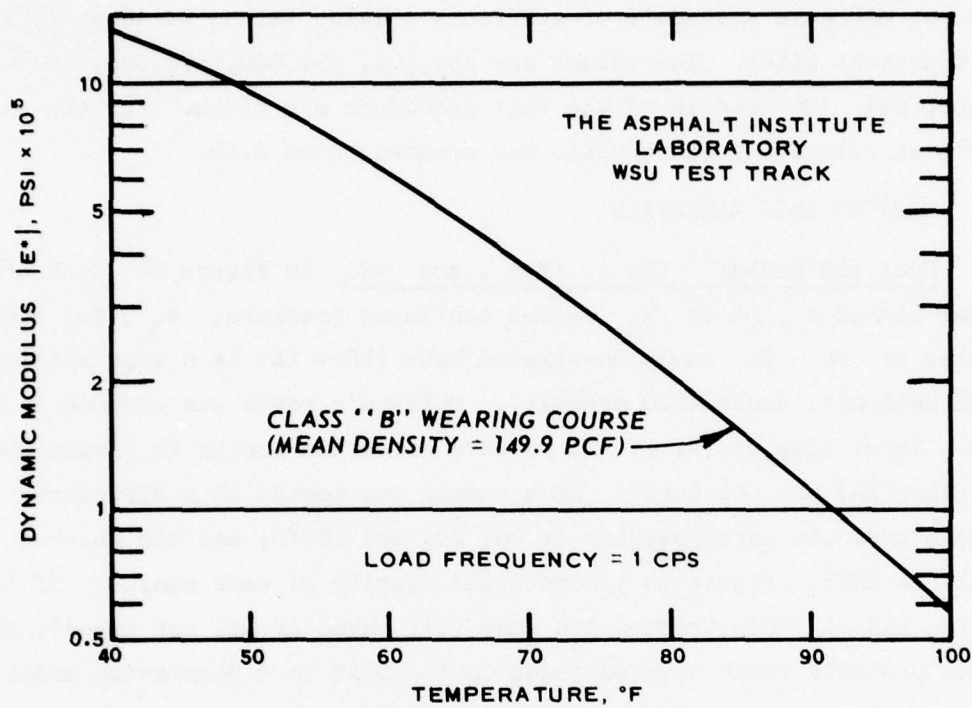


Figure 12. Dynamic modulus versus temperature relationships for asphalt treated base and asphalt concrete surface course (after Cook and Krukarll)

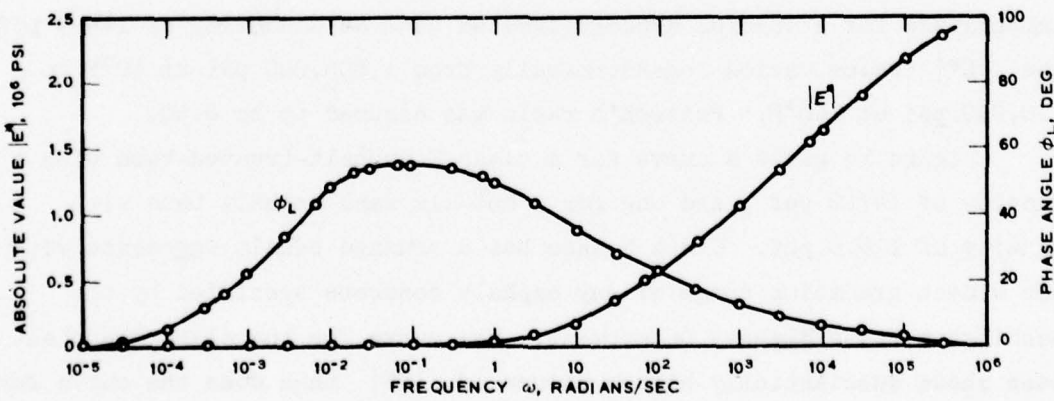


Figure 13. Magnitude and phase angle of complex elastic modulus,  $E^*$ , as a function of angular frequency at  $77^{\circ}\text{F}$  (after Pagen<sup>28</sup>)

MRD<sup>21</sup> (Stiffness Modulus, v). In the evaluation of San Francisco Airport, MRD gave a summary of stiffness modulus values of AC at 70°F for four test sites. The values are 450,000, 550,000, 570,000, and 600,000 psi. No details of the test procedure are given. For the same four test sites, Poisson's ratio was assumed to be 0.40.

#### TREATED BASE MATERIALS

Cook and Krukar<sup>11</sup> ( $M_R$ ,  $|E^*|$ , and  $v$ ). In Figure 14, Cook and Krukar showed a plot of  $M_R$  versus confining pressure,  $\sigma_3$ , for four samples of SS - Kh emulsion-treated base (SS - kh is a slow setting grade cationic, emulsified asphalt). Poisson's ratio was assumed to be 0.40. Three samples (B, C, and D) were cured six months in plastic bags, the other (A) was not cured. Each sample was tested at a different temperature; the cured samples at 40, 70, and 100°F, and the uncured sample at 80°F. Figure 14 presents the density of each sample. If the samples had all been treated the same (all cured or all not cured), the curves probably would have ascended on the plot in a decreasing order of temperature, i.e., D, A, C, and D (see Figure 11 for temperature effect on E). This did not occur, however, probably because curing raised the  $M_R$  values of curves B, C, and D. The effects of density are not readily apparent.

Figure 15 shows a curve of dynamic modulus,  $|E^*|$ , versus temperature for a special asphalt-treated base at a density of 144.9 pcf. The  $|E^*|$  value varies logarithmically from 1,600,000 psi at 40°F to 110,000 psi at 100°F. Poisson's ratio was assumed to be 0.40.

Figure 16 gives a curve for a class F asphalt-treated base with a density of 147.2 pcf, and one for a hot-mix sand asphalt base with density of 116.6 pcf. Class F base has a crushed basalt aggregate with the widest gradation range of any asphalt concrete specified by the Washington State Highway Department. The curve for the class F asphalt base shows substantially higher values of  $|E^*|$  than does the curve for the hot-mix sand asphalt base because the density of the former material is considerably higher. The effect of different aggregate gradations is

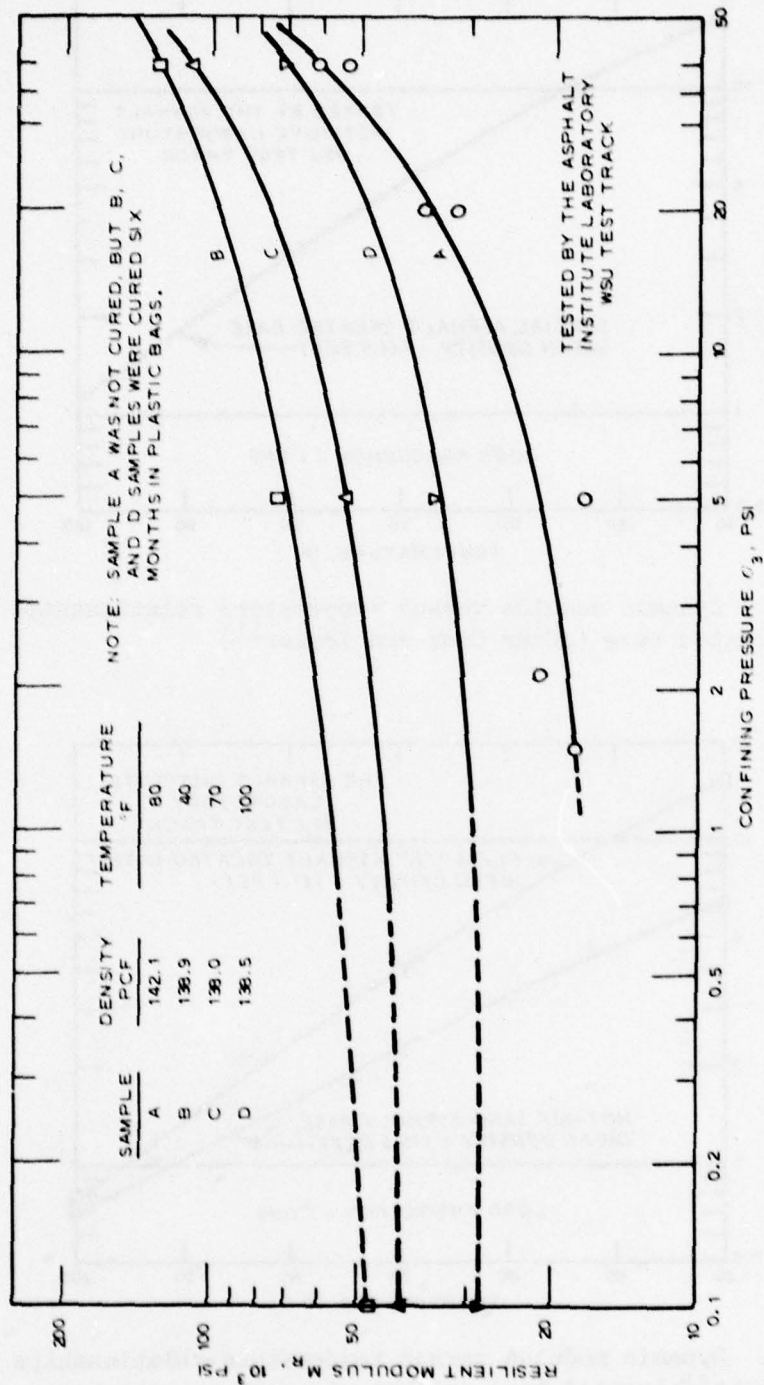


Figure 14. Resilient modulus versus confining pressure relationship for SS - K<sub>1</sub> emulsion-treated base (after Cook and Kruckar<sup>11</sup>)

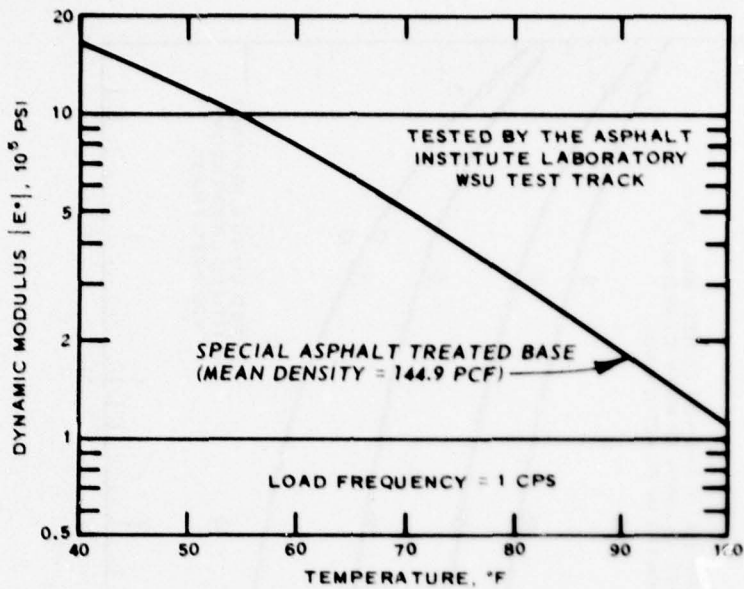


Figure 15. Dynamic modulus versus temperature relationships for asphalt-treated base (after Cook and Krukar<sup>11</sup>)

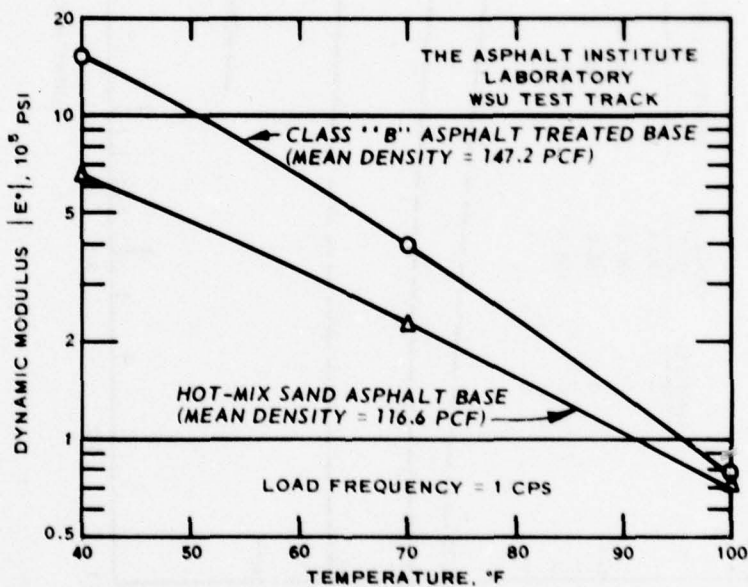


Figure 16. Dynamic modulus versus temperature relationships for class F asphalt-treated base and hot-mix sand asphalt base (after Cook and Krukar<sup>11</sup>)

also probably reflected in the different  $|E^*|$  values. Poisson's ratio was assumed to be 0.40.

Barker et al.<sup>29</sup> ( $E$ ,  $v$ ). Because the tensile strength of cement- and lime-stabilized material is lower than the compressive strength, Barker et al. determined the properties of these materials in indirect tensile testing. Cement- and lime-stabilized clay test specimens were 4.0 in. in diameter by 2.5 in. in height. Clayey gravelly sand material was molded into a 6-in.-diam by 4.5-in.-high specimen. The specimens under study were impact compacted to field conditions of density and moisture. Accurate measurement of horizontal deformations was not possible; therefore, Poisson's ratios were not obtained in the series of tests described in Reference 29. Barker found marked increases in  $E$  with increases in cement content. Table 4 lists the modulus values

Table 4

Tensile Strength and Modulus of Elasticity of Cement-Stabilized Materials (After Barker et al.<sup>29</sup>)

Material	Indirect Tensile Strength, psi	Modulus of Elasticity $E$ , psi
Lean clay		
3.0 percent cement	14.7	8,400
10.0 percent cement	42.5	46,900
3.5 percent lime	7.3	13,500
Clayey gravelly sand		
3.0 percent cement	18.4	31,100
10.0 percent cement	141.0	223,000

determined in the testing. Poisson's ratio was assumed to be 0.25 for all materials shown in Table 4.

MRD<sup>21</sup> ( $E$ ,  $v$ ). MRD found the cement-treated base at San Francisco International Airport to have an elastic modulus of 1,100,000 psi and a Poisson's ratio of 0.30. These values were determined using ASTM Designation C469-65.<sup>6</sup>

#### UNTREATED BASE MATERIALS

Dorman and Klomp<sup>14</sup> (Dynamic E). Untreated bases are subject to the same kinds of variations in elastic constants as are subgrade materials, discussed later. One kind of variation that should be mentioned here, however, is the apparent dependency of the dynamic elastic modulus of an untreated base material on the modulus of the underlying subgrade. Figure 17 gives the relationship that Dorman and Klomp found from wave velocity measurements. The ratios of modulus of elasticity of the

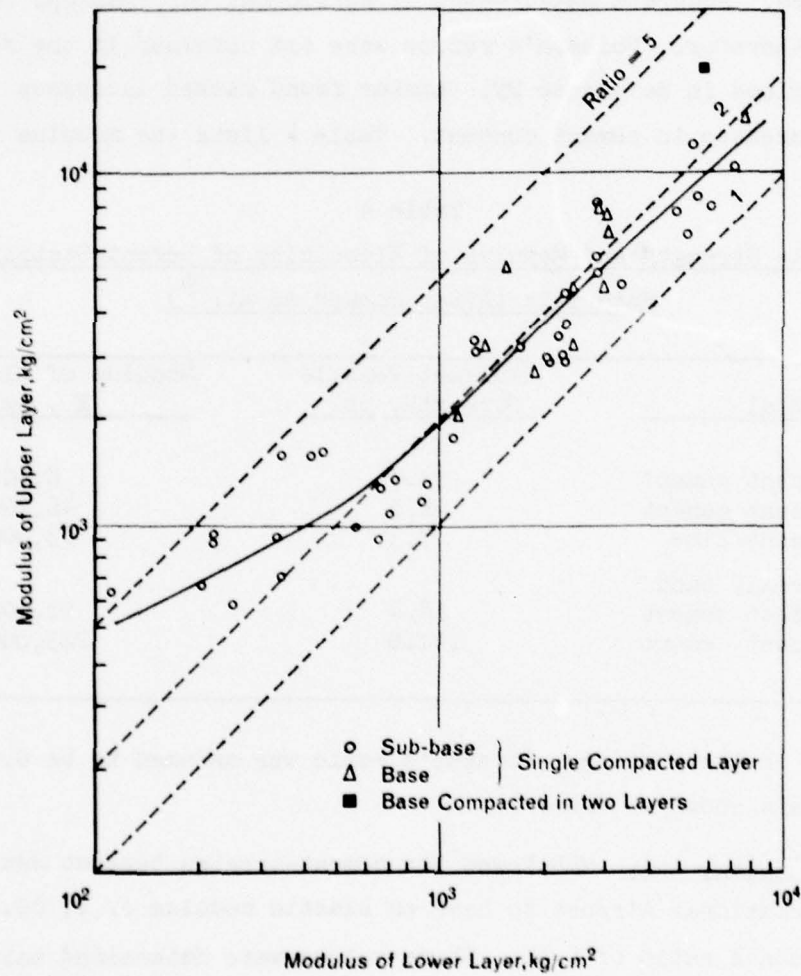


Figure 17. Dynamic moduli of unbound granular layers (after Dorman and Klomp<sup>14</sup>)

untreated base materials to modulus of elasticity of the subgrades for the many cases tested all fall in the range from 1 to 5. The average ratio is approximately 2.

Cook and Krukar<sup>11</sup> ( $M_R$ ). Cook and Krukar performed  $M_R$  tests on samples of an untreated base material (crushed basaltic rock) at three different water contents (W/C), 7.4 percent, 3.0 percent (dried in air), and saturated under vacuum. All samples were compacted at 7.4 percent W/C.

Figure 18 shows the relationship of  $M_R$  to confining pressure,  $\sigma_3$ , for the three samples. The curve for the sample with the lowest W/C (3.0 percent) plots well above the curves for the other two samples, which are nearly coincident.  $M_R$  increases with increasing confining pressure, and there appears to be a tendency for all curves to coalesce at very high confining pressures.

Figure 19 presents the same samples on a background of  $M_R$  versus bulk stress,  $\theta$ . Bulk stress, or the first stress invariant, is the sum of the principal stresses ( $\theta = \sigma_1 + \sigma_2 + \sigma_3$ ). The driest samples continues to show the highest values of  $M_R$ , and  $M_R$  increases with increasing  $\theta$ .

Glynn and Kirwan<sup>13</sup> ( $M_R$ ). Figures 20-22 show the relationship of modulus of resilient axial deformation (same as  $M_R$ ) to cell pressure  $\sigma_3$ , i.e., confining pressure for a gravel with a dry density of 127.8 pcf and a moisture content of 9.4 percent, a gravel with a dry density of 131.4 pcf and a moisture content of 7.15 percent, and a crushed stone with a dry density of 128.1 pcf and a moisture content of 7.85 percent, respectively. The deviator stress ( $\sigma_1 - \sigma_3$ ; 10 or 20 psi in Figure 20, and 10, 20, or 30 psi in Figures 21 and 22) is indicated for each point plotted. While not overwhelming, the evidence indicates that  $M_R$  increases with increasing density and decreasing moisture content and is not significantly affected by deviator stress.

Allen<sup>30</sup> ( $M_R$ ). Allen has summarized the results of repeated load triaxial tests to determine  $M_R$  for several untreated base materials

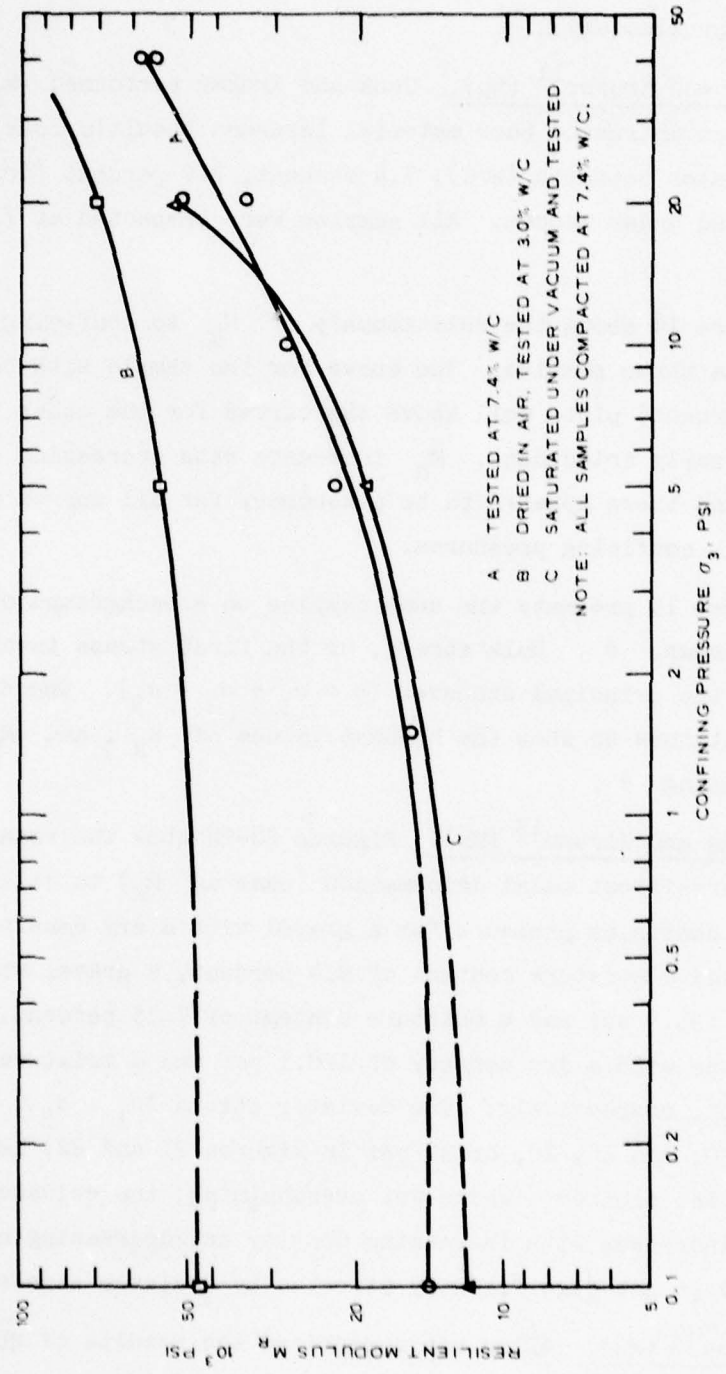


Figure 18. Resilient modulus versus confining pressure relationship for untreated base material (after Cook and Krikarli)

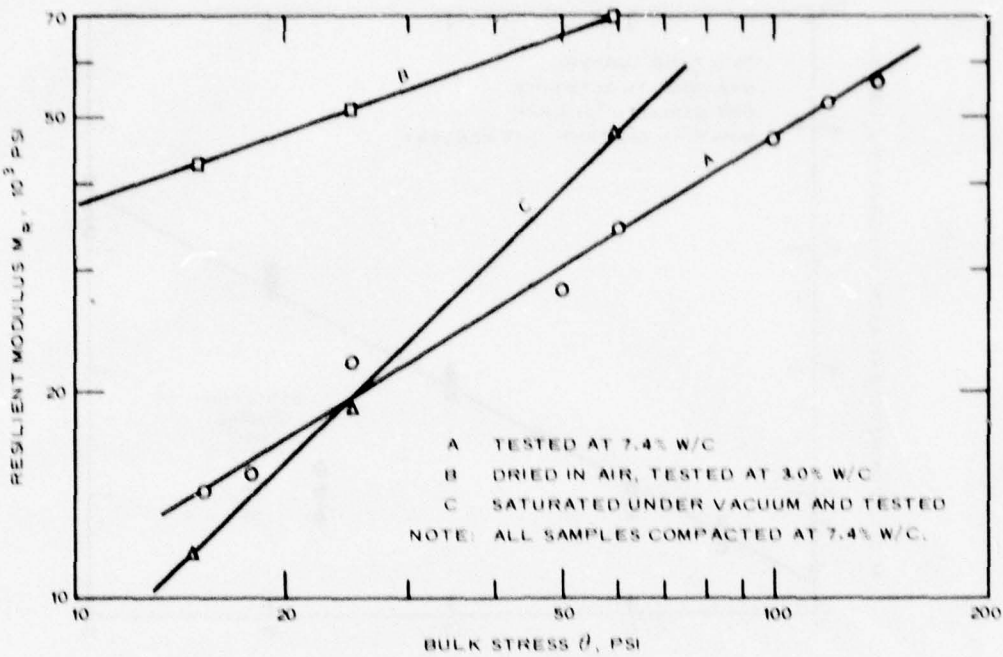


Figure 19. Resilient modulus versus bulk stress relationship for untreated base material (after Cook and Krukar<sup>11</sup>)

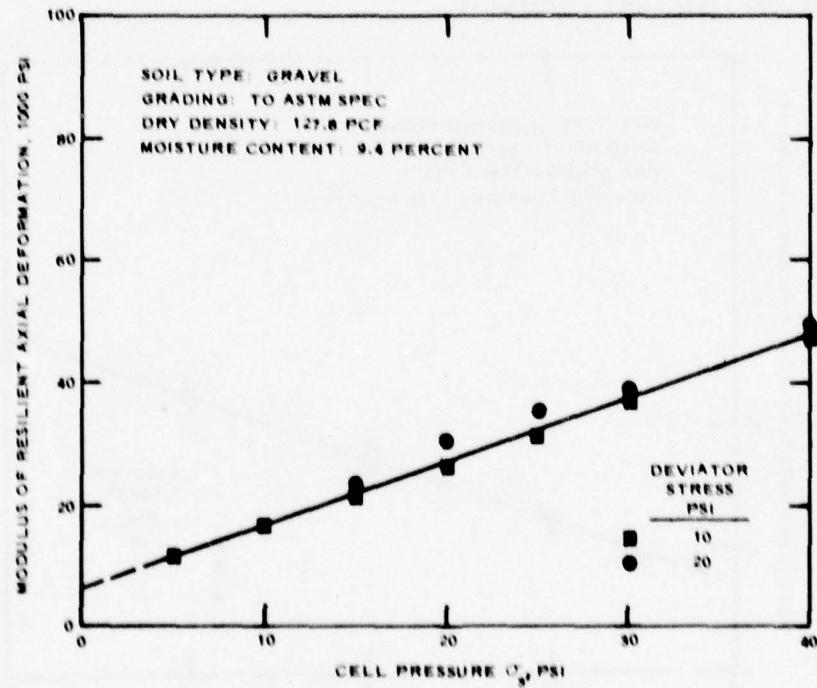


Figure 20. Modulus versus cell pressure ( $\sigma_3$ ), test series 3 (after Glynn and Kirwan<sup>13</sup>)

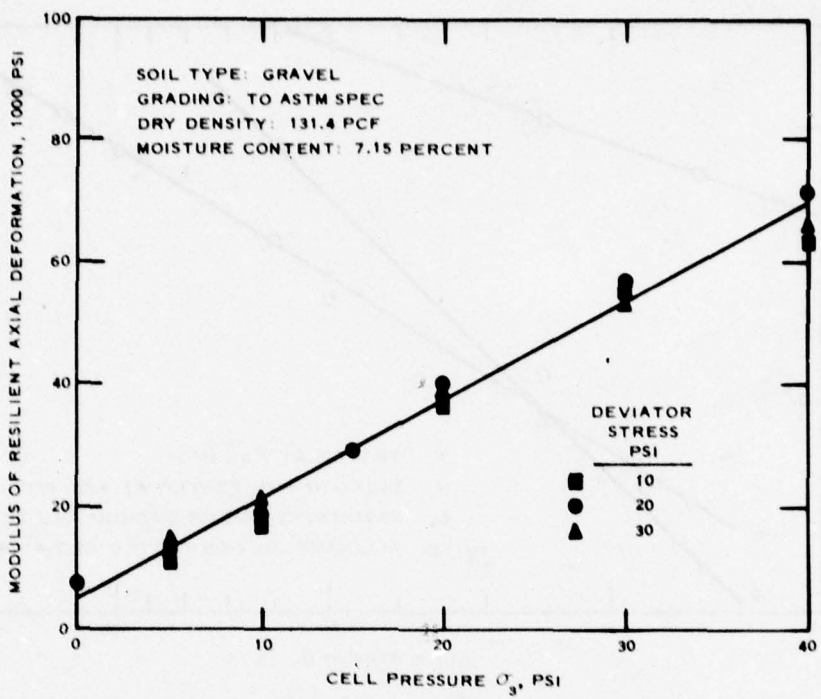


Figure 21. Modulus versus cell pressure ( $\sigma_3$ ), test series 4  
 (after Glynn and Kirwan<sup>13</sup>)

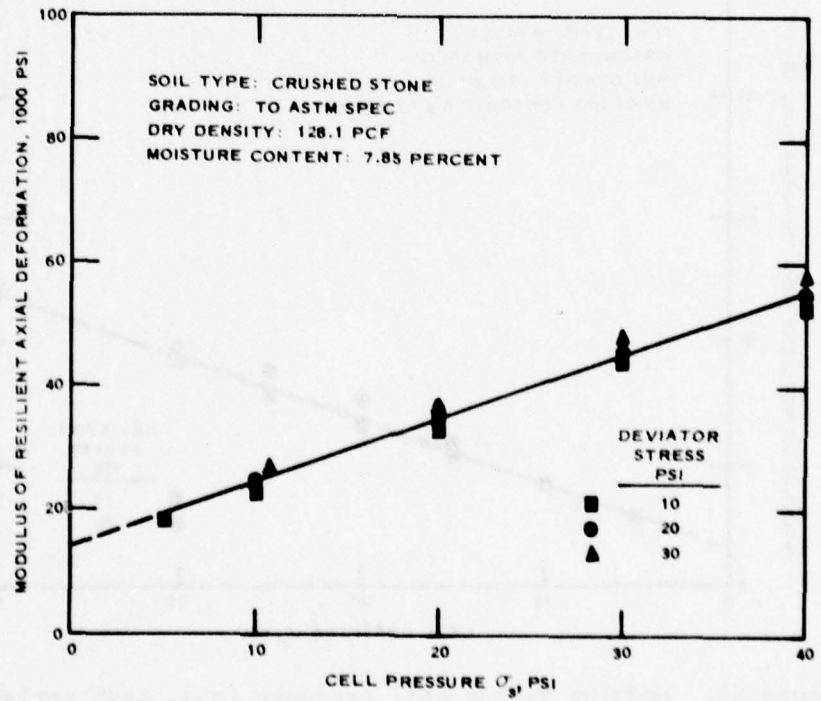


Figure 22. Modulus versus cell pressure ( $\sigma_3$ ), test series 5  
 (after Glynn and Kirwan<sup>13</sup>)

in Table 5. This table presents the researcher(s), the material tested, the range of  $M_R$  values found, and comments on the test conditions. The variation in values of  $M_R$  for a given material and between materials is seen to be quite wide in some cases. From the table, it appears that stress level had a greater effect on  $M_R$  than did the other test factors (frequency and duration of load, moisture content, gradation, void ratio, dry density, and rate of deformation); however, such a conclusion on the basis of the data shown can only be considered tentative.

Table 5  
Summary of Repeated-Load Triaxial Tests to Evaluate the Resilient Properties of Granular Materials (After Allen<sup>30</sup>)

Researcher	Material	Resilient Modulus, psi	Comments
1. Seed and Chan	Silty sand	21,300 to 27,300	Varied frequency and duration of load
2. Haynes and Yoder	Gravel and crushed stone	28,000 to 63,000	Varied moisture content and gradation
3. Biarez	Rounded aggregate	16,700 to 54,500	Varied stress levels and void ratio
4. Trollope, Lee and Morris	Poorly graded dry sand	35,000 to 95,000	Varied stress levels, dry density, rate of deformation
5. Dunlap	Well graded aggregate	30,000 to 160,000	Varied stress levels
6. Mitry	Dry gravel	$7,000\sigma_3^{0.55}$ to $1,900\sigma_3^{0.61}$	Varied stress levels
7. Schiffley	Crushed gravel	$13,000\sigma_3^{0.50}$ to $9,000\sigma_3^{0.50}$	Varied moisture content
8. Kasianchuk	Aggregate base aggregate subbase	$3,830\sigma_3^{0.53}$ to $2,900\sigma_3^{0.47}$	Varied stress levels
9. Hicks and Finn	Aggregate base	$5,400\sigma_3^{0.50}$ to $21,000\sigma_3^{0.50}$	Varied moisture content

NOTES:  $\sigma_3$  is confining pressure;  $\theta$  is bulk stress =  $\sigma_1 + \sigma_2 + \sigma_3$ .

Allen<sup>30</sup> (v). Allen has summarized Hicks' study of some of the factors that influence the resilient Poisson's ratio of untreated base materials from tests similar to those conducted at WES. In Figure 23, a plot of resilient  $v$  against the principal stress ratio,  $\sigma_1/\sigma_3$ , shows that the  $v$  for the dry specimen is approximately twice that of the wet one and that the various confining pressures had some effect on

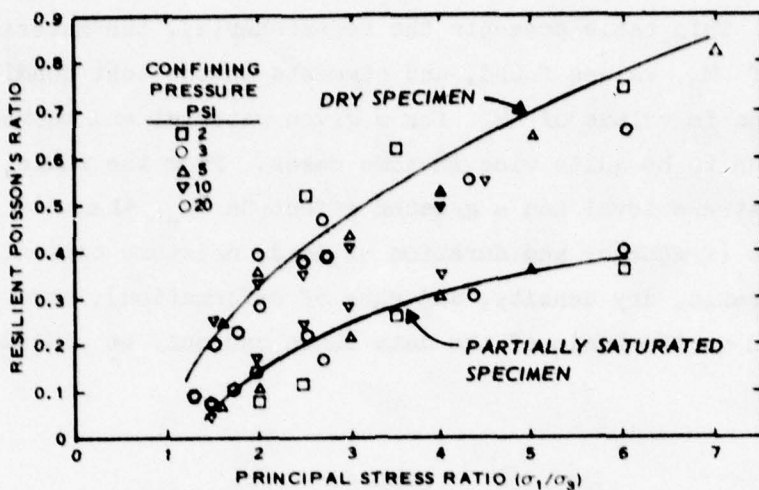


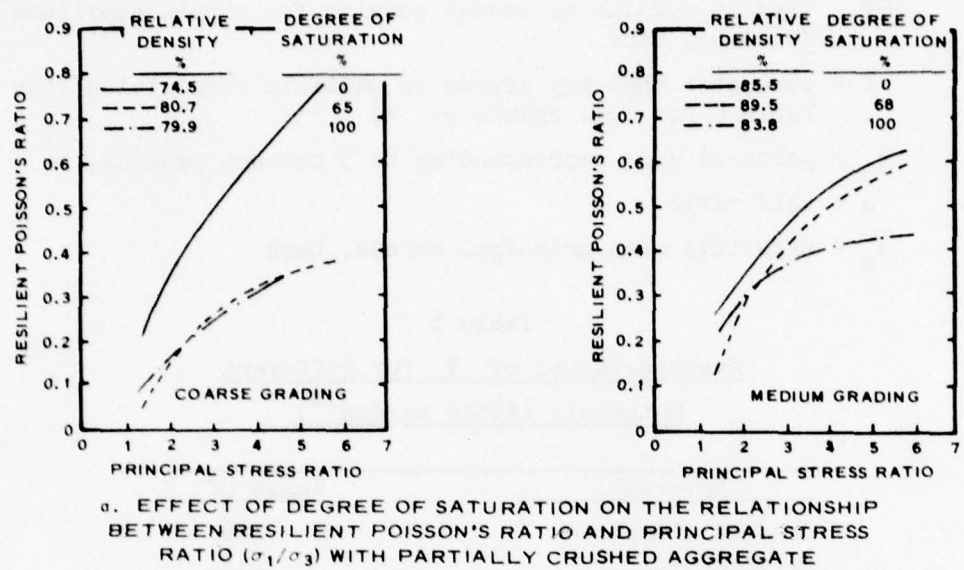
Figure 23. Secant Poisson's ratio as a function of principal stress ratio with partially crushed aggregate, low density, coarse grading (after Hicks; summarized by Allen<sup>30</sup>)

the results. In Figure 24a, Allen (Hicks) shows two plots, one for a coarsely graded material and the other for a medium-graded material. Each contains curves for samples at 0 and 100 percent saturation and at an intermediate saturation. A relative density is indicated for each curve. Figure 24b also shows  $v$  versus  $\sigma_1/\sigma_3$  plots for a coarsely graded and a finely graded material. In these plots, the samples are dry, and relative densities are indicated.

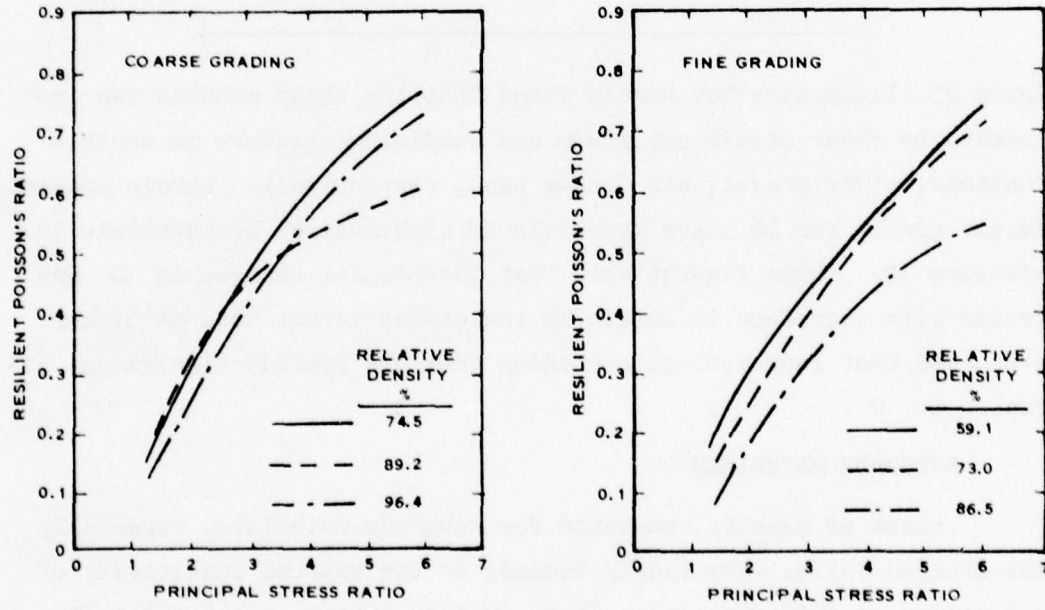
On the basis of examination of the four plots, it can be concluded tentatively that water content is the most significant factor (the drier the sample, the higher the  $v$ ) and that increases in relative density usually correspond to decreases in resilient  $v$ .

Hardin 15 (G). In tests on 19 gravel samples, Hardin extended his earlier work with soils to arrive at the following expression for gravels, which summarized the factors that cause variations in the shear moduli of coarse materials.

$$G_{\max} = Y \left[ 2 + D_5 \left( \frac{\sigma_0}{\sigma_0} - 0.2/3 \right) \right] \frac{(2.973 - e)^2}{(1 + e)} \frac{1}{\sigma_0^{1/2}}$$



a. EFFECT OF DEGREE OF SATURATION ON THE RELATIONSHIP  
BETWEEN RESILIENT POISSON'S RATIO AND PRINCIPAL STRESS  
RATIO ( $\sigma_1/\sigma_3$ ) WITH PARTIALLY CRUSHED AGGREGATE



b. EFFECT OF DENSITY ON THE RELATIONSHIP BETWEEN  
RESILIENT POISSON'S RATIO AND PRINCIPAL STRESS  
RATIO ( $\sigma_1/\sigma_3$ ) WITH PARTIALLY CRUSHED AGGREGATE  
AND DRY SAMPLES

Figure 24. Resilient Poisson's ratio versus principal stress ratio (after Hicks; summarized by Allen<sup>30</sup>)

where

$G_{max}$  = maximum shear modulus, which is equal to the initial tangent modulus or secant modulus for strain amplitude  $\leq 0.00001$ , bars

$Y$  = parameter that may depend on particle composition (see Table 6 for some values of  $Y$ )

$D_5$  = particle size corresponding to 5 percent passing, mm

$e$  = void ratio

$\sigma_o$  = effective mean principal stress, bars

Table 6

Average Values of Y for Different Materials (After Hardin<sup>18</sup>)

Material	Value of Y
Crushed limestone	146
River gravel	143
Standard Ottawa sand	110
Natural soils	132

Figure 25 illustrates how Hardin found that the shear modulus was influenced by shear strain amplitude and confining pressure in crushed limestone, river gravel, and Ottawa sand, respectively. Hardin presents similar graphs for 16 other materials or combinations of materials in Reference 18. These figures show that incremental changes in  $G$  are greater with increases in strain at low stress levels than at higher levels and that increases in confining pressure provide significant increases in  $G$ .

#### SUBGRADE MATERIALS

Values of elastic constants for subgrade materials, especially fine-grained soils, vary widely because of the extreme sensitivity of such values to soil properties (type, water content, etc.) and to in situ and/or test conditions (confining pressure, strain amplitude, etc.). It is important to note that elastic constants determined in the laboratory often are not accurate for field conditions. Terzaghi and Peck<sup>31</sup>

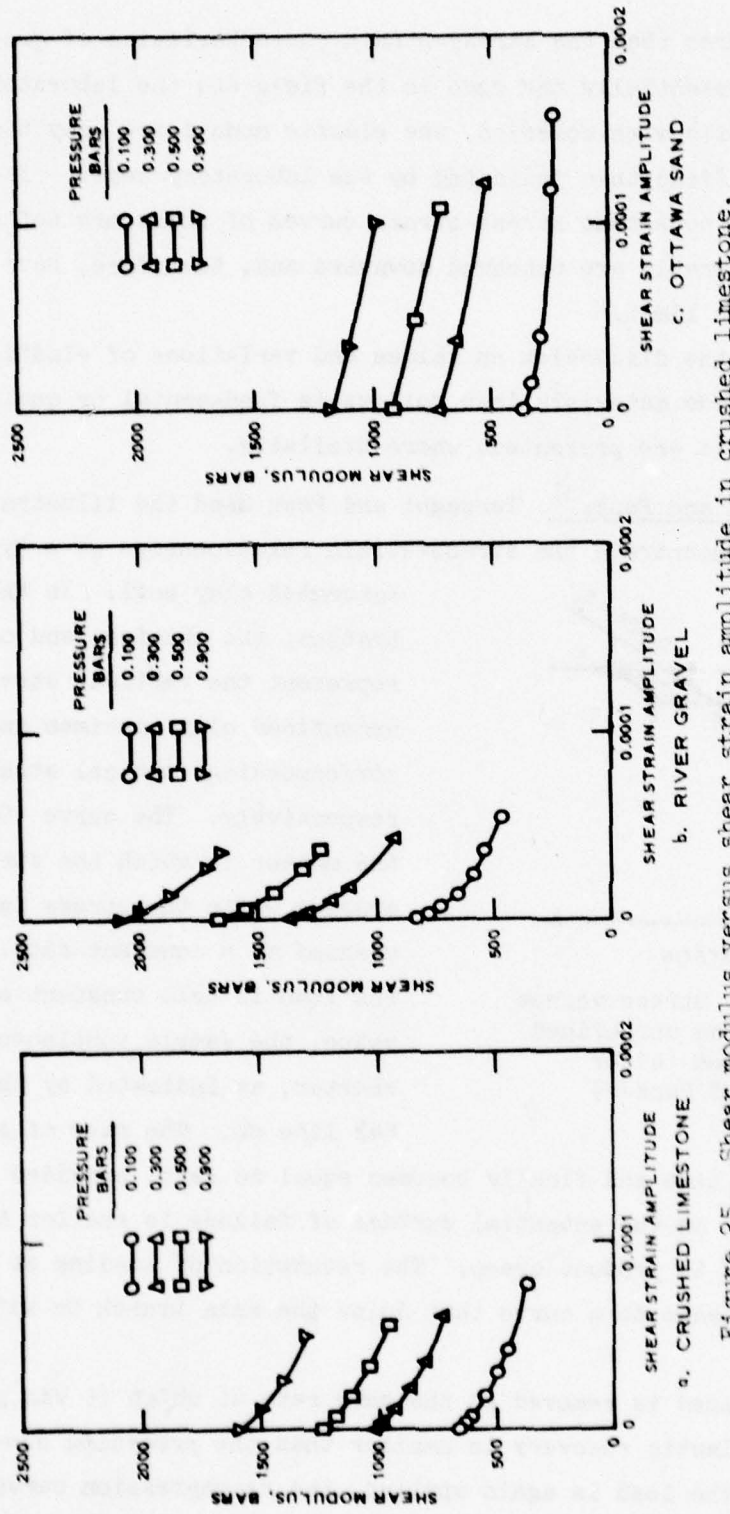


Figure 25. Shear modulus versus shear strain amplitude in crushed limestone, river gravel, and Ottawa sand (after Hardin<sup>18</sup>)

and Bowles<sup>32</sup> agree that the stress-strain characteristics of granular materials are essentially the same in the field and the laboratory; however, for soils with cohesion, the elastic moduli are many times greater in the field than indicated by the laboratory tests. It also is important to note that stress-strain curves of soils are not straight lines; they generally are concaved downward and, therefore, have no definite elastic limit.

Much of the discussion on values and variations of elastic constants in subgrade materials that follows is fundamental or qualitative. Quantitative data are presented, where available.

Terzaghi and Peck.<sup>31</sup> Terzaghi and Peck used the illustration in Figure 26 to demonstrate the stress-strain relationships of a typical

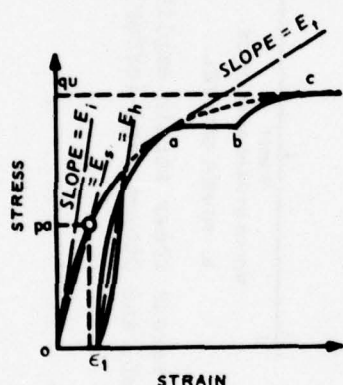


Figure 26. Stress versus strain for an unconfined clay specimen (after Terzaghi and Peck<sup>31</sup>)

saturated clay soil. In this illustration, the abscissa and ordinate represent the vertical stress on an unconfined clay specimen and the corresponding vertical strain, respectively. The curve Oc shows the manner in which the strain increases while the stress is increased at a constant rate. If the load is held constant at some value, the sample continues to get shorter, as indicated by the horizontal line ab. The rate of shortening decreases with time and finally becomes equal to zero, provided the shearing stress on the potential surface of failure is smaller than the stress required to produce creep. The resumption of loading at the original rate leads to a curve that joins the main branch Oc without any break.

If the load is removed at the same rate at which it was previously applied, the elastic recovery is smaller than the preceding compression. If the load is again applied, the recompression curve joins

the main branch without any breaks, and the decompression and recompression curves enclose a hysteresis loop. As soon as the stress becomes equal to the unconfined compressive strength,  $q_u$ , of the material, the specimen fails by shearing or bulging.

Since for most soils the stress-strain curve Oc in Figure 26 is curved throughout its entire length, the relation between stress and strain for soils, unlike that of elastic materials, cannot be expressed by a single numerical value  $E$ . In order to compare the stress-strain properties of different soils or those of the same soil under different conditions, one of the following four quantities may be used: the initial tangent modulus  $E_i$ , the tangent modulus  $E_t$ , the secant modulus  $E_s$ , or the hysteresis modulus  $E_h$ . These quantities are equal, respectively, to the slopes (stress per unit of strain) of the dash-dotted lines in Figure 26. The secant modulus  $E_s$  represents the average slope of the stress-strain curve for the range in stress between zero and some arbitrary value  $P_a$ .

If an undisturbed clay specimen is first tested and then remolded at unaltered W/C and tested again, it may be observed that the values of  $q_u$  and  $E$  are very much smaller for the remolded than for the undisturbed material, but the general character of the stress-strain diagram remains unaltered. The magnitude of the decrease of strength and stiffness depends on the degree of sensitivity of the clay. If the remolded specimens are allowed to age without change in water content, their strength and stiffness increase at a rate that decreases with time, but it is doubtful whether they would ever attain values corresponding to those for the undisturbed specimens.

The stress-strain characteristics of partly confined, normally loaded clays are similar to those of fine-grained and saturated loose sands. However, at a given confining pressure, the values of confined compressive strength,  $q_c$ , and  $E$  for clay are very much smaller than the corresponding values for sand. If a unidirectional stress is added to an all-around pressure in clay, the relation between this stress and the corresponding strain is similar to that shown in Figure 27 for loose sand.

Figure 27 shows a plot of initial tangent modulus versus confining pressure,  $p_c$ , for dense and loose sands. The  $E_i$  of confined, normally loaded clays increases like that of a loose sand, in simple proportion to  $p_c$ ; that is

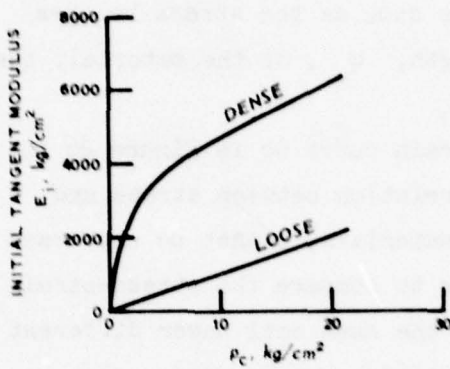


Figure 27. Initial tangent modulus versus confining pressures for sand (after Terzaghi and Peck<sup>31</sup>)

without permitting the water content of the specimen to change, the value of  $C$  ranges from about 10 for highly colloidal clays to 100 for silty or slightly sandy clays.

Lambe and Whitman<sup>33</sup> ( $E$  and  $v$ ). Lambe and Whitman determined that it is difficult to find the  $E_i$  accurately because the slope of the stress-strain curve changes rapidly even at small strains. They also found that the  $E_i$  modulus as determined from the first loading of a triaxial test usually is much less than the modulus computed from wave velocity.

Lambe and Whitman stated that the effect of the actual state of stress on modulus is not clear, but the best available information shows that modulus depends on the average of the initial principal stresses; that is,

$$E \propto \sqrt{\sigma_v + \frac{2K_o}{3}}$$

where

$\sigma_v$  = vertical stress

$K_o$  = the coefficient of lateral stress at rest

The equation is true only when  $1/2 < K_o < 2$  and when the factor of safety against failure is two or greater.

The elastic modulus decreases and Poisson's ratio increases as strain level increases. Lambe and Whitman presented a relationship between  $\sigma_v$ ,  $\sigma_h$ , and  $\epsilon_v$ , which is

$$\sigma_v - \sigma_h = \sqrt{\frac{\epsilon_v}{a + b\epsilon_v}}$$

where  $a$  and  $b$  are constants and subscripts  $h$  and  $v$  mean "horizontal" and "vertical," respectively. The general form of this empirical expression indicates that the modulus depends heavily on stress level.

Lambe and Whitman made the following general statements:

- a. The modulus of a soil decreases with:
  - (1) An increase in deviator stress.
  - (2) A soil disturbance.
- b. The modulus of a soil increases with:
  - (1) An increase in consolidation stress.
  - (2) An increase in overconsolidation ratio.
  - (3) An increase in aging.
  - (4) An increase in strain rate.

Lambe and Whitman also stated that during the early range of strains for which the concepts of theory of elasticity are useful, the Poisson's ratio is varying with strain and for sands becomes constant only for large strains that imply failure; then it has a value greater than 0.5. Poisson's ratio is less than 0.5 only during the early stages of strain where the specimen decreases in volume. Because of this behavior, it is difficult to make an exact evaluation of  $\nu$ . For early stages of a first loading of a sand, when particle rearrangements are important,  $\nu$  typically has values of about 0.1 to 0.2. During cyclic loading,  $\nu$  becomes more of a constant, with values from 0.3 to 0.4. However, satisfactory estimates of  $\nu$  of low saturated and fully

saturated soils are 0.35 and 0.5, respectively, for most computations.\*

Barkan<sup>10</sup> (E). Barkan concluded that the E modulus of sand containing no silt or clay does not change drastically with grain size. Table 7 shows how E varies with sands of different grain sizes.

Table 7  
Grain Size of Sand and E Moduli  
(After Barkan<sup>10</sup>)

<u>Grain Size of Sand, mm</u>	E <u>kg/cm<sup>2</sup></u>
1.25-1.50	450
1.00-1.25	520
0.60-0.80	620
0.35-0.60	480
0.30-0.35	480
0.20-0.30	620

For clay, Barkan found that the E modulus depended on water content, grain size, and porosity. Figure 28 shows how E values obtained

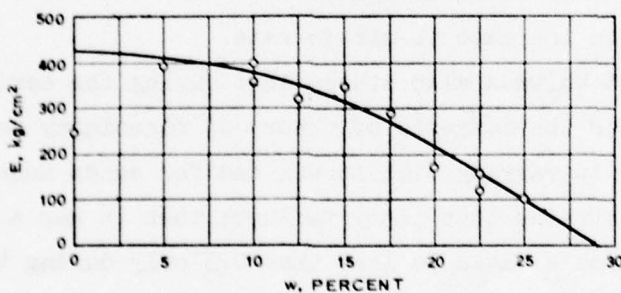


Figure 28. E versus water content for a clay (after Barkan<sup>10</sup>)

\* Although values  $\geq 0.5$  for Poisson's ratio have been observed in the laboratory, these upper limits are not valid for use in elastic theory since the bulk modulus of elasticity, defined as  $E/3(1 - 2v)$ , calculates to infinity if  $v = 0.5$ .

from compression tests on clay cubes varied with water content. An empirical formula that expresses the E modulus of clay in terms of water content is

$$E = E_0 \left( 1 - \frac{W^2}{W_0^2} \right)$$

where

$E_0$  = value of modulus with zero moisture content

W = moisture content of clay at time of interest

$W_0$  = moisture content of the clay for which the modulus is very small

Figure 29 presents Barkan's relationship between E of a clay and its void ratio, e. In a change of void ratio from 0.32 to 0.93, the value of E changes fourteenfold, from 1700 to 120 kg/cm<sup>2</sup>.

Table 8 gives the values of E modulus determined by Barkan for nine different soils. It is apparent that soil name alone is no clue to an E value.

Barkan summarized his study of E values for soils with the following conclusions:

On the basis of these data, it is possible to conclude that Young's modulus for clayey soils depends to a large degree on physiomechanical properties. While the values of E for sands change comparatively little, those for clays and clays with silt and sand may change greatly depending on the moisture content, the void ratio, and, to a lesser degree, the grain size. Since the data now available are not sufficient for generalizations concerning the effects of these characteristics on Young's modulus, it is not possible to recommend any values of E for cohesive soils for use in design computations. It is necessary to determine the design values of E in each case by direct testing of undisturbed soil taken from the construction site.

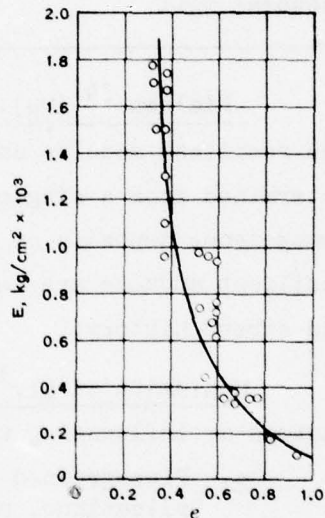


Figure 29. E versus void ratio for a clay (after Barkan<sup>10</sup>)

Table 8  
Elastic Moduli for Nine Soils (After Barkan<sup>10</sup>)

Soil Description	$E$ , kg/cm <sup>2</sup>
Plastic silty clay with sand and organic silt	310
Brown saturated silty clay with sand	440
Dense silty clay with some sand	2,950
Medium moist sand	540
Gray sand with gravel	540
Fine saturated sand	850
Medium sand	830
Loess	1,000-1,300
Loessial soil	1,200

Nielsen<sup>34</sup> ( $M_R$ ). As indicated by this reference, for some soils the resilient modulus can be significantly greater than the modulus determined from a single static test and is an aeolotropic property in homogeneous deposits of fine-grained soils. Factors that influence the resilient modulus are method of compaction, initial compaction moisture, and stress history.

Monismith et al.<sup>35</sup> ( $M_R$ ). These researchers listed the following factors as influencing the resilient moduli of soils:

- a. Fine-grained soils--stress intensity, number of stress applications, age at initial loading (thixotropy), compaction method, compaction density, water content, and subsequent changes in these.
- b. Untreated granular materials--confining pressure, stress level, duration of stress application, rate of application, rate of deformation, type and gradation of aggregate, void ratio, and degree of saturation.

The influence of stress intensity is the most important factor considered.

Robnett and Thompson<sup>36</sup> ( $E_R$ ). The findings of Robnett and Thompson reinforce the opinion of Monismith as to the importance of stress intensity in resilient modulus testing. They state that it is apparent

that any adequate characterization of subgrade soil support must recognize the stress dependent nature of the resilient modulus,  $E_r$ . They also recognized the important influence of compaction moisture content and density on the resilient properties of soil.

Figure 30 presents the load-time relationship of the resilient modulus testing equipment used by Robnett and Thompson.

Figure 31 shows resilient modulus in relationship to degree of saturation for eight different soils. The plot indicates that the resilient moduli decreases with an increasing degree of saturation.

Figures 32 and 33 show the influence of compaction moisture content on resilient modulus. Figure 32 is a graph of  $E_r$  versus applied deviator stress, with  $\sigma_3 = 0$ , for three soil types. For each soil type, relationships are shown for water contents of optimum and optimum plus 2 percent. At an applied deviator stress of 5 psi (Figure 32), decreasing the moisture content by 2 percent increased  $E_r$  by 27 to 63 percent for the three soils. The effect of moisture content is fairly constant with applied deviator stress. Figure 33, which is a graph of  $E_r$  versus compaction moisture content relative to optimum, shows the effects of moisture content on seven soil types in addition to those shown in Figure 32. The  $E_r$ 's of all 10 soil types decrease, some more drastically than others, with increasing moisture content.

Figure 34 shows the influence of density on the curves of resilient moduli versus applied deviator stress (axial stress since

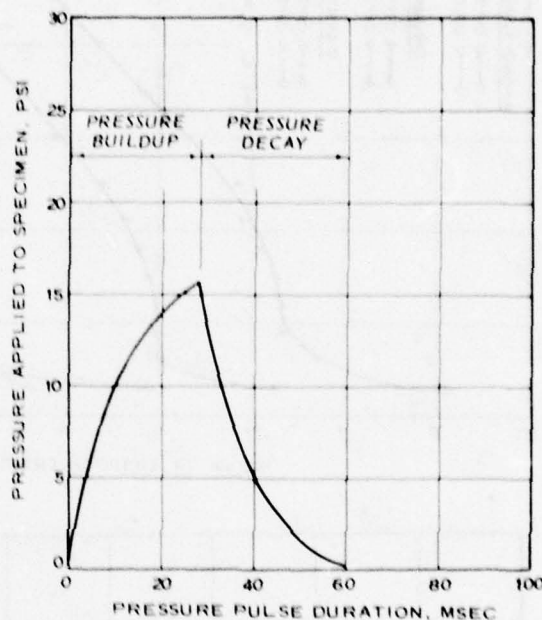


Figure 30. Typical specimen load-time relation developed by the resilient testing equipment (after Robnett and Thompson<sup>36</sup>)

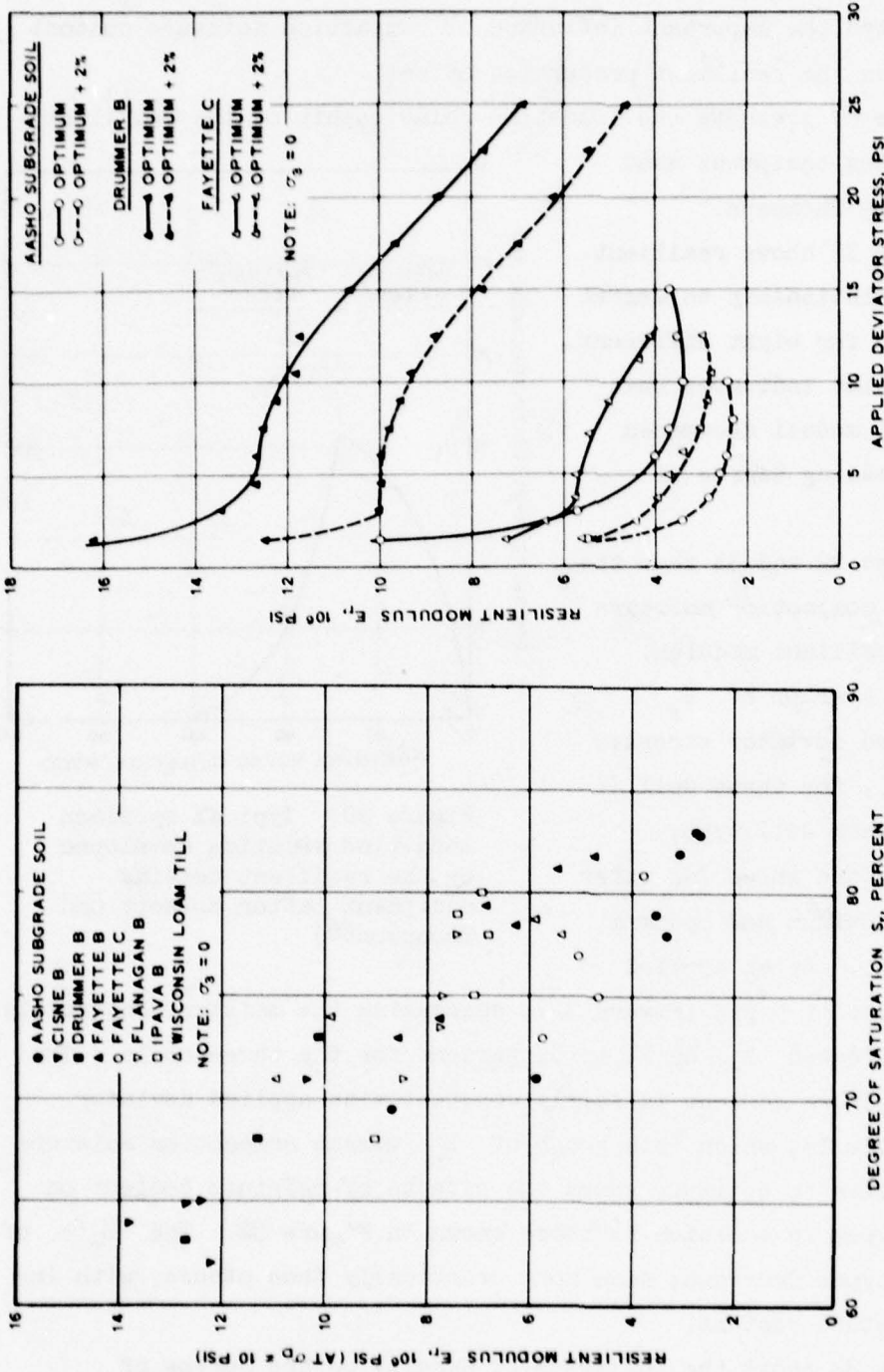


Figure 31. Resilient modulus versus degree of saturation for eight soils (after Robnett and Thompson<sup>36</sup>)

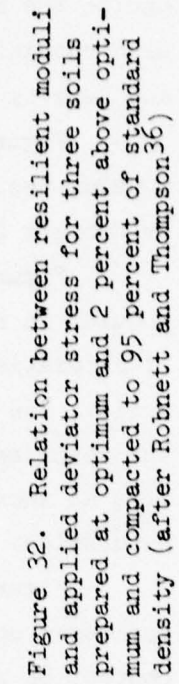


Figure 32. Relation between resilient moduli and applied deviator stress for three soils prepared at optimum and 2 percent above optimum and compacted to 95 percent of standard density (after Robnett and Thompson<sup>36</sup>)

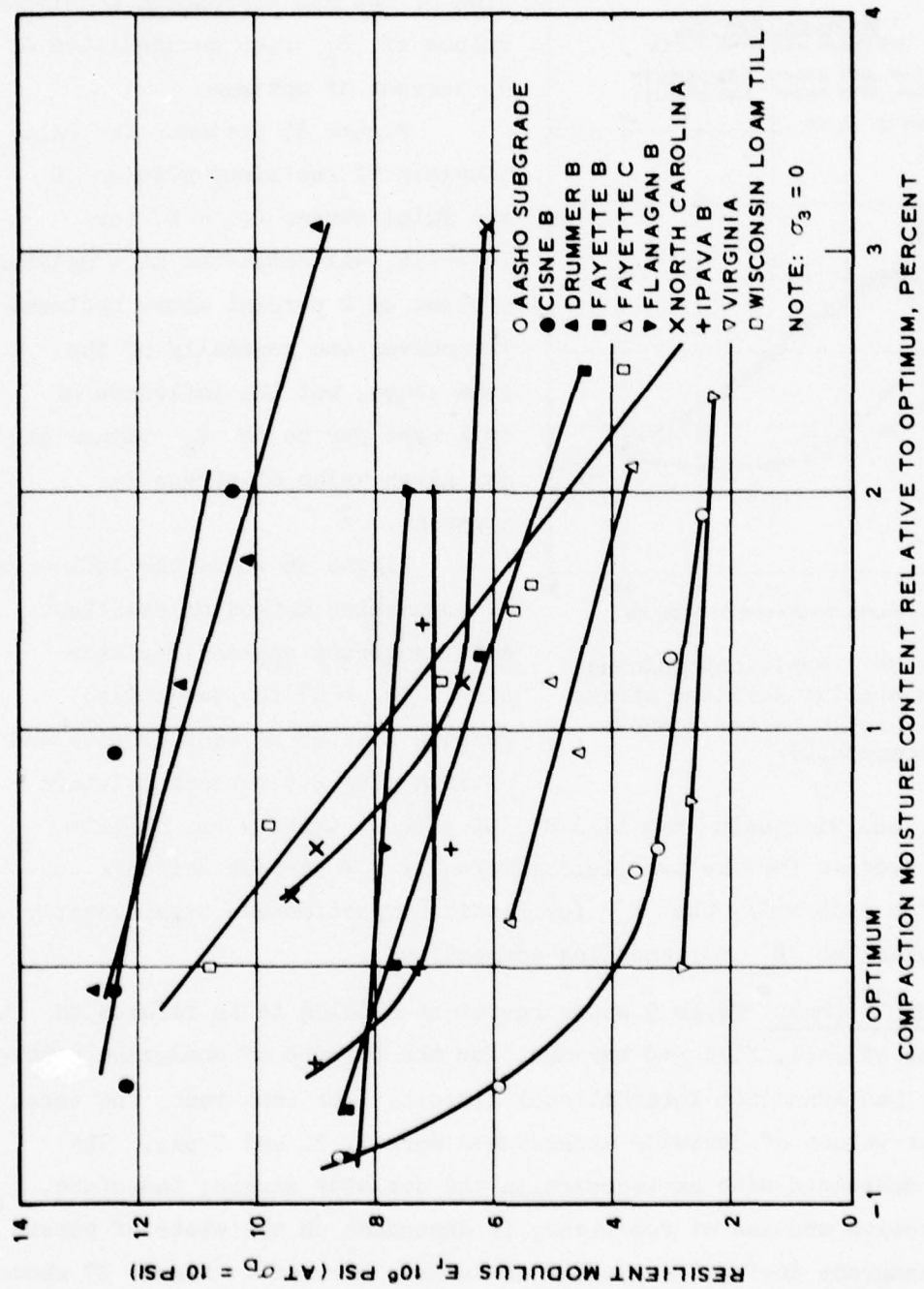


Figure 33. Relation between resilient moduli (at  $\sigma_D = 10$  psi) and compaction moisture content for phase 1 soil samples compacted to 95 percent AASHO T-99 density (after Bonnett and Thompson 36).

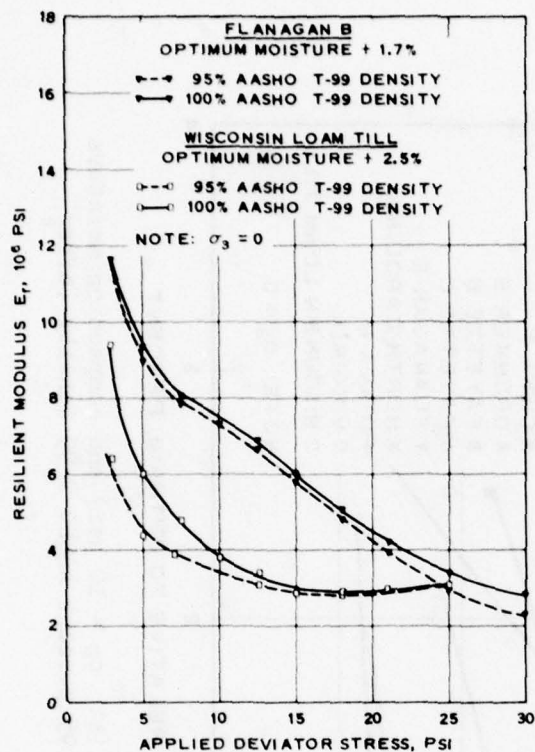


Figure 34. Resilient modulus versus applied deviator stress for two soils (after Robnett and Thompson<sup>36</sup>)

content, and Wisconsin loam till at 100 percent density and optimum plus an average for the two field samples of 2.7 percent moisture content. For each soil, the  $E_r$  for static compaction was significantly higher than the  $E_r$  for kneading compaction.

MRD<sup>21</sup> ( $M_R$ ). Table 9 shows resilient modulus tests results on two types of soil, fill and bay mud, for the purpose of analyzing conditions at San Francisco International Airport. For each test, the three different values of deviator stress used were 1, 3, and 5 psi. The modulus decreased with an increase in the deviator stress; therefore, the effective modulus of resiliency is dependent on the state of stress of the subgrade during the passage of various aircraft. Figure 37 shows the dependency of  $M_R$  on repeated deviator stress for four samples from Table 9.

$\sigma_3$  was zero) for two soils. It is apparent that densities of 100 percent of optimum correspond to higher values of  $E_r$  than do densities of 95 percent of optimum.

Figure 35 presents the relationship of resilient modulus  $E_r$  and axial stress ( $\sigma_3 = 0$ ) for 10 soils, all compacted at a moisture content of 2 percent above optimum. The curves are generally of the same shape, but the influence of soil type per se on  $E_r$  values at any given value of stress is apparent.

Figure 36 shows the influence of compaction method on resilient modulus versus applied deviator stress ( $\sigma_3 = 0$ ) for two soils: Fayette B at 95 percent density and optimum plus 2.5 percent moisture

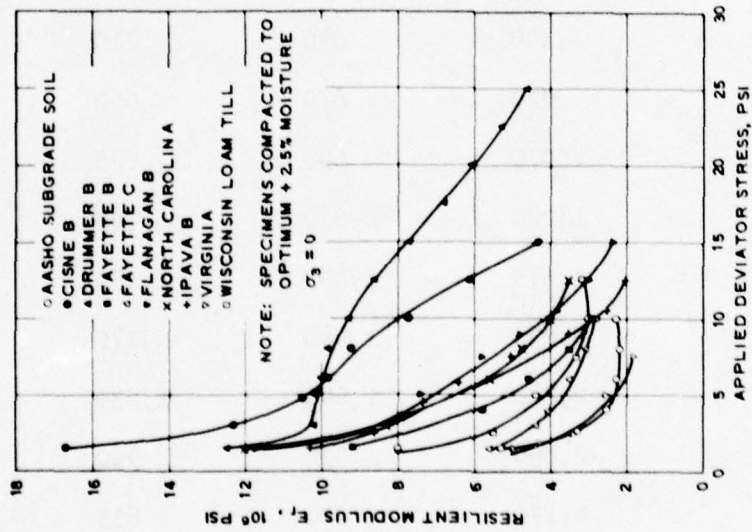
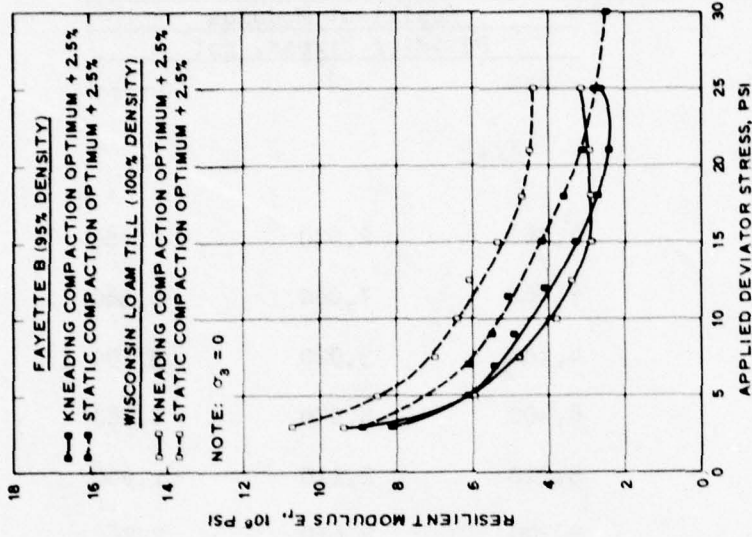


Figure 35. Relation between resilient moduli and applied stress for phase 1 soil samples compacted at optimum +2 percent moisture to 95 percent AASHO T-99 density (after Robnett and Thompson<sup>36</sup>)

Figure 36. Typical influence of compaction method on resilience (after Robnett and Thompson<sup>36</sup>)

Table 9  
Summary of Resilient Modulus Test Results (After  
Materials Research and Development<sup>21</sup>)

<u>Sample No.</u>	Resilient Modulus Deviator Stress, psi		
	<u>1</u>	<u>3</u>	<u>5</u>
<u>Fill</u>			
1L-2-2	4,050	2,930	2,780
1R-1-1	7,860	7,080	6,380
10L-1-1	4,780	3,920	3,790
10R-1-1	6,400	5,070	4,580
10R-6-1	3,210	2,110	1,900
F-1-1	3,300	2,610	2,760
<u>Bay Mud</u>			
1L-1-3	1,340	840	710
1L-2-3	810	670	650
1L-3-3	970	690	625
1L-6-2	1,280	870	785
1R-1-3	1,675	1,400	1,150
10L-1-2	2,065	1,440	1,170
10R-1-2	2,680	1,640	1,230
S-1-2	2,040	1,330	960
S-2-3	1,170	700	635

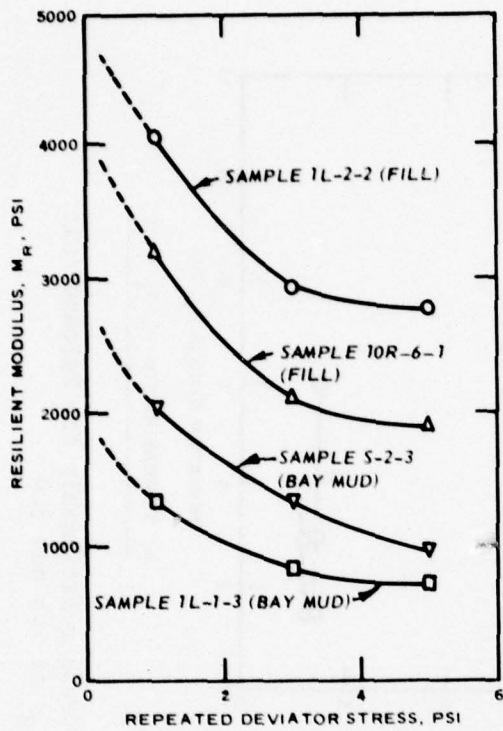


Figure 37. Typical examples of the stress sensitivity of the resilient modulus of soils (after Materials Research and Development<sup>21</sup>)

increasing the stress ratio from 1.5 to 3.0 decreased  $M_R$  for all four soil conditions. The changes in  $M_R$  with deviator stress are not consistent.  $M_R$  decreases with increases in deviator stress for curves A and C and increases with increases in deviator stress for curves B and D.

Foster and Heukelom<sup>37</sup> (E). Table 10 presents modulus values determined for six soils by Foster and Heukelom using wave velocity tests. The E values range from a low of  $80 \text{ kg/cm}^2$  to a high of  $9000 \text{ kg/cm}^2$ ; peats and clays have considerably lower values than do the more granular soils.

Yoder<sup>20</sup> (v). Yoder indicated that Poisson's ratio for a soil is a "tenuous value which has not been determined experimentally with any degree of exactitude."

Cook and Krukar<sup>11</sup> ( $M_R$ ).

Figure 38 presents two plots showing the results of repeated load triaxial compression tests on 6-in.-diam by 12-in.-high specimens, which were used in Cook and Krukar's analysis of subgrade soil (Palouse silt) under test tracks at WSU. These plots illustrate relationships of resilient modulus to deviator stress and are both for the same soil, at the same four moisture contents and densities on each. The difference between them is that the stress ratios,  $\sigma_d/\sigma_3$ , were 1.5 and 3.0 for Figures 38a and 38b, respectively. The shapes of the curves (A, B, C, and D) are nearly the same from one to the other; however, in-

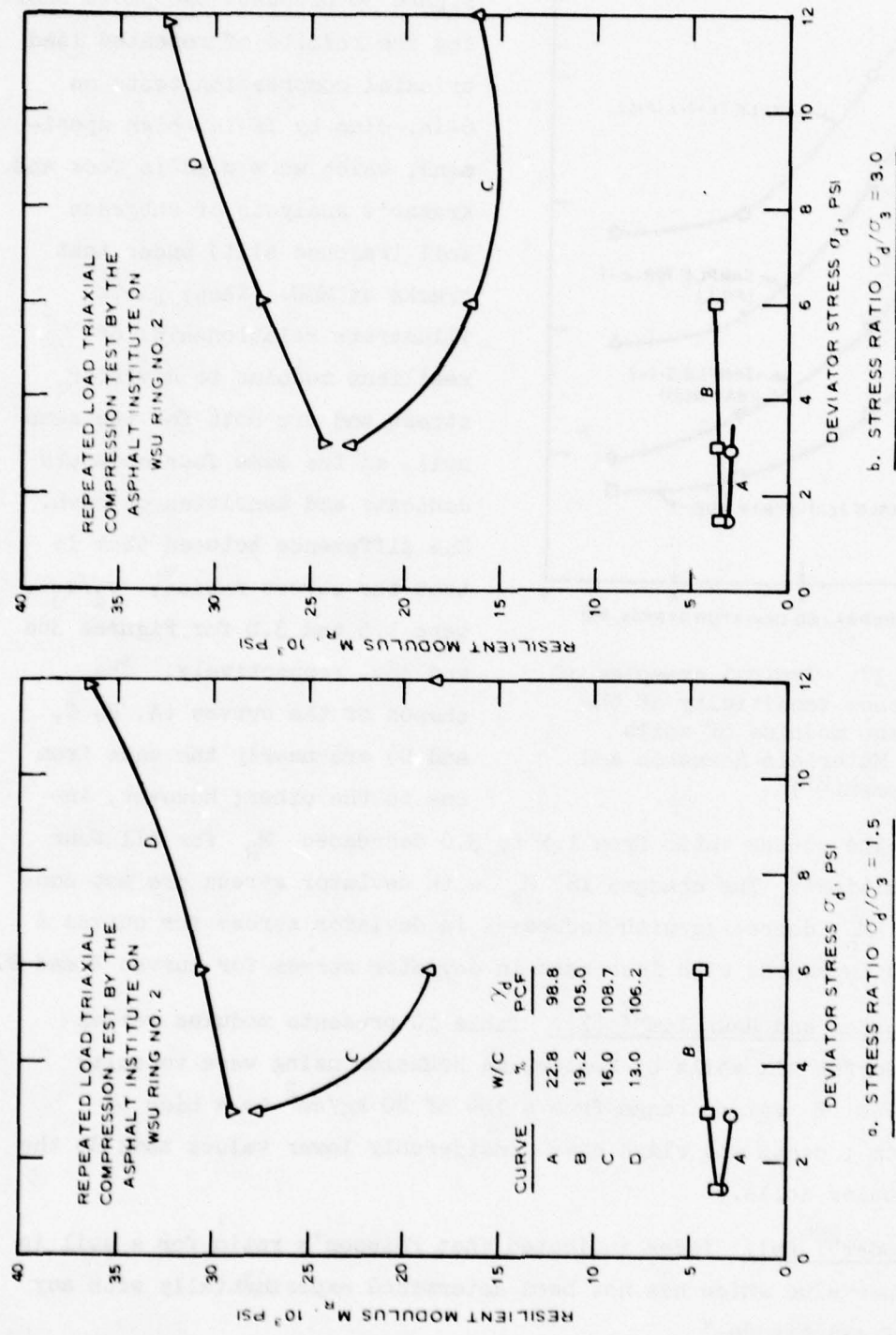


Figure 38. Resilient modulus deviator stress relationship for Palouse silt  
for stress ratios  $(\sigma_d/\sigma_3)$  of 1.5 and 3.0

Table 10  
Wave Velocities and Subgrade Modulus Values Observed on Various  
Soils (After Foster and Heukelom<sup>37</sup>)

<u>Type of Soil</u>	Wave Velocity m/sec	Subgrade Modulus, E	
		kg/cm <sup>2</sup>	psi
Peat	50-110	80-330	1,130-4,670
Clay	90-150	440-1,200	6,230-17,000
Sand	120-180	800-1,800	11,300-25,500
Sandy clay	150-200	1,200-2,200	17,000-31,100
Clay gravel	190-320	2,100-6,000	29,700-84,900
Moraine*	250-400	3,500-9,000	49,500-127,000

\* Glacial deposit.

Morgan and Scala<sup>24</sup> ( $v$ ). According to Morgan and Scala, the theoretical upper limit of 0.5 for  $v$  is appropriate to assume for a saturated clay loaded under undrained conditions. Sands should be assigned a value from 0.3 to 0.4. For first loadings, values from 0.11 to 0.91 were determined for dense sands initially loaded to high stress in a conventional triaxial test. While looking for evidence that  $v$  was influenced by stress level, they found that little work had been done on the subject. Their report indicated that Brown and Pell found no systematic variation of  $v$  with stress on a clay subgrade and that values varied randomly between 0.2 and 0.6.\*

Barkan<sup>10</sup> ( $v$ ). Working with Katsenelenbogen, Barkan studied the effects of the moisture content of clay and an admixture of clay on  $v$  in compression and in a consolidometer. Their study revealed that  $v$  does not depend on moisture content but that increasing sand content has the effect of decreasing  $v$ . They also found the average value for pure clay to be 0.50 and for clay with 30 percent sand to be 0.42. They further generalized that  $v$  is smaller for sands than for clays and

---

\* Ibid. p. 50.

suggested that  $\nu$  for clays lies close to 0.5 and for sands from 0.30 to 0.35.

Barkan calculated values of  $\nu$  of 0.3 for sands and from 0.41 to 0.43 for clays. He reported that G. I. Polrovsky computed  $\nu$  from 0.38 to 0.40 for artificially prepared clay and that Ramspeck determined values of  $\nu$  on the basis of wave velocity measurements and found values of 0.5 for moist clay, 0.44 for loess, and from 0.31 to 0.47 for sandy soils. Barkan also stated that N. A. Tsytovich recommends values from 0.15 to 0.25 for sandy soils, 0.30 to 0.35 for clay with some sand and silt, and 0.35 to 0.40 for clays.

Bowles<sup>32</sup> ( $\nu$ ). Bowles suggested the values of  $\nu$  in Table 11.

Table 11

Typical Range of Values for Poisson's Ratio,  
 $\nu$  (After Bowles<sup>32</sup>)

Type of Soil	$\nu$
Clay, saturated	0.4-0.5
Clay, unsaturated	0.1-0.3
Sandy clay	0.2-0.3
Silt	0.3-0.35
Sand (dense)	0.2-0.4
Coarse (void ratio = 0.4-0.7)	0.15
Fine-grained (void ratio = 0.4-0.7)	0.25
Rock	0.1-0.4*

\* Depends somewhat on type of rock.

These vary from 0.1 for rock and unsaturated clay to 0.5 for saturated clay.

Lysmer et al.<sup>28</sup> (G). The shear modulus of a soil can be computed from the results of Rayleigh wave velocity measurements using the following equation:

$$Y = n \sqrt{\frac{G}{\rho}}$$

where

$\gamma$  = Rayleigh wave velocity

$n$  = factor depending upon Poisson's ratio  $\nu$

$G$  = shear modulus

$\rho$  = mass density

$\rho$  and  $\nu$  must be determined by conventional means.

Lysmer et al. reported that Hardin and Drnevich studied the factors affecting the shear moduli of soils and concluded that the most significant were strain amplitude, effective mean principal stress, void ratio, number of cycles of loading, and degree of saturation of cohesive soils. Of less importance were octahedral shear stress, overconsolidation ratio, effective stress strength parameters, and time effects.

Lysmer et al. also made the following comments on the factors that influence the shear moduli of soils:

The interrelationship of the parameters is very complex and presents a difficult problem if definitive and comprehensive expressions are sought to describe the behavior of soils subjected to dynamic loading. Laboratory programs have been conducted using forced and free longitudinal, torsional, shear and triaxial compression vibratory testing. All investigations have shown that the modulus values and damping factors for soils are strongly influenced by the strain amplitude. While many of the other factors, especially confining pressure and void ratio, are of great importance in laboratory studies, in situ vibratory testing in the field has the advantage that the need to account for the influence of a majority of these parameters is eliminated. The effects of sample disturbance are also eliminated. This fact is of major importance when saturated clays are involved.

Hardin<sup>38</sup> (G). Hardin revealed that the shear modulus of soils may vary between the extreme limits of values commonly less than 1,000 psi to values greater than 50,000 psi. The relationship between shear modulus and strain level is extremely variable but can be simplified by normalization as outlined in Reference 38. The normalized values are, however, still variable because a given strain does not have the same effect on all soils or on the same soil under different states

of stress. Also, the normalized relationship is affected by percent saturation, number of cycles, and rate of loading. Table 12 gives values of maximum shear moduli for 19 different soils. The largest value is 14 times the smallest value listed in the table.

#### RELATIONSHIPS OF ELASTIC CONSTANTS TO OTHER PARAMETERS IN SOILS

Since laboratory and field procedures for directly determining elastic constants are relatively complicated and expensive, it is desirable to express the constants in terms of more conveniently measured material properties or in terms of results of more readily performed tests. Many researchers have attempted to do this, and the work of several of them (not already covered in the section of the report called "Values and Variations of Elastic Constants") is outlined (but not necessarily completely described) in the following paragraphs. No significant relationships of this type were found for wearing surfaces or treated base materials; accordingly, the following discussion pertains solely to untreated base materials and subgrade materials, i.e. soils. The elastic constant(s) discussed in a paragraph is (are) shown in parentheses at the end of the paragraph heading. Quantitative data and symbols are given in the same terms as used by the referenced authors.

#### EQUATIONS RELATING MODULUS AND STATE OF STRESS

Hicks<sup>39</sup> and Dunlap<sup>40</sup> ( $M_R$ ). Two expressions from Hicks and one from Dunlap that relate resilient modulus to the state of stress existing in a material are:

$$\underline{a.} \quad M_R = K_1 \sigma_3^2 \quad (\text{Hicks}).$$

$$\underline{b.} \quad M_R = K'_1 \theta^2 \quad (\text{Hicks}).$$

$$\underline{c.} \quad M = K''_2 + 2K''_3 \sigma_r \quad (\text{Dunlap}).$$

Table 13 lists the values of  $K_1$ ,  $K_2$ ,  $K'_1$ ,  $K'_2$ ,  $K''_1$ , and  $K''_2$ . The three factors,  $\sigma_3$ ,  $\theta$ , and  $\sigma_r$ , represent confining stress,

Table 12  
Values of Maximum Shear Modulus (After Hardin<sup>38</sup>)

<u>Soil Identification</u>	<u>Percent Saturation</u>	G max* psi
WES sand	Dry	18,830
St. John's sand	100	12,580
Air Force silty sand	33	8,050
Air Force silty clay	91	5,200
Vicksburg loess	73	12,130
Vanceburg	91	14,290
Allen	44	11,000
Kentucky 55	100	6,020
Longhorn	70	18,360
West Virginia shale	69	11,740
Virginia clay	94	11,290
Dover	86	16,810
Prestonsburg sand	47	11,220
Kirtland No. 10-36	40	12,840
Louisiana clay	100	1,350
San Francisco clay	100	4,800
Ellsworth	66	10,030
Cheeks	98	9,790
Nevada clay	99	4,940

---

\* G max = maximum shear modulus = the initial tangent modulus or secant modulus for strain amplitude  $\geq 0.00001$ .

Table 13

Material Constant Values Proposed for Various Granular  
Materials (After Hicks<sup>39</sup> and Dunlap<sup>40</sup>)

Description of Material	Constants	
Expression: $M_R = K_1 \sigma_3^{K_2}$		
	<u><math>K_1</math></u>	<u><math>K_2</math></u>
Dry, partially crushed gravel	10,094	0.580
Dry, crushed gravel	13,126	0.550
Partially saturated, partially crushed gravel	7,650	0.591
Partially saturated, crushed gravel	8,813	0.569
Saturated, partially crushed gravel	9,894	0.528
San Diego base	12,225	0.540
Gonzales Bypass base	15,000	0.480
Gonzales Bypass subbase	10,000	0.400
Morro Bay base	11,800	0.390
Morro Bay subbase	6,310	0.430
Expression: $M_R = K'_1 \theta^{K'_2}$		
	<u><math>K'_1</math></u>	<u><math>K'_2</math></u>
San Diego base	3,933	0.61
Dry, crushed gravel	2,156	0.71
Partially saturated, crushed gravel	2,033	0.67
Morro Bay subbase	2,900	0.47
Morro Bay base	3,030	0.53
Expression: $M = K''_2 + 2K''_3 \sigma_r$		
	<u><math>K''_2</math></u>	<u><math>K''_3</math></u>
Crushed limestone	4,856	390
Crushed limestone after 36,000 repetitions	37,710	1082

bulk stress that equals  $\sigma_1 + \sigma_2 + \sigma_3$ , and radial stress in a triaxial test, respectively.

Morgan and Scala<sup>24</sup> ( $E_s$ ,  $M_R$ , and  $E_t$ ). Morgan and Scala reported the following equations attributable to Brown and Pell, Seed et al., and Holden:

- a.  $E_s = 2040J_1^{0.57}$  (Brown and Pell) where  $E_s$  = calculated value of in situ secant modulus and  $J_1$  = first stress invariant =  $\sigma_1 + \sigma_2 + \sigma_3$ .
- b.  $M_R = 1900J_1^{0.61}$  (Seed et al.) where  $M_R$  = secant modulus of resiliency at a constant confining pressure determined from a triaxial test and  $J_1 = \sigma_1 + \sigma_2 + \sigma_3$ .
- c.  $E_t = a + b\sigma_{oct} - c\tau_{oct}$  (Holden) where  $E_t$  = tangent modulus of resiliency,  $a$ ,  $b$ , and  $c$  = constants,  $\sigma_{oct} = 1/3J_1 = 1/3(\sigma_v + 2\sigma_r)$  from a triaxial test, and  $\tau_{oct} = \sqrt{2/3(\sigma_v - \sigma_r)}$ . Subscripts v and r refer to vertical and radial, respectively.

Nielsen<sup>34</sup> (M). The USN Civil Engineering Laboratory (USNCEL) acknowledged Dunlap's equation relating resilient modulus to the state of stress in a material as useful to explain the response of granular soils to repeated loadings. USNCEL also pointed out that Dunlap's modulus is the slope of the initial portion of the stress-strain curve in a triaxial test and is defined as follows:

$$M = k_2 + 2k_3\sigma_r$$

where

$M$  = modulus of deformation measured in the direction of the applied stress,  $\sigma_z$

$k_2$  = modulus of deformation when  $\sigma_r = 0$

$k_3$  = constant of proportionality expressing the influence of  $\sigma_r$  on  $M$

$\sigma_r$  = radial (lateral) stress in triaxial test

Figure 39 illustrates the equation. For a single, slowly applied normal stress that continually increased until the sample fails, molding moisture and unit weight have significant influence on the deformation constants,  $k_2$  and  $k_3$ . Under repetitive stresses, these constants are

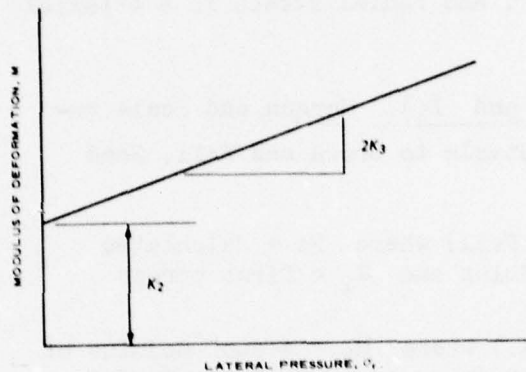


Figure 39. Relationship between modulus of deformation and lateral pressure proposed for granular material (after Dunlap<sup>40</sup>)

influenced by the number of load repetitions applied to the specimen.

Glynn and Kirwan<sup>13</sup> ( $E_r$ ). Glynn and Kirwan offer the general expression, suggested by earlier work of Barkan:

$$E_r = E_o(1 + \alpha\sigma)$$

where

$E_r$  = resilient modulus in a confined state

$E_o$  = initial modulus in an unconfined state

$\alpha$  = constant for any one soil

$\sigma$  = stress component

Wang et al.<sup>41</sup> For resilient modulus of a highly plastic soil, Wang et al. used

$$M_R = K_1 + (K_2 - \sigma_d)K_3 \quad \text{for } \sigma_d < K_2$$

$$M_R = K_1 + (\sigma_d - K_2)K_4 \quad \text{for } \sigma_d > K_2$$

where

$K_1, K_2, K_3$ , and  $K_4$  = material constants

$\sigma_d$  = deviator stress

RESILIENT MODULUS OF CLAY IN TERMS  
OF PLASTICITY INDEX (PI), DENSITY,  
AND MOISTURE CONTENT

Glynn and Kirwan<sup>13</sup> have developed a relationship between

resilient modulus, PI, moisture content, and density (Figure 40). The term  $r_w$  is the ratio of the actual moisture content to the optimum

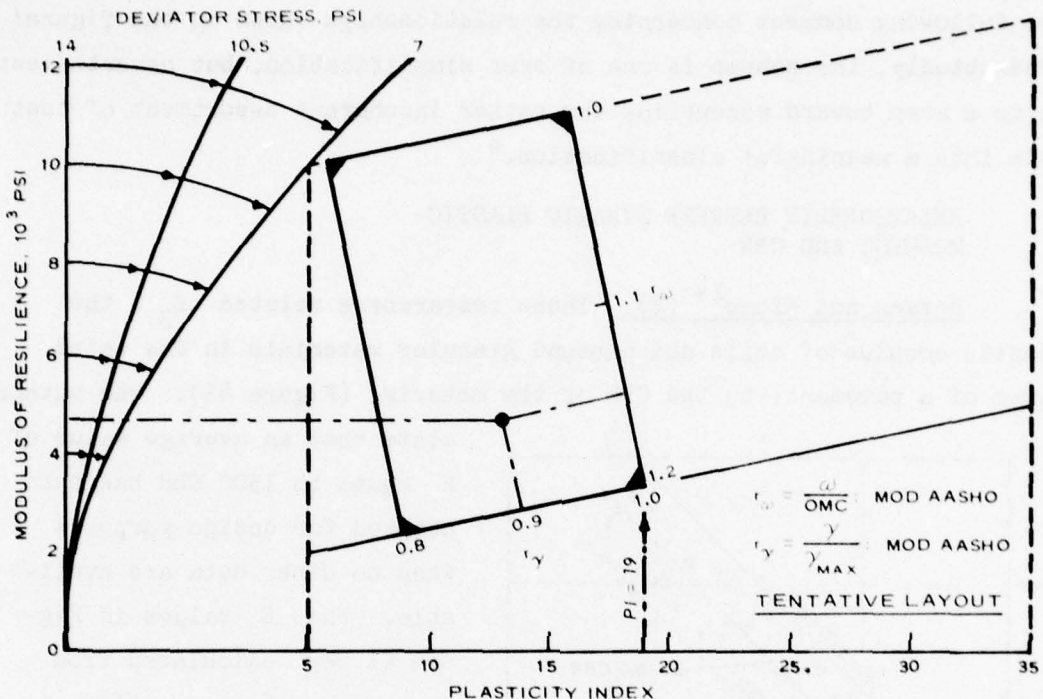


Figure 40. Dynamic stress response of clays  
(after Glynn and Kirwan<sup>13</sup>)

moisture content, and  $r_y$  is the ratio of dry density to the maximum dry density of the modified AASHO test. Glynn and Kirwan did not offer an example showing how to use Figure 40. Apparently, the rectangle on which scales for  $r_y$  and  $r_w$  are presented must be moved along the axis on which  $r_y$  is shown until the value of 1.0 for  $r_y$  lines up with the measured PI. The lines designated by long and short dashes in Figure 40 are for a clay with a PI of 19,  $r_w$  of 1.15, and  $r_y$  of 0.9. For these parameters, the modulus of resilience is approximately 4900 psi for a deviator stress of 7 psi; 4800 psi for a deviator stress of 10.5 psi; and 4700 psi for a deviator stress of 14 psi. Figure 40 is limited to deviator stresses between 7 and 14 psi, densities from 80 to 100 percent of modified AASHO, moisture contents from 100 to 120 percent of optimum, and PI's from 5 to 25. However, it is comprehensive in that a method is

suggested whereby resilient moduli can be established from fairly simple soils testing. It also considers moisture content, density, and stress, which are three major influences on resilient moduli. The authors offer the following comment concerning the relationships shown in the figure: "Undoubtedly, the scheme is one of over simplification, but nevertheless, it is a step toward assembling the rather incoherent assortment of test data into a meaningful classification."

#### RELATIONSHIP BETWEEN DYNAMIC ELASTIC MODULUS AND CBR

Dorman and Klomp<sup>14</sup> ( $E_3$ ). These researchers related  $E_3$ , the elastic modulus of soils and unbound granular materials in the third layer of a pavement, to the CBR of the material (Figure 41). The authors

state that an average value of  $E$  equal to 1500 CBR has been adopted for design purposes when no other data are available. The  $E$  values in Figure 41 were calculated from wave propagation or stiffness measurements.

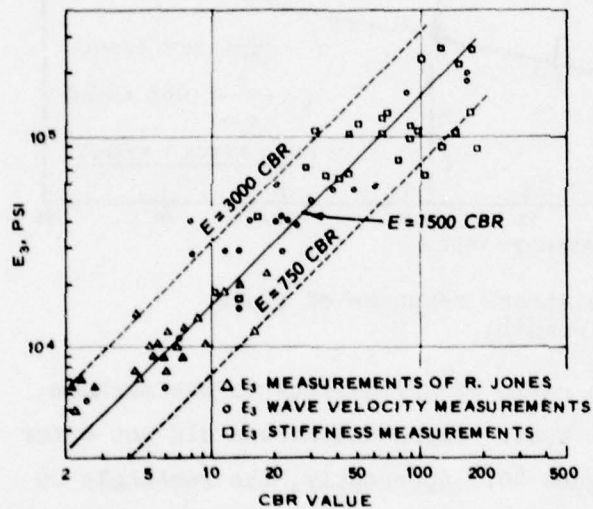


Figure 41. Relation between dynamic modulus and CBR (after Dorman and Klomp<sup>14</sup>)

stress under a pavement. They concluded from this study that no relationship existed between  $E_r$  and CBR and observed that soils of similar CBR can exhibit substantially different resiliencies.

#### RELATIONSHIP BETWEEN MODULUS OF ELASTICITY AND PLATE BEARING VALUE

The Asphalt Institute<sup>12</sup> developed an approximate relationship

Robnett and Thompson<sup>36</sup> ( $E_r$ ). These authors developed a graph, Figure 42, of soaked CBR versus resilient modulus,  $E_r$ , determined at a stress level equivalent to the calculated vertical compressive

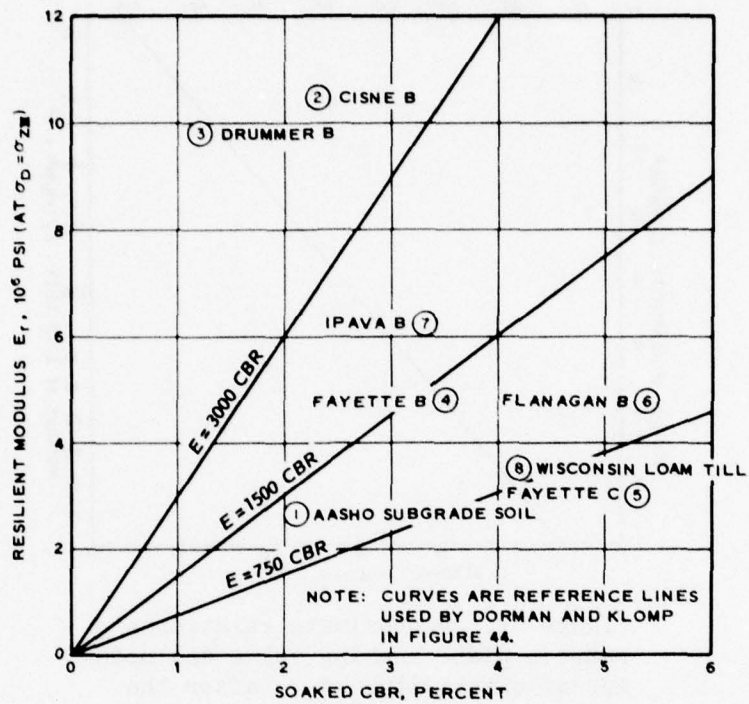


Figure 42. Resilient modulus versus soaked CBR  
(after Robnett and Thompson<sup>36</sup>)

between subgrade modulus of elasticity and bearing value (Figure 43). The plate bearing test uses a 30-in.-diam bearing plate, 0.5-in. deflection, and 10 repetitions of load. The equation of the line in Figure 43 is  $E_s$  (psi) = 480 (bearing value) - 5000.

#### EQUATION FOR SHEAR MODULUS OF SOILS

Hardin's equation for the shear modulus of gravels has been presented earlier in the report. His summary equation for the shear modulus of soils<sup>18</sup> (excluding gravels and gravelly soils) is

$$\frac{G}{G_{\max}} = \frac{1}{1 + \gamma_h}$$

with

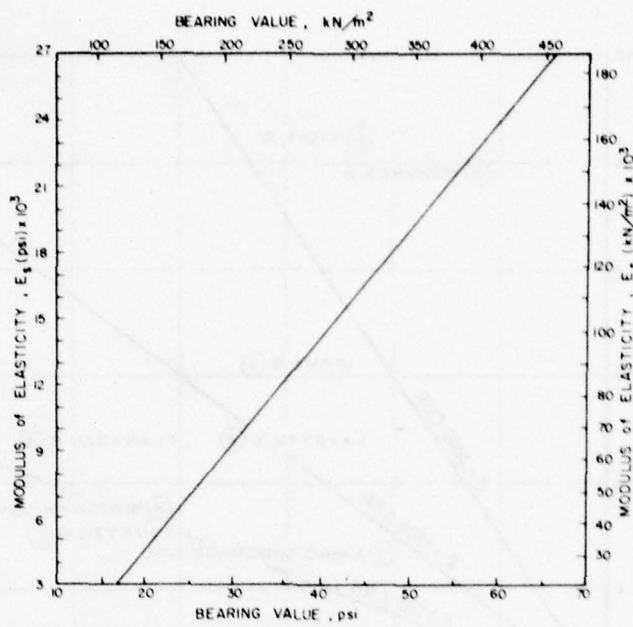


Figure 43. Approximate relationship between plate bearing value and modulus of elasticity,  $E_s$  (after the Asphalt Institute<sup>12</sup>)

$$\gamma_h = \frac{\gamma}{\gamma_r} \left[ 1 + ae_{xp} - \left( \frac{\gamma}{\gamma_r} \right)^{0.4} \right]$$

where  $\gamma_h$  = hyperbolic strain

$G$  = secant shear modulus for a given strain amplitude and cycle

$G_{max}$  = maximum shear modulus, initial tangent modulus, or secant modulus for strain amplitude  $\leq 0.00001$

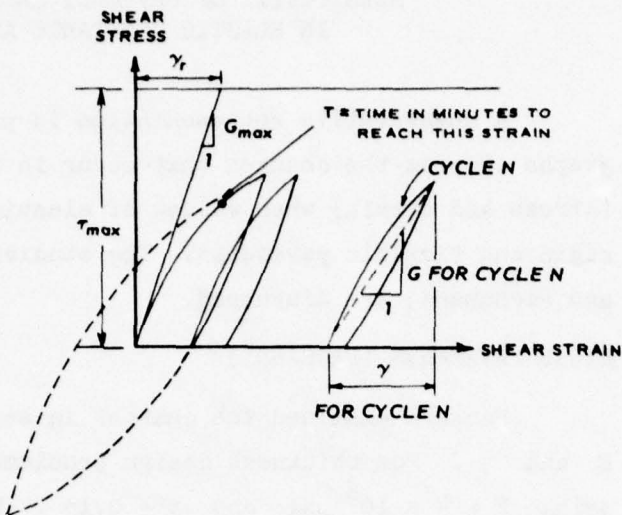
$\gamma$  = shear strain

$\gamma_r$  = reference strain =  $\tau_{max}/G_{max}$ , defined by the intersection of the initial tangent line and strength asymptote in Figure 44 and empirically related to  $G_{max}$

$e_{xp}$  = base of natural logarithms

$a$  = defined by one of the following equations, depending on the type of soil

Figure 44. Schematic single shear-stress strain relation (after Hardin<sup>18</sup>)



$$a = \begin{cases} \left[ \left( \frac{3.85}{N} \right) - 0.85 \right] T^{0.025} & \text{for clean dry sand} \\ 1.6(1 + 0.02S) \frac{T^{0.2}}{N^{0.6}} & \text{for nonplastic soils with fines and low-plasticity soils} \\ 0.2(1 + 0.2S) \frac{T^{0.75}}{N^{0.15}} & \text{for high-plasticity soils with liquid limit} > 50 \end{cases}$$

where

$N$  = number of cycles of loading

$T$  = time in minutes to reach a normalized strain equal to one

$S$  = percent saturation

For pavement evaluation, Hardin suggested that the type of soil (including PI and particle size) and  $S$  would have to be estimated from available knowledge of the subgrade or from a core sample;  $G_{max}$  would be measured by nondestructive vibratory testing;  $N$  would come from traffic records;  $\gamma$  would be determined by the finite-element analysis; and  $T$  would depend on the speed of the aircraft. (The complete procedure for determining  $G$  also requires the measurement or estimation of the void ratio,  $e$ , and involves several intermediate steps not shown in this report.)

## SENSITIVITY OF PAVEMENT RESPONSES TO CHANGES IN ELASTIC CONSTANTS AND THICKNESS

A quantitative representation is provided in the following paragraphs showing the changes that occur in values of pavement responses (stress and strain) when values of elastic constants are changed in rigid and flexible pavements. The studies of two researchers, Packard and Pichumani, are discussed.

### RIGID PAVEMENTS (PACKARD<sup>4</sup>)

Packard examined the changes in stress that occur with changes in  $E$  and  $\nu$ . For thickness design problems in PCC, Packard recommended using  $E = 4 \times 10^6$  psi and  $\nu = 0.15$ . He gave the following approximate effects of variations in  $E$  and  $\nu$  from the recommended values.

#### CHANGE IN $E$ ( $\nu = 0.15$ )

A reduction in  $E$  from 4,000,000 to 3,000,000 psi decreases the stress 5 percent. An increase in  $E$  from 4,000,000 to 5,000,000 psi increases stress 4 percent.

#### CHANGE IN $\nu$ ( $E = 4 \times 10^6$ psi)

An increase in  $\nu$  from 0.15 to 0.20 and from 0.15 to 0.25 increases stress 4 and 8 percent, respectively.

### RIGID PAVEMENTS (PICHUMANI<sup>5</sup>)

Pichumani made a parametric study of both rigid and flexible pavement systems, using the Airfield Pavement (AFPAV) Code to show the effect of input material properties on theoretical predictions of pavement response. The AFPAV Code is an analytical model based on the finite element structural analysis technique and was developed for the Air Force Weapons Laboratory (AFWL) by J. E. Crawford. The following discussion is an excerpt from Pichumani's report.

#### BASE CONDITIONS OF STUDY

Load. The load used was the static load of a C-5A aircraft, i.e., 30 kips on each wheel of a 12-wheel assembly.

Parameters Varied. Table 14 presents the rigid pavement parameter variations studied.

#### VARIATION IN E OF SURFACE COURSE

Unchanged Parameters (Table 15). In the surface course, thickness,  $h$ , was 10 in. and  $\nu$  was 0.20; in the subgrade,  $E$  was 6000 psi and  $\nu$  was 0.45. The surface course rested directly on the subgrade.

Results (Table 15). A decrease in surface course  $E$  from 6,600,000 to 3,000,000 psi resulted in an increase in surface deflection from 0.098 to 0.116 in. (18 percent).

#### VARIATION IN h OF SURFACE COURSE

Unchanged Parameters (Table 15). In the surface course,  $E$  was 6,600,000 psi and  $\nu$  was 0.20; in the subgrade,  $E$  was 6,000 psi and  $\nu$  was 0.45. The surface course rested directly on the subgrade.

Results (Table 15). When surface course  $h$  was increased from 10 to 14 in., the corresponding change in surface deflection was from 0.098 to 0.081 in. (a decrease of 17 percent).

#### VARIATION IN E OF SUBGRADE

Unchanged Parameters (Table 16). The surface course rested directly on the subgrade. The surface course  $E$  was 6,600,000 psi with  $\nu$  of 0.20 and  $h$  of 10 in.; the subgrade  $\nu$  was 0.45.

Results (Table 16). A change in subgrade  $E$  from 6000 to 3000 psi increased surface deflection from 0.098 to 0.166 in., a 69 percent increase; a further decrease of  $E$  to 1000 psi caused the deflection to increase to 0.387 in., a 295 percent increase over the deflection of 0.098 when  $E$  was 6000 psi.

#### EFFECT OF BASE COURSE

In this permutation, a base course was inserted between the surface course and the subgrade.

Unchanged Parameters (Table 17). The constant parameters were

Table 14  
Rigid Pavement Parameter Variations Studied (After Pichumani<sup>5</sup>)

Thickness h, in.	Modulus of Elasticity, E psi	Surface Course Parameters		Layer	Subgrade Parameters		Poisson's Ratio $\nu$
		Poisson's Ratio $\nu$	Poisson's Ratio $\nu$		Thickness h, in.	Modulus of Elasticity E, psi	
10.0	6,600,000	0.20	1	600	6,000	6,000	0.45
10.0	5,000,000	0.20	1	600	6,000	6,000	0.45
10.0	3,000,000	0.20	1	600	6,000	6,000	0.45
10.0	6,600,000	0.20	1	600	6,000	6,000	0.45
12.0	6,600,000	0.20	1	600	6,000	6,000	0.45
14.0	6,600,000	0.20	1	600	6,000	6,000	0.45
10.0	6,600,000	0.20	1	600	6,000	6,000	0.45
10.0	6,600,000	0.20	1	600	3,000	3,000	0.45
10.0	6,600,000	0.20	1	600	1,000	1,000	0.45
10.0	6,600,000	0.20	1	12	24,000	24,000	0.35
10.0	6,600,000	0.20	2	588	6,000	6,000	0.45
10.0	6,600,000	0.20	1	18	36,000	36,000	0.35
10.0	6,600,000	0.20	2	582	6,000	6,000	0.45
				24	60,000	60,000	0.35
				576	6,000	6,000	0.45

Table 15  
Effect of Parameter Variations in Surface Course on Rigid Pavement Deflection (After Pichumani<sup>5</sup>)

<u>Parameters</u>		<u>Maximum Elastic Surface Deflection, in.</u>	<u>Remarks</u>
<u>E , psi</u>	<u>h , in.</u>		
6,600,000	10	0.098	
5,000,000	10	0.105	E modulus only varied
3,000,000	10	0.116	
6,600,000	10	0.098	
6,600,000	12	0.088	Thickness, h , only varied
6,600,000	14	0.081	

Note: The surface course rested directly on the subgrade; the E modulus and Poisson's ratio of the subgrade were 6000 psi and 0.45, respectively.

Table 16  
Effect of Parameter Variations in Subgrade on Rigid Pavement Deflection (After Pichumani<sup>5</sup>)

<u>Parameters</u>		<u>Maximum Elastic Surface Deflection</u>
<u>E</u>	<u>v</u>	<u>in.</u>
<u>psi</u>		
6,000	0.45	0.098
3,000	0.45	0.166
1,000	0.45	0.387

Note: The surface course with E modulus = 6,600,000 psi and Poisson's ratio, v , = 0.20 rested directly on the subgrade.

Table 17

Effect of Base Course on Rigid Pavement Response  
(After Pichumani<sup>5</sup>)

Parameters			Maximum Elastic Surface Deflection in.
<u>h</u> , in.	<u>E</u> , psi	<u>v</u>	
12	24,000	0.35	0.093
18	36,000	0.35	0.090
24	60,000	0.35	0.084

Note: The surface course parameters were  $E$  modulus = 6,600,000 psi, Poisson's ratio,  $v$ , = 0.20, and thickness,  $h$ , = 10 in.; the subgrade parameters were  $E$  = 6,000 psi and  $v$  = 0.45.

$E$  = 6,600,000 psi,  $v$  = 0.20, and  $h$  = 10 in. for the surface course;  $E$  = 6,000 psi and  $v$  = 0.45 for the subgrade; and  $v$  = 0.35 for the base course.

Results (Table 17). Variations were made in  $E$  and  $h$  of the base course. When the subgrade  $E$  was 24,000 psi and its  $h$  was 12 in., the surface deflection was 0.093 in. This value is only slightly lower than in the comparable "no base course" case (0.098 in.). When the base course  $E$  was 60,000 psi and its  $h$  was 24 in., the resulting pavement response (0.084 in.) was very close to the 0.081-in. deflection in the no base course case where the  $E$  of the surface course was the same (6,600,000 psi), but its  $h$  was 4 in. thicker, i.e. 14 in. thick (compare bottom data line of Table 17 with bottom data line of Table 15).

#### FLEXIBLE PAVEMENTS (PICHUMANI<sup>5</sup>)

##### BASE CONDITIONS OF STUDY

Load. The load was the same as for the rigid pavement study, i.e. the static load of a C-5A.

Parameters Varied. Table 18 lists the values of  $E$ ,  $v$ , and  $h$  in the surface course, base course, subbase, and subgrade assumed as

Table 18  
Assumed Layer Properties of Flexible Pavement  
(After Pichumani<sup>5</sup>)

Layer	E Modulus psi	Poisson's Ratio, $\nu$	Thickness h, in.
Surface course	150,000	0.25	3
Base course	50,000	0.30	6
Subbase	25,000	0.35	24
Subgrade	5,000	0.45	$\infty$

reference values in this study. Table 19 presents the variations of these values studied. Only the value of one parameter in one layer was varied for each permutation. All other values remained the same as given in Table 18.

#### EFFECT OF E IN EACH LAYER

Tables 20 and 21 show that the surface elastic deflections were not changed significantly by variations in the E modulus of the surface course, base course, and subbase within the range of values presented in Table 19. However, Table 22 indicates that variations in Young's modulus of the subgrade affected the surface deflection very significantly. For example, a 67 percent reduction in the E modulus of the surface course (i.e. from 1,500,000 to 500,000 psi) resulted in an increase of only 8 percent in surface deflection (from 0.157 to 0.170 in.), while a 50 percent reduction in the subgrade E modulus (from 5,000 to 2,500 psi) increased the surface deflection by more than 60 percent (from 0.183 to 0.299 in.).

Pichumani observed that even though the E modulus values of the base course and subbase may not be very significant for surface elastic deflections, they are very important in determining the state of stress in the upper layers of the pavement system. Therefore, it is necessary to determine the E moduli of the various layers as accurately as possible since structural failure of the pavement system can be caused

Table 19  
Flexible Pavement Parameter Variations Studied  
(After Pichumani<sup>5</sup>)

<u>Layer</u>	<u>Parameter Varied</u>	<u>Symbol</u>	<u>Unit</u>	<u>Values of Parameter Varied</u>		
Surface course	E		psi	1,500,000; 500,000; 150,000		
Surface course	v		--	0.20;	0.25;	0.30
Surface course	h		in.	3.0;	4.5;	6.0
Base course	E		psi	75,000; 50,000; 37,500		
Base course	v		--	0.25;	0.30;	0.35
Base course	h		in.	6.0;	9.0;	12.0
Subbase	E		psi	37,500; 25,000; 12,500		
Subbase	v		--	0.30;	0.35;	0.40
Subbase	h		in.	15.0;	24.0;	33.0
Subgrade	E		psi	5,000; 2,500; 1,250		
Subgrade	v		--	0.40;	0.45;	0.495
Existing ground profile	E		psi	5,000; 50,000; 500,000		

Note: E = modulus of elasticity ; v = Poisson's ratio ; h = layer thickness.

Table 20  
Effect of Parameter Variations in Surface Course  
on Flexible Pavement Deflection  
(After Pichumani<sup>5</sup>)

Parameters			Maximum Elastic Surface Deflection		Remarks
E , psi	v	h , in.	in.		
1,500,000	0.25	3.0	0.157	E modulus only varied	
500,000	0.25	3.0	0.170		
150,000	0.25	3.0	0.183		
150,000	0.20	3.0	0.183	Poisson's ratio, v , only varied	
150,000	0.25	3.0	0.183		
150,000	0.30	3.0	0.182		
150,000	0.25	3.0	0.183	Thickness, h , only varied	
150,000	0.25	4.5	0.174		
150,000	0.25	6.0	0.168		

Note: The properties of the other layers are given in Table 18.

Table 21  
Effect of Parameter Variations in Base Course  
and Subbase on Flexible Pavement Deflection  
(After Pichumani<sup>5</sup>)

Parameters			Maximum Elastic Surface Deflection in.	Remarks
E , psi	v	h , in.		
<u>Base Course</u>				
37,500	0.30	6	0.187	E modulus only varied
50,000	0.30	6	0.183	
75,000	0.30	6	0.178	
50,000	0.25	6	0.183	Poisson's ratio, v , only varied
50,000	0.30	6	0.183	
50,000	0.35	6	0.182	
50,000	0.30	6	0.183	Thickness, h , only varied
50,000	0.30	9	0.174	
50,000	0.30	12	0.167	
<u>Subbase</u>				
12,500	0.35	24	0.207	E modulus only varied
25,000	0.35	24	0.183	
37,500	0.35	24	0.171	
25,000	0.30	24	0.182	Poisson's ratio, v , only varied
25,000	0.35	24	0.183	
25,000	0.40	24	0.183	
25,000	0.35	15	0.197	Thickness, h , only varied
25,000	0.35	24	0.183	
25,000	0.35	33	0.168	

Note: The properties of the other layers are given in Table 18.

Table 22  
Effect of Parameter Variations in Subgrade on Flexible  
Pavement Deflection (After Pichumani<sup>5</sup>)

Parameters		Maximum Elastic Surface Deflection in.	Remarks
E , psi	v		
5,000	0.450	0.183	E modulus only varied
2,500	0.450	0.299	
1,250	0.450	0.493	
5,000	0.400	0.215	Poisson's ratio, v , only varied
5,000	0.450	0.183	
5,000	0.495	0.141	

Note: The properties of the other layers are given in Table 18.

by critical load stresses exceeding the inherent strength of the pavement materials.

#### EFFECT OF v IN EACH LAYER

Tables 20 and 21 show that surface deflections were not significantly affected by v of the surface course, base course, or subbase for the range of thicknesses studied; however, Table 22 shows that v of the subgrade influenced the deflections significantly. A v of 0.40 for the subgrade gave a maximum surface deflection of 0.215 in., while a v of 0.495 gave a maximum deflection of only 0.141 in.

#### EFFECT OF h IN UPPER LAYERS

Increasing the thicknesses of the upper pavement layers (i.e., the surface course (Table 20), base course (Table 21), and subbase (Table 21)) decreased the surface deflections. For example in Table 21, when the subbase thickness (originally 24 in.) was altered to 15 and 33 in., an increase of 8 percent (0.183 to 0.197 in.) and a decrease of 8 percent (0.183 to 0.168 in.) in surface deflection, respectively, resulted.

#### EFFECT OF E OF EXISTING GROUND

In the finite element idealization of the pavement system, the total depth of the pavement structure was assumed to be 50 ft, and the subgrade was considered to have a constant E modulus. The total built-up depth of an existing WES flexible pavement test section was only 12 ft. All other parameters of the WES section were exactly the same as assumed by Pichumani in this exercise. The E modulus of the ground below the built-up subgrade was not known. However, based on the reported CBR value of 2 to 4, the E modulus of the ground was assumed to be the same as that of the subgrade. To illustrate the importance of knowing the E modulus of the existing ground below a depth of 12 ft, a parametric study assuming three different moduli values (5,000, 50,000, and 500,000 psi) was conducted. The maximum surface deflection of 0.183 in. with an E modulus of 5,000 psi was reduced by one third to 0.121 in. when the existing ground was assumed to have an E modulus of 50,000 psi. An E modulus of 500,000 psi below 12 ft further reduced the maximum surface deflection to 0.108 in., a reduction of about 40 percent. Therefore, it appears that it is necessary to determine the properties of the pavement system to an appreciable depth.

## RELATIONSHIPS BETWEEN VIBRATORY TEST RESULTS AND ELASTIC CONSTANTS

In the following paragraphs, brief discussions are given of the principal mathematical models of pavement response to vibratory tests, vibrator wave patterns, comments on relating vibrator results and elastic constants, extrapolation of constants from low to high stress levels, and results of preliminary studies to establish a relationship between the WES 16-kip vibrator test results and elastic modulus.

### MATHEMATICAL MODELS

In the study of how the elastic constants of  $E$ ,  $v$ , or  $G$  are to be extracted from vibratory test results, it is obviously desirable to know how the soil or pavement is affected by the vibratory load. The two types of models that describe the response are the lumped mass model and the linear elastic half-space model. The primary difference between these two models is that the former one assumes that there is a finite mass of soil, which acts as a spring for the foundation and vibrates together with it, while the latter model assumes no finite mass of soil. Several particular models that fit into one of these two types are described briefly in the following paragraphs.

#### LINEAR LUMPED MASS MODEL (TSCHEBOTARIOFF<sup>42</sup>)

For the lumped mass model, Tschebotarioff presented the equation

$$f_n = \frac{1}{2\pi} \sqrt{\frac{K'Ag}{W_s + W_v}}$$

where

$f_n$  = natural frequency of system

$K'$  = dynamic modulus of soil reaction, or volume spring coefficient

$A$  = contact area between base of foundation and soil

$g$  = acceleration of gravity

$W_s$  = weight of vibrating soil

$W_v$  = weight of vibratory loading device

Figure 45 shows the conditions of loading, and Figure 46 illustrates how the soil vibrates together with the vibrator. Tschebotarioff offers that there cannot be a clearly defined limit for the soil mass  $W_s$  as indicated by Figure 45. Figure 46 shows that the motions of the soil are more complex than the motion of the vibrator. He suggests that the term  $W_s$  should be considered as referring to an equivalent weight of soil with no clearly defined physical boundaries.

The pertinent point to be made by the equation for  $f_n$  is that the elastic constants of the soil are assumed present in the terms  $W_s$  and  $K'$ ; however, the process by which they can be extracted from this simple model, which is for a single-mass system and assumes no damping, is not clear. Then, of course, the equation assumes a homogeneous soil mass. Working with a layered pavement system obviously renders the system much more complicated.

#### LINEAR LUMPED MASS MODEL (YANG<sup>43</sup>)

Yang uses the linear spring-mass-dashpot model to describe the frequency sweep measurements done with a vibrator. He computes an effective  $E$  value for the entire pavement and subgrade system by calculating the area under the measured frequency response curve. By neglecting damping and inertial terms, he arrives at the following expression for the  $E$  modulus:

$$E = \frac{1}{2a} \left( \frac{1}{\frac{1}{2F} \int_1^{\infty} \frac{z(\mu)}{\mu} d\mu} \right)$$

where

$a$  = radius of vibrator baseplate

$F$  = force amplitude

$z(\mu)$  = peak-to-peak response

$\mu$  = ratio of frequency to natural frequency

Yang applies the single lumped-mass spring model, which exhibits only one resonance peak, to the entire multipeaked frequency response spectrum.

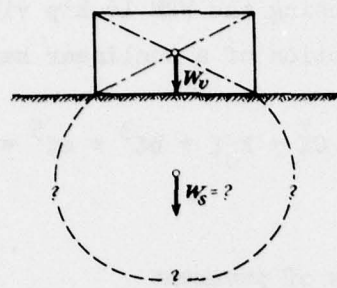


Figure 45. Sketch illustrating the equation

$$f_n = 1/2\pi \sqrt{K'Ag/W_s + w_v}$$

(after Tschebotarioff<sup>42</sup>)

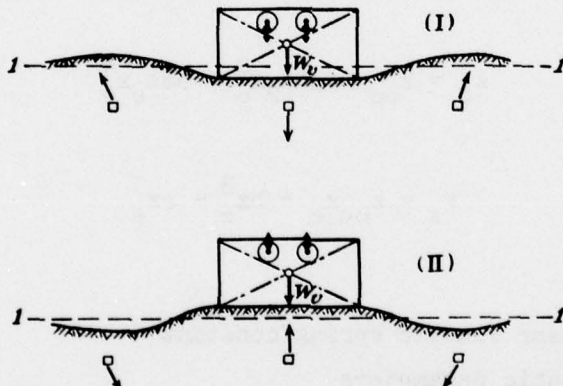


Figure 46. Probable nature of the soil-surface deformation around a vibrator inducing vertical oscillations (after Tschebotarioff<sup>42</sup>)

## NONLINEAR LUMPED MASS MODEL WEISS<sup>2</sup>

In his study of the dynamic stiffness of pavements, Weiss developed a nonlinear model that describes the response of pavement systems to vibratory loading. The nonlinear dynamic load-deflection curves that are measured using the WES 16-kip vibrator are described by solving the equation of motion of a nonlinear harmonic oscillator

$$m\ddot{\xi} + C\ddot{\xi} + k_o\xi + b\xi^3 + e\xi^5 = F_D$$

where

$m$  = effective mass of pavement

$\xi$  = dynamic deflection of the pavement surface

$C$  = damping constant

$k_o$  = spring constant that depends on static load of vibrator

$b$  = third-order nonlinear plastic parameter

$e$  = fifth-order nonlinear elastic parameter

$F_D$  = dynamic load

The spring constant  $k_o$  is related to the static load by the equations

$$k_o = k_{oo} + 3be_2x_e^2 + 5e_4x_e^4$$

$$F_s = k_{oo}x_e + bx_e^3 + ex_e^5$$

where

$k_{oo}$  = linear elastic spring constant

$e_2, e_4$  = elastic parameters

$x_e$  = static elastic deflection of pavement surface beneath the vibrator baseplate

$F_s$  = static load of vibrator

The elastic constants appear in the expressions for the elastic parameters  $k_{oo}$ ,  $b$ , and  $e$ . For example, for a subgrade the expression for the parameter  $k_{oo}$  is

$$k_{oo} = \frac{2\pi a^2 Q_1 G_1 \Psi}{l_o}$$

where

$k_{oo}$  = linear elastic parameter of a nonlinear pavement

$a$  = radius of the vibrator baseplate

$Q$  = function of Poisson's ratio

$G$  = shear modulus of homogeneous elastic half-space

$\Psi$  = expansion parameter

$l_o$  = finite depth of influence of the static strain field

More general expressions for  $k_{oo}$ ,  $b$ , and  $e$  for the case of a layered pavement appear in Reference 2. Weiss's procedure was developed to describe the measured nonlinear dynamic load-deflection curves. However, Weiss<sup>3</sup> has also developed a linear model of the frequency response spectrum while a nonlinear model of the frequency response spectrum is under study. The linear model is found to be inadequate to describe the frequency response spectrum.

The nonlinear dynamical theory of Weiss can also be applied to the laboratory resilient modulus measurement.<sup>3</sup> This theory gives an analytical expression for the resilient modulus in terms of the dynamic deviator stress, static confining pressure, frequency, and a set of basic soil parameters including the Young's modulus. The nonlinear dynamical theory can be used to extract the static elastic Young's modulus value from the measured dynamic resilient modulus.

#### FINITE ELEMENT ELASTIC HALF-SPACE MODEL (WAAS<sup>44</sup>)

Waas has developed a finite element computer program that calculates the response of a foundation resting on a linear layered elastic half-space to a dynamic load applied to the top of the foundation. A rigid lower layer is required by the finite element approach. By this method, torsional and vertical vibrations of circular footings on, or embedded in, homogeneous and inhomogeneous soil or pavement layers over rock are studied. The approach is a numerical method for layered

elastic media, which extends the earlier result of Lysmer<sup>45</sup> for the homogeneous elastic half-space.

The method assumes that the equation of motion to be solved for each finite element is

$$\ddot{m\mu} + C\dot{\mu} + k\mu = \underline{P}(t)$$

where

$m$  = mass of finite element

$\mu$  = displacement of a nodal joint

$C$  = viscoelastic damping constant

$k$  = spring constant

$\underline{P}$  = driving force

$t$  = time

The displacements, damping constants, masses, and spring constants of the finite element nodes are collected into a displacement matrix ( $\mu$ ), a mass matrix ( $m$ ), and a stiffness matrix ( $k$ ). The stiffness matrix is complex because it includes the viscoelastic effects, i.e., it includes both  $k$  and  $C$ . The matrix form of the equations of motion are solved subject to the boundary conditions imposed by the particular program. The result is a theoretical frequency response spectrum that depends on the values of the elastic moduli of the layered system and on the depth of the lower rigid layer.

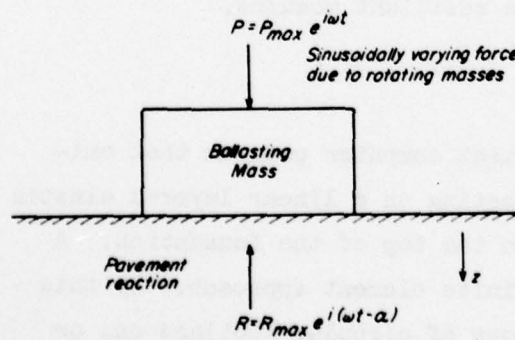


Figure 47. Schematic of force system for Royal Dutch Shell Machine (after Lysmer et al.<sup>28</sup>)

#### LINEAR ELASTIC HALF-SPACE MODEL (LYSMER ET AL.<sup>28</sup>)

A linear elastic half-space model was advanced by Lysmer et al. in their development of a nondestructive pavement evaluation method based on the wave propagation method.

Figure 47 shows the idealized system assumed for the half-space

model. Pertinent equations are as follows:

$$P = P_{\max} e^{i\omega t}$$

$$R = R_{\max} e^{i(\omega t - \alpha)}$$

$$z = z_{\max} e^{i(\omega t - \beta)}$$

where

P = force due to rotating masses

e = base of natural logarithms

i = -1

$\omega$  = angular frequency of rotating masses

t = time

R = pavement reaction

$\alpha$  = phase lag of R behind P

z = deflection of pavement under center of loading

$\beta$  = phase lag of z behind P

The elastic constants in the half-space model are contained in the  $R_{\max}$  and  $\alpha$  terms in a very complex relationship developed by Lysmer.

#### VIBRATOR WAVE PATTERNS

The motion of the soil or pavement surface in direct contact with a vibratory baseplate is in phase with the plate and vibrates with it; however, the soil motion is out of phase and complicated at positions away from the plate. Additional comments on vibrator wave patterns are given below.

#### LYSMER ET AL.

Lysmer et al.<sup>28</sup> stated that two wave types can exist in elastic media, dilational (P-waves) and rotational (S-waves or shear waves). Under special conditions, the two basic wave types combine to form other waves with special names, such as Rayleigh waves, Love waves, and Stonely waves.

## BARKAN AND WES

Barkan<sup>10</sup> disclosed that when a vibrator is placed on the soil and vibrates as a solid body with one degree of freedom, then theoretically the resonance curve of the forced vertical vibrations has a maximum. However, measured resonance curves have several peaks. This phenomenon of multiple peaks is exhibited in Figure 48, which shows graphs of deflection versus frequency for nine test sites, all on rigid pavements. Data for these graphs were collected using the WES 16-kip vibrator at a constant dynamic load of 10 kips. Within the given frequency range of 5 to 100 Hz, five or six peaks are generally apparent. Barkan says that some investigators explain these multiple peaks by coincidences of the natural frequencies of the soil layers and the frequencies of propagating waves.

## WES

Figure 49 shows a comparison of pressures on a pavement surface created by a wheel of a 727 aircraft and the WES 16-kip vibrator. The pressure over a point created by the aircraft builds up from zero as the tire begins to approach the point, reaches a maximum of 172 psi as the center of the tire is over the point, and decreases back to zero as the tire leaves the point. The pressure created by the vibrator is a combination of static and dynamic pressures. When the load mass is lowered to the pavement, a static pressure of 63 psi is created. If the dynamic load is 15 kips, the resulting total maximum pressure is 122 psi and the minimum pressure is 4 psi. The maximum surface pressure that can be created by the vibrator is 71 percent of the pressure of one wheel of the 727 aircraft (122 psi : 172 psi). To duplicate the time that a point is loaded by the 727 moving at 20 mph, the vibrator must be operated at a frequency of approximately 17 Hz; however, the vibrator cannot be operated for one cycle of loading, which would simulate the passage of an aircraft, due to mechanical and control limitations. Also, only the pavement response to the dynamic load can be measured with the existing system that uses velocity transducers.

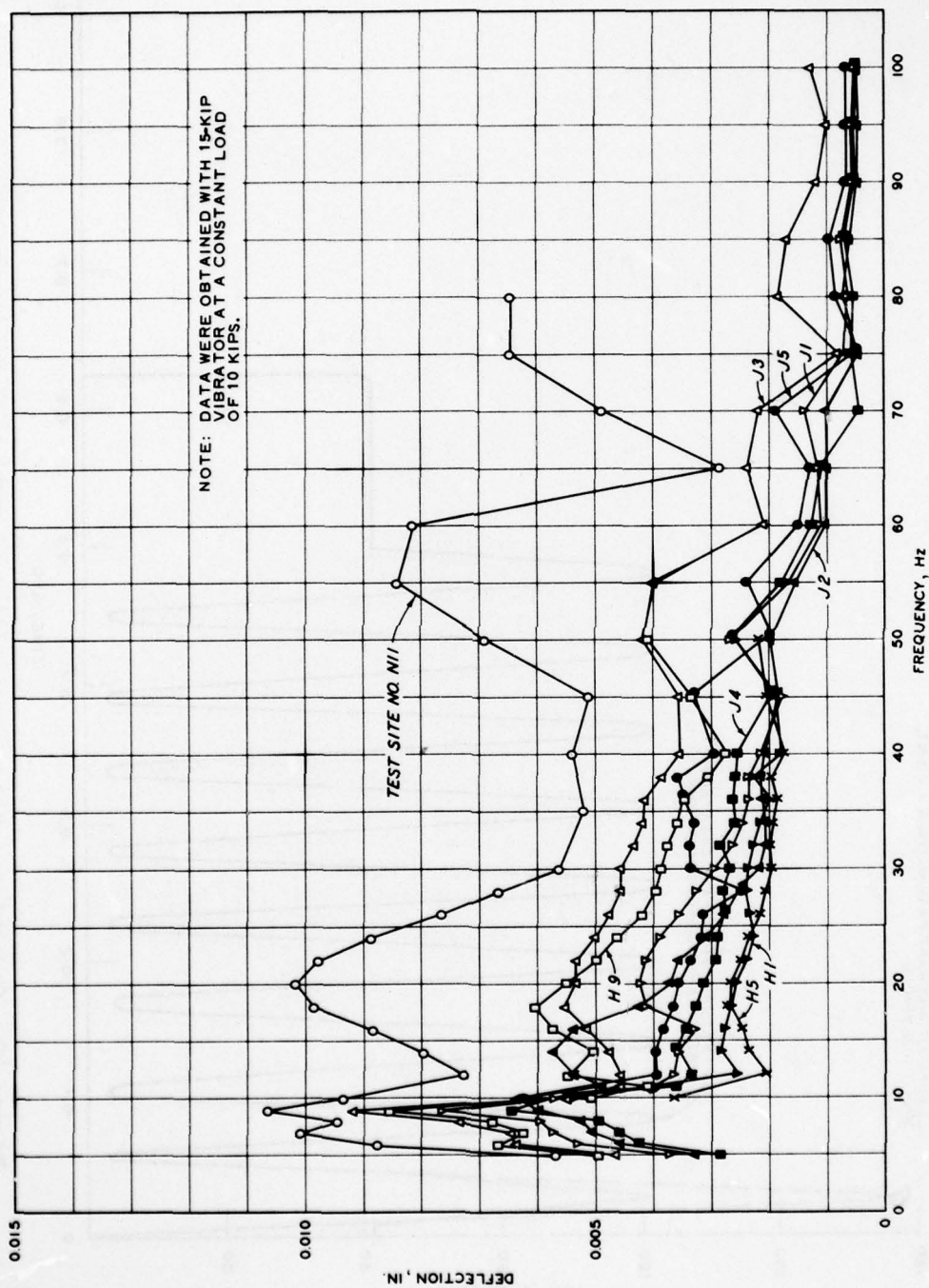


Figure 48. Deflection versus frequency for rigid pavements

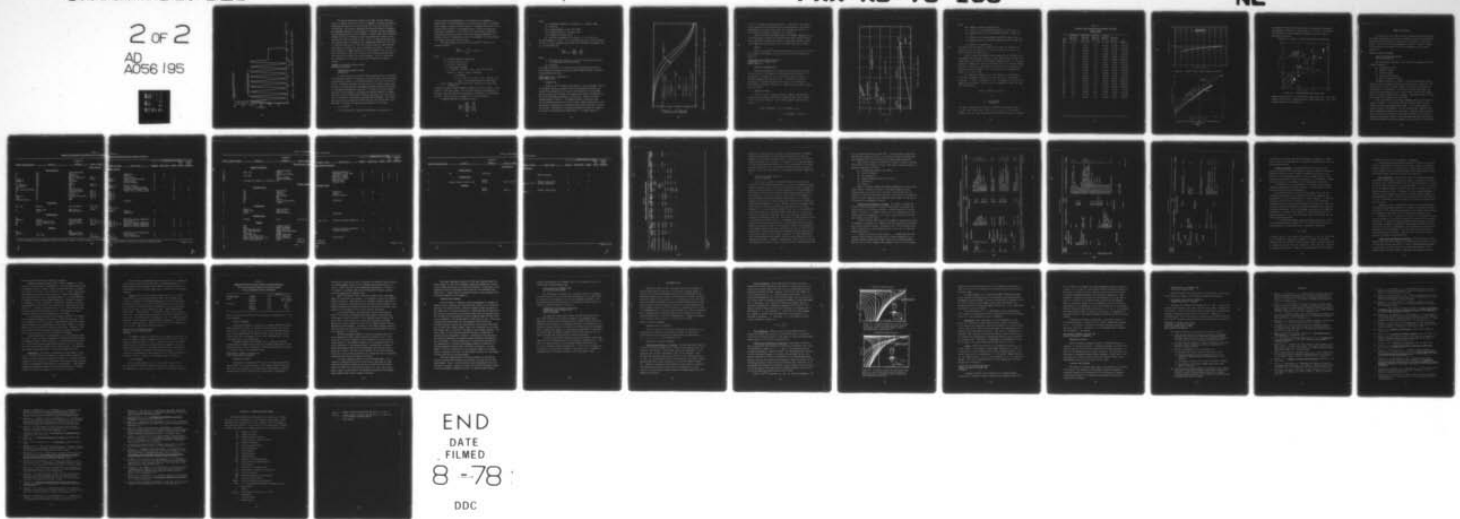
AD-A056 195 ARMY ENGINEER WATERWAYS EXPERIMENT STATION VICKSBURG MISS F/G 1/5  
LITERATURE REVIEW - ELASTIC CONSTANTS FOR AIRPORT PAVEMENT MATE--ETC(U)  
MAR 78 J L GREEN DOT-FA73WAI-377

UNCLASSIFIED

2 of 2  
AD  
A056 195

FAA-RD-76-138

NL



END  
DATE  
FILED  
8-78  
DDC

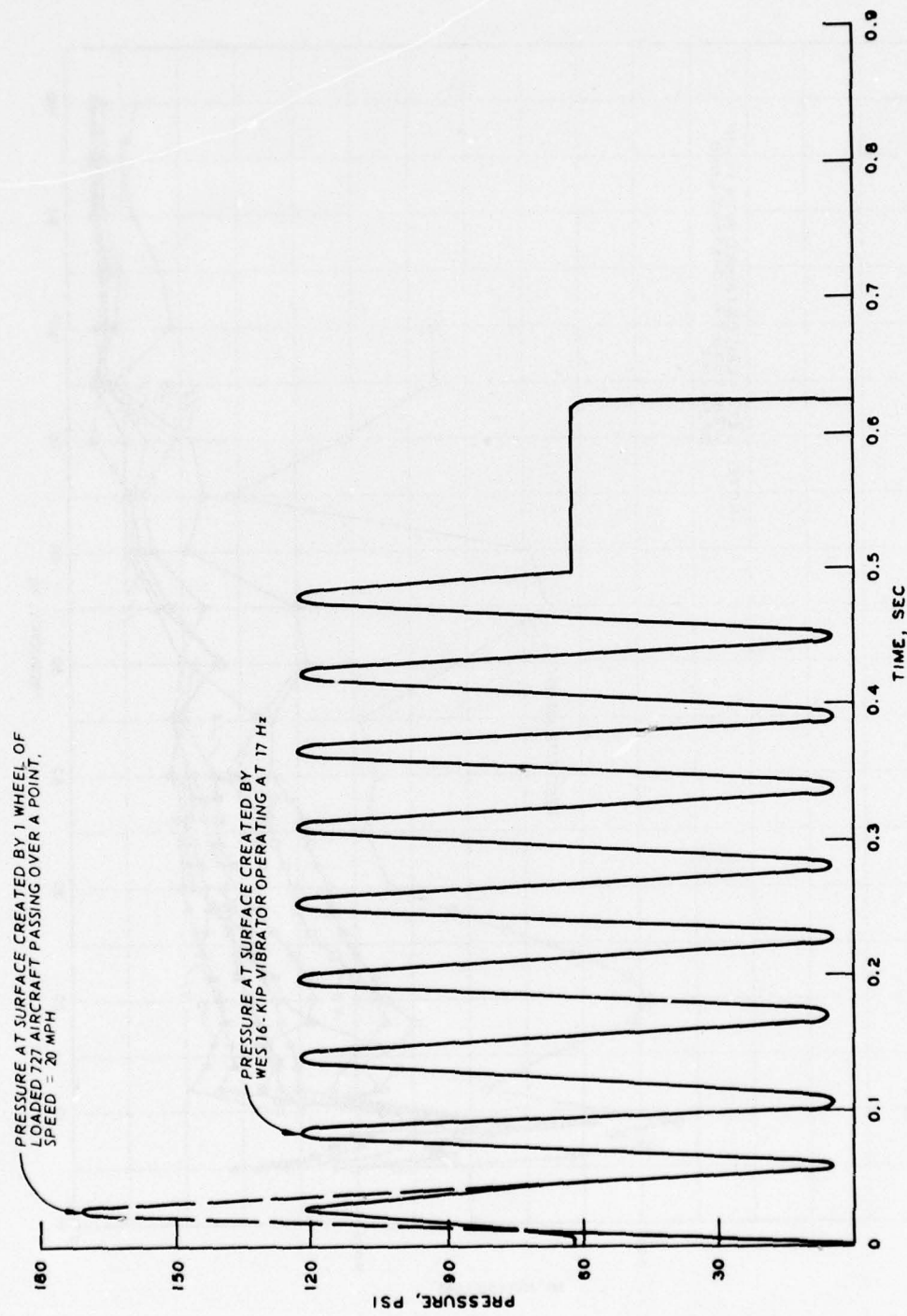


Figure 49. Comparison of pressure created by 727 aircraft and WES vibrator

The surface pressures created by one wheel of most other aircraft are smaller than for the 727; for example, the surface pressures created by one wheel of the DC-9 and the 737 in psi are 165 and 151, respectively. The tests to determine the resilient moduli of pavement and subgrade materials can be designed to reproduce the axial pressures created by any aircraft or the vibrator. However, there are differences between the state of stresses in the field under the vibrator or aircraft and the resilient modulus test. First, in resilient modulus testing, the specimen is confined in the longitudinal direction, and stress is constant at any point in the test specimen; however, under the aircraft and the vibrator, the stress attenuates with depth. Secondly, the confining, or chamber pressure, in the resilience tests can be carefully controlled to any level; however, the confining pressures under the aircraft and vibrator can only be assumed. Little is known about the configuration or the mass of the soil influenced by vibratory loading.

#### COMMENTS ON RELATING VIBRATOR RESULTS AND ELASTIC CONSTANTS

#### TRANSPORTATION RESEARCH BOARD CONFERENCE<sup>46</sup>

At the Transportation Research Board Conference held in September 1973, discussion group C reviewed the 10 overlay design procedures based on deflection, curvature, or stiffness known to be in use in the United States. The group concluded that priority one in research needs should be given to establishing the "fundamental deflection basin relationship to performance and material properties." Further, the group observed that most of the evaluation procedures had several features in common, but none of the procedures was universally applicable due to the variations in materials, environment, and measuring techniques. They found that users of the procedures believed that they had insufficient feedback data to validate and improve the procedures at that time.

#### A. J. SCALA<sup>47</sup>

In his discussion of Cogill's presentation on utilization of

surface deflection measurements in the evaluation of highways, A. J. Scala states: "The interpretation of the deflection bowl of a pavement under loading in terms of elastic moduli or strength coefficients of the various layers would be of inestimable value in both the design and evaluation of pavements." He further lists four pertinent references (Texas Transportation Institute, Utah State Highway Department, N. I. Viswani, and C. P. Valkering) of which he recommended the Texas system as the most useful model at that time.

The Texas Transportation Institute system<sup>48</sup> is based on the Burmister equation

$$\frac{4\pi E_1}{3P} wr = \int_{x=0}^{\infty} v \cdot J_0(x) dx$$

where

$E_1$  = Young's modulus of upper layer

P = vertical load at point 0

w = vertical displacement

r = cylindrical coordinate

$v = 1 + 4Nm e^{-2m} - N^2 e^{-4m}/1 - 2N(1 + 2m^2)e^{-2m} + N^2 e^{-4m}$ ,

where e = base of natural logarithms

m = parameter

$N = (1 - E_2/E_1)/(1 + E_2/E_1) = (E_1 - E_2)/(E_1 + E_2)$

where  $E_2$  = Young's modulus of lower layer

$J_0(x)$  = Bessel function of the first kind and zero order with argument x

A computer program, ELASTIC MODULUS, computes the elastic moduli of each layer of a two-layer system. The required inputs are the thickness of the upper layer and deflections measured by a Dynaflect on the pavement surface. Poisson's ratio is assumed as 0.5 for both layers.

In ELASTIC MODULUS, the equation used is

$$\frac{w_1 r_1}{w_2 r_2} = \frac{F\left(\frac{E_2}{E_1}, \frac{r_1}{h}\right)}{F\left(\frac{E_2}{E_1}, \frac{r_2}{h}\right)}$$

where

$w_1$  = deflection measured at a distance  $r_1$  from the load

F = function

$E_2$  = Young's modulus of the lower layer

$E_1$  = Young's modulus of the upper layer

h = thickness of upper layer

$w_2$  = deflection measured at a distance  $r_2$  from the load

The only unknown is  $E_2/E_1$ . By a convergent process of trial and error, a value of  $E_2/E_1$  usually can be found that satisfies the equation and  $E_1$  is calculated from

$$\frac{4\pi E_1}{3P} w_1 r_1 \approx F\left(\frac{E_2}{E_1}, \frac{r_1}{h}\right)$$

where

P = vertical force acting at a point in the horizontal surface of a two-layer elastic half-space

$E_2 = E_1(E_2/E_1)$

The authors warn that for calculations involving deflections under a heavy vehicle the moduli computed by ELASTIC MODULUS should be reduced by approximately one half.

#### EXTRAPOLATION OF G FROM LOW TO HIGH STRESS LEVELS

LYSMER ET AL.

Lysmer et al.<sup>28</sup> recognized that because strain amplitudes induced by vibratory testing are smaller than those induced by aircraft, the results from vibratory in situ tests can be expected to yield higher values of moduli and indicate less damping than would be appropriate for use in the functional evaluation of structures. Lysmer discusses a proposed method in which G and damping properties obtained from in situ vibratory tests may be used to obtain similar properties for the description of behavior at strain amplitudes greater than those induced by the test. The method is contained in Figure 50, which is a graph of the ratio of shear modulus at shear strain  $\gamma$  to shear modulus at

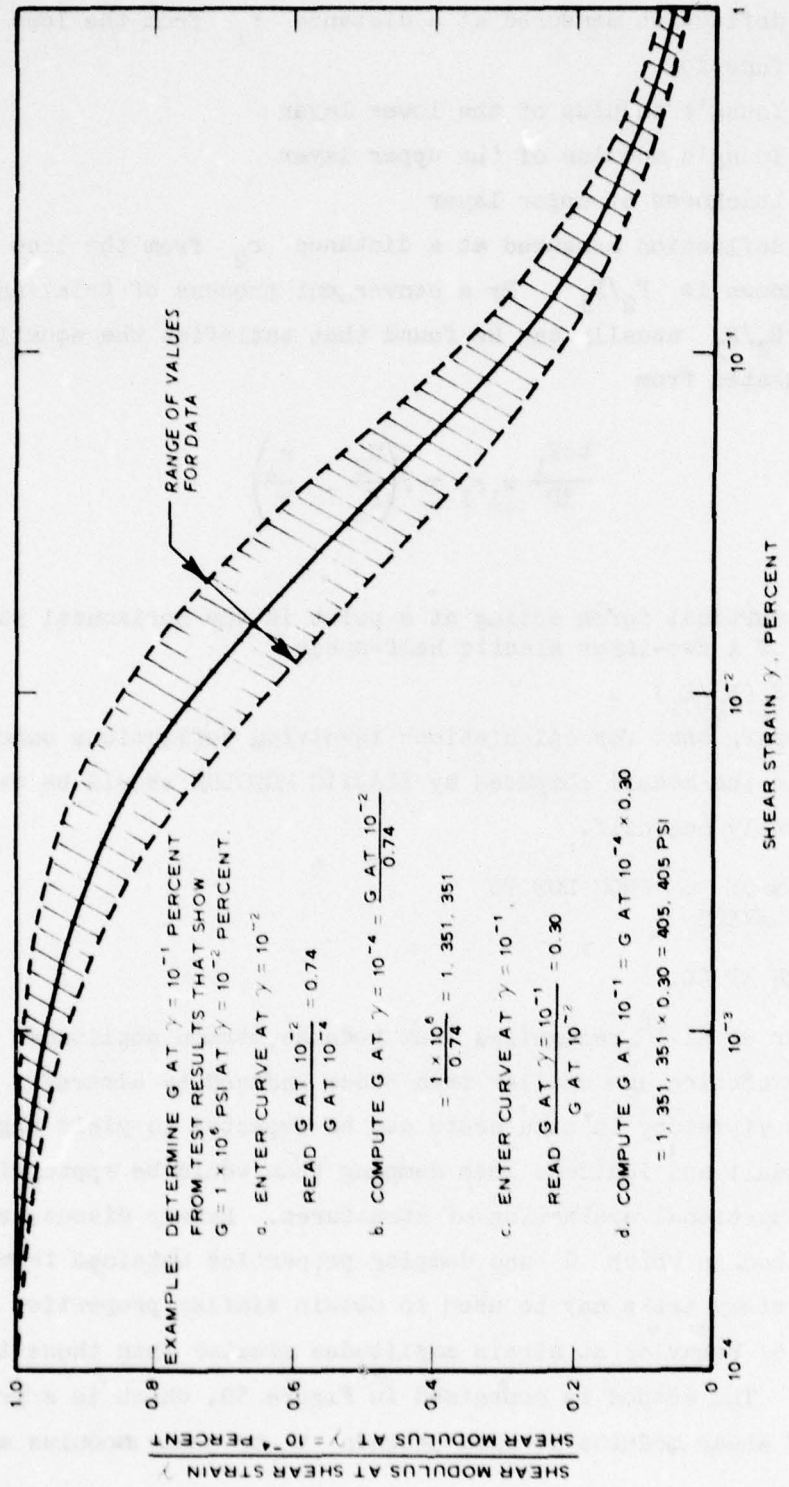


Figure 50. Variation of shear modulus with shear strain for sands (after Lysmer et al. 28)

$\gamma = 10^{-4}$  in percent versus shear strain  $\gamma$  in percent. The modulus versus shear-strain relationship can be approximated for any sand by determining the modulus at any strain and reducing this value for other strains by using the average line in Figure 50.

Lysmer found that information about the dynamic response of soils other than sands is limited and suggested that moduli obtained from a test on gravelly soils may be modified to approximate values at other strain amplitudes in accordance with the method proposed for sands.

#### HARDIN

Hardin's procedure<sup>18</sup> whereby shear moduli at any strain level may be calculated from results at a given strain level is illustrated in Figure 25.

#### PRELIMINARY RELATIONSHIP ESTABLISHED BETWEEN WES 16-KIP VIBRATOR AND ELASTIC MODULUS

#### DYNAMIC STIFFNESS MODULUS

The DSM is measured with the WES 16-kip vibrator and proposed for use by WES in a procedure for evaluating airport pavements. It is defined as the ratio of load to deflection, when the load is a specific, steady-state vibratory load. A complete description of procedures for determining DSM and applying it in the evaluation of pavements is given in Reference 1. Figure 51 shows a sample computation for DSM.

#### EQUATION FOR DSM

As part of this literature review, a special study was made to establish a preliminary relationship between the WES 16-kip vibrator results and elastic modulus. The following equation gave the best results:

$$DSM = 1.909526(t_1 \times E_1) + 0.508105(t_2 \times E_2)$$

$$+ 27.809179(E_S) - 871,471$$

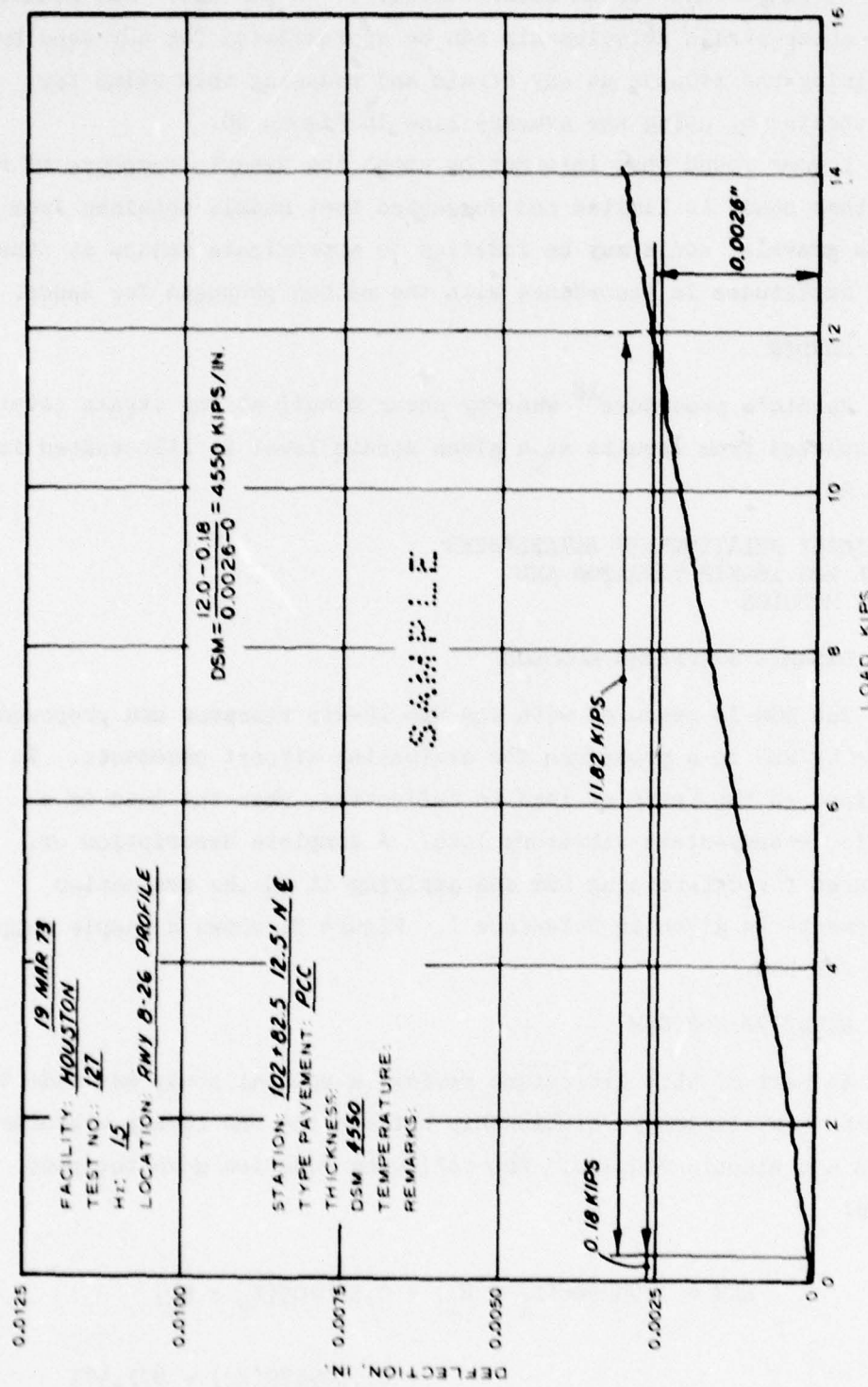


Figure 51. Sample DSM calculation

where

DSM = dynamic stiffness modulus, lb/in.

$t_1$  = thickness of bound pavement material in layer one, in.

$E_1$  = average modulus of bound pavement material in layer one,  
psi

$t_2$  = thickness of unbound pavement material in layer two, in.

$E_2$  = average modulus of unbound pavement material in layer two,  
psi

$E_3$  = modulus of subgrade, psi

The regression coefficient, 27.809179, has to have the dimension of inches, and the constant, 871,471, must be pounds per inch, but the other constants are dimensionless.

Table 23 shows the pavement layer properties and the DSM's used to establish the regression equation. DSM's were adjusted to what their values would have been at a mean pavement temperature of 70°F. Modulus values were computed for the bound pavement and for the unbound pavement materials, respectively, from Figures 52 and 53, which are unpublished works by Dr. Walter Barker of WES. The modulus of the subgrade was taken as  $E_3 = 1500 \times CBR$ .

The regression equation is not satisfactory for estimating the  $E$  values of pavements dissimilar to those used in its development, especially  $E$  values of subgrades per se. An example will show how the equation can be abused. For the case of no pavement or base, the equation would reduce to

$$DSM = 27.809179E_3 - 871,471$$

or

$$E_3 = \frac{871,471 + DSM}{27.809179}$$

The value of DSM cannot be negative; therefore, the smallest value of  $E_3$  that could result (when  $DSM = 0$ ) is 31,337 psi. Since actual values of  $E_3$  are often considerably less than 31,000 psi, this example

Table 23  
Pavement Layer Properties and Dynamic Stiffness  
Moduli (DSM)

Test Site No.	Bituminous Material Thickness $t_1$ , in.	Bituminous Material Modulus $E_1$ , psi	Granular Material Thickness $t_2$ , in.	Granular Material Modulus $E_2$ , psi	Subgrade Modulus $E_S$ , psi	DSM lb/in.
N18	3.25	58,000	6.0	33,000	27,000	630,000
N20	6.0	56,000	6.0	33,000	27,000	1,170,000
N22	6.0	56,000	7.0	33,500	27,000	740,000
N23	6.0	56,000	7.0	33,500	27,000	700,000
W1	9.0	82,000	5.0	34,000	30,000	1,080,000
W2	12.0	91,000	6.0	33,000	30,000	2,060,000
B1	17.5	79,250	6.0	27,000	21,000	2,680,000
B2	12.0	70,000	9.0	31,500	21,000	920,000
B3	10.5	67,000	10.5	35,500	25,500	1,170,000
P1	10.0	65,500	8.0	38,000	10,500	1,020,000
P2	8.5	62,500	7.5	26,000	9,000	560,000
P5	6.0	56,000	6.0	46,000	22,500	790,000
P13	15.0	98,000	5.0	34,000	30,000	3,000,000
P14	14.0	95,000	5.0	34,000	30,000	2,630,000
NV1	13.0	72,000	19.0	63,750	18,000	2,460,000
NV2	13.0	72,000	25.0	79,750	18,000	1,880,000
NV3	8.0	56,000	12.0	53,000	18,000	570,000
NV4	18.0	79,500	12.0	66,000	18,000	3,160,000
S4	9.0	82,000	15.0	21,500	6,000	350,000
S7	3.0	56,000	21.0	52,000	6,000	570,000

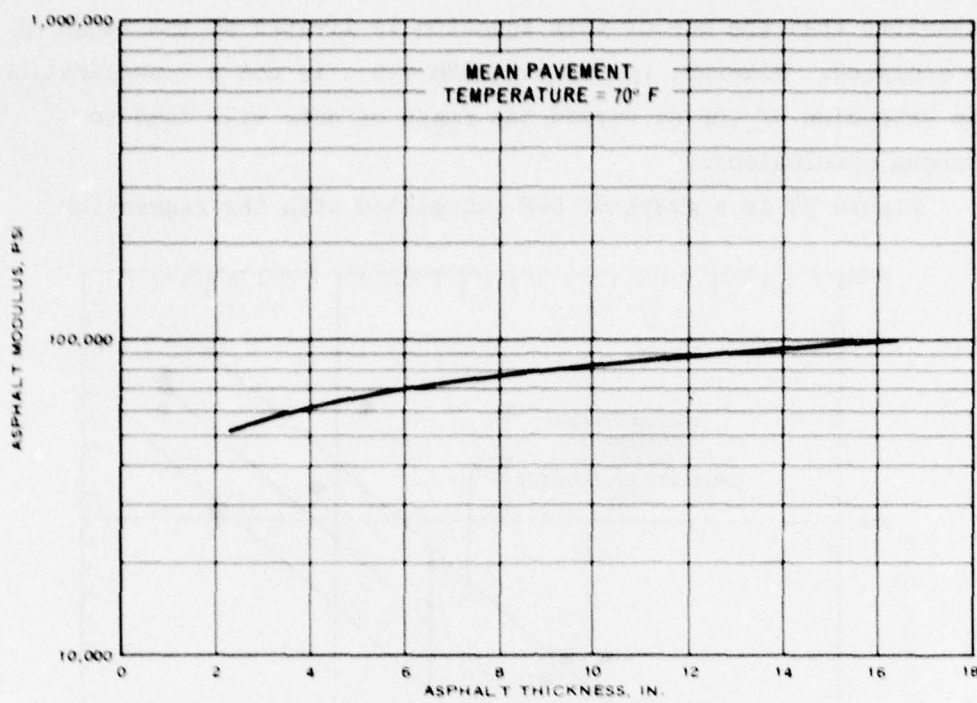


Figure 52. Asphalt modulus versus asphalt thickness

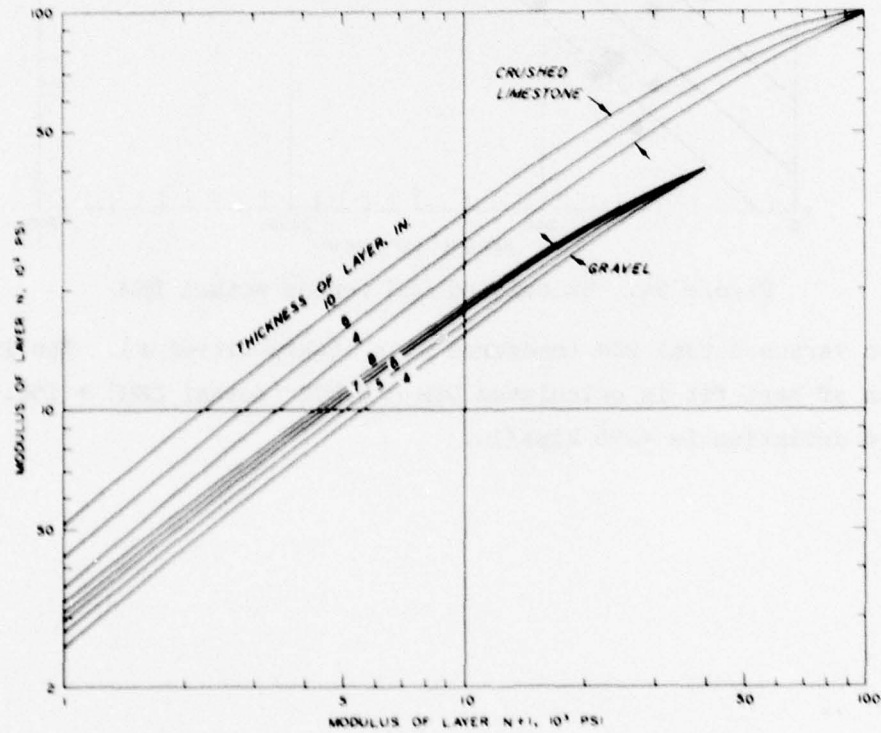


Figure 53. Modulus of layer  $N$  versus modulus of layer  $N+1$

illustrates that the use of this equation is limited to the range of data analyzed. However, in reality,  $DSM = 0$ , is not a consideration since extension of curves beyond the range of data will lead to erroneous conclusions.

Figure 54 is a graph of DSM calculated with the regression

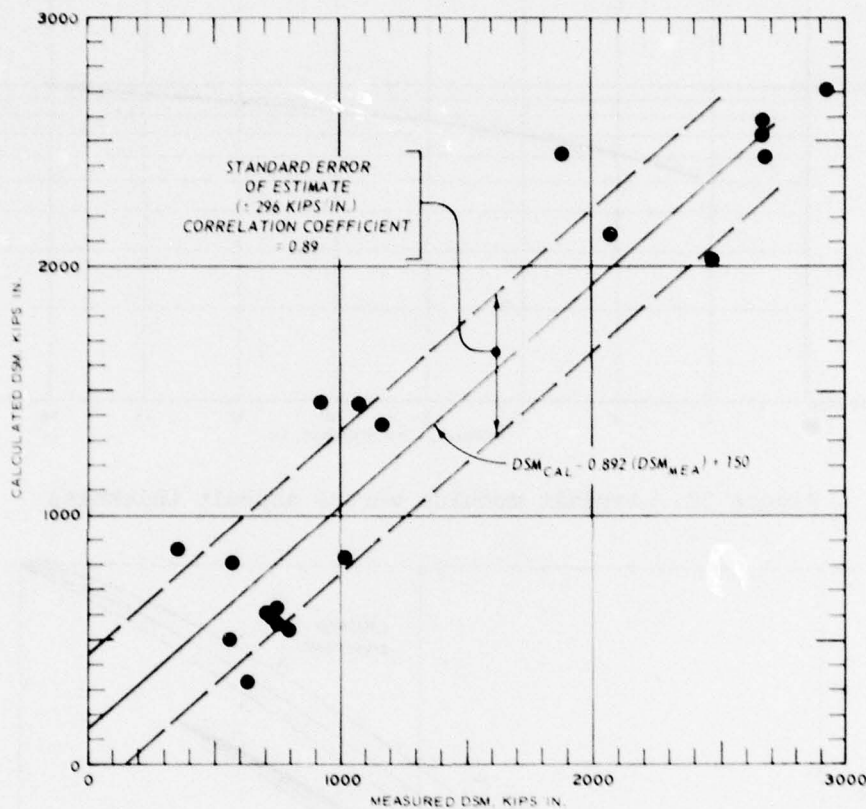


Figure 54. Calculated DSM versus actual DSM

equation versus actual DSM (measured with 16-kip vibrator). The linear equation of best fit is calculated  $DSM = 0.892$  (actual  $DSM$ ) + 150. The standard deviation is  $\pm 296$  kips/in.

## SUMMARY DISCUSSION

To this point, this study has been concerned almost entirely with the direct presentation of pertinent information from the literature and has essentially refrained from evaluation or discussion of that information. Thus in the following paragraphs, an effort is made to summarize, evaluate, or otherwise discuss the information that has been presented.

### REVIEW OF ELASTIC CONSTANTS

#### ELASTIC CONSTANT TEST METHODS AND SPECIFIC VALUES

The test methods reviewed in this study can be grouped into five general categories:

- a. Compression testing.
- b. Flexure testing.
- c. Tension testing.
- d. Wave velocity testing.
- e. Natural frequency testing.

A summary reference, or index, to the test methods and specific values of elastic constants reported herein is given in Table 24. This table shows the elastic constant symbol (as used by the researcher); the material; the researcher or reference; the figure and table; the type of test and category of test (listed above); and the test characteristics (whether quasi-static or dynamic, and whether state of stress and loading rate frequency were considered).

Table 25 presents the minimum and maximum values cited herein for elastic constants. It is evident that the specific values for each constant can have an extremely wide range. It is doubtful that the elastic constants determined by one test procedure are compatible with those determined by another test procedure. Certainly, test procedures that do not account for factors that cause variations in the elastic constants will produce values for the same materials that are different from those obtained from test procedures that do account for the factors.

Table 24

<u>Elastic Constant Symbol</u>	<u>Material</u>	<u>Researcher or Reference</u>	<u>Figure or Table</u>
<u>Elastic Modulus</u>			
	<u>Wearing Surface</u>		
E	PCC	ASTM C469-65, MRD	
E	PCC	CRD-C21	
E	PCC	ASTM C597-71	
E	PCC	Murillo, CRD-C21-58	Table 2
Dynamic E	PCC	Barkan	Table 1
Dynamic E	PCC	CRD-C18-59	
E	PCC	Popov	
E , Dynamic E	PCC	Neville	Figs. 5-8
E , Dynamic E	PCC	WES	Table 3
E*	AC	WSU, AI	
M <sub>R</sub> , flexural stiffness	AC	Glynn and Kirwan	
E	AC	Klomp and Niesman	Fig. 9
E	AC	Izatt et al.	Fig. 10
E	AC	Witczak	Fig. 11
Dynamic E	AC	Cook and Krukar (WSU)	Fig. 12
E*	AC	Pagen	Fig. 13
Stiffness modulus	AC	MRD	
<u>Treated Base</u>			
M <sub>R</sub> ,  E*	Emulsion	Cook and Krukar	Fig. 12, 14,
E	Cement, lime	Barker et al.	15, 16
E	Cement	MRD, ASTM 469-65	Table 4
<u>Untreated Base</u>			
M <sub>R</sub>	Various	Dorman and Klomp	Fig. 17
Dynamic E	Crushed basaltic rock	Cook and Krukar	Fig. 18, 19
M <sub>R</sub>	Gravel, untreated stone	Glynn and Kirwan	Fig. 20, 21, 22
M <sub>R</sub>	Various	Allen	Table 5
<u>Subgrade</u>			
M <sub>R</sub>		WES	
Dynamic E		Dorman and Klomp	
E <sub>i</sub>	Clay, sand	Terzaghi and Peck	Fig. 28
			(Continued)

\* The five categories are (a) compression testing, (b) flexure testing, (c) tension testing, (d) wave velocity, and (e) impact testing.

Table 24

Methods for and Specific Values of Elastic Constants

Figure or Table	Type of Test	Category*	Characteristics of Test			
			Quasi-Static	Dynamic	State of Stress	Loading Rate Frequency
<u>Elastic Modulus</u>						
Table 2	Compression	a	x			
Table 1	Flexure	b	x			
	Pulse Velocity	d		x		
Figs. 5-8	Rupture, three-point beam	a	x			
Table 3	Sound generator	d		x		x
	Natural frequency	e		x		
Fig. 9						
Fig. 10						
Fig. 11					x	
Fig. 12					x	
Fig. 13					x	x
	Stiffness	b				
Fig. 12, 14, 15, 16						
Table 4	Tension	c				
	Compression	a	x			
Fig. 17	Repetitive triaxial compression	a		x	x	
Fig. 18, 19	Wave velocity	d		x		
Fig. 20, 21, 22	Repetitive triaxial compression	a		x	x	x
Table 5	Repetitive triaxial compression	a		x	x	
Fig. 28	Repetitive triaxial compression	a		x	x	x
	Wave velocity	d		x		
	Triaxial compression	a	x		x	

(d) wave velocity testing, and (e) natural frequency testing.

(Sheet 1 of 3)

2

Table 24 (Continued)

<u>Elastic Constant Symbol</u>	<u>Material</u>	<u>Researcher or Reference</u>	<u>Figure or Table</u>
<u>Elastic Modulus (Con</u>			
<u>E</u>			
<u>E</u>	Sand, clay	Lambe and Whitman	
<u>E<sub>r</sub></u>		Barkan	
<u>H<sub>R</sub></u>	Fill, mud	Robnett and Thompson	
<u>M<sub>R</sub></u>		MRD	
<u>E<sub>m</sub></u>		Cook and Krukar	
<u>E</u>	All materials singly or in combination	Foster and Heukelom	
		WES	
<u>Poisson's Ratio</u>			
<u>Wearing Surface</u>			
<u><math>\mu</math></u>	PCC	ASTM C469-65	
<u><math>\mu</math></u>	PCC	CRD-C21	
<u><math>\mu</math></u>	PCC	CRD-C18-59	
<u><math>\mu</math></u>	PCC	Yoder and PCA	
<u><math>\mu</math></u>	PCC	MRD	
<u><math>\mu</math></u>	PCC	Neville	
<u><math>\mu</math></u>	AC	Glynn and Kirwan (TTI)	
<u><math>\mu</math></u>	AC	Orchard	
<u>Treated Base</u>			
<u><math>\mu</math></u>	Emulsion	Cook and Krukar	
<u><math>\mu</math></u>	Cement, lime	Barker et al.	
<u><math>\mu</math></u>	Cement	MRD, ASTM 469-65	
<u>Untreated Base</u>			
<u><math>\mu</math></u>	Granular	Allen	Fig. 23, 24
<u>Subgrade</u>			
<u><math>\mu</math></u>	Clay	Terzaghi and Peck	
<u><math>\mu</math></u>	Sand	Lambe and Whitman	
<u><math>\mu</math></u>	Saturated clay, sand	Morgan and Scala	
<u><math>\mu</math></u>	Clay, clay admixtures	Barkan w/Katsenelenbogen	
<u><math>\mu</math></u>	Sand, clay	Barkan	
<u><math>\mu</math></u>	Artificial clay	Barkan (Pokrovsky)	
<u><math>\mu</math></u>	Clay, loess, sandy soils	Barkan (Ramspeck)	
<u><math>\mu</math></u>	Sandy; silty, sandy clay; clay	Barkan (Tsytovich)	
<u><math>\mu</math></u>	Rock to saturated clay	Bowles	Table 11

(Continued)

ble 24 (Continued)

<u>Figure or Table</u>	<u>Type of Test</u>	<u>Category</u>	<u>Characteristics of Test</u>			<u>State of Loading Rate</u>
			<u>Quasi-Static</u>	<u>Dynamic</u>	<u>Stress</u>	
<u>Modulus (Continued)</u>						
	Triaxial compression	a	x			x
	Compression on clay cubes	a	x			
	Repetitive triaxial	a		x	x	x
	Repetitive triaxial	a		x	x	x
	Repetitive triaxial	a		x	x	x
	Wave velocity	d		x		
	Vibratory (DSM)	a		x		x
<u>Poisson's Ratio</u>						
	Compression	a	x			
	Flexure	b	x			
	Natural frequency	e			x	
	Compression	a	x		x	
	Compression	a	x			
Fig. 23, 24	Repetitive triaxial compression	a		x	x	x
	Repetitive triaxial compression	a		x	x	x
	Triaxial compression	a	x		x	
	Wave velocity			x		

Table 11  
(Continued)

(Sheet 2 of 3)

Table 24 (Concluded)

<u>Elastic Constant Symbol</u>	<u>Material</u>	<u>Researcher or Reference</u>	<u>Figure or Table</u>
<u>Shear Modulus</u>			
<u>Wearing Surface</u>			
G	PCC	CRD-C18-59	
<u>Untreated Base</u>			
G	Crushed limestone, gravel, sand	Hardin Hardin	Fig. 25, 26, 27
<u>Subgrade</u>			
G		Hardin Hardin	Table 12

24 (Concluded)

Figure or Table	Type of Test	Category	Characteristics of Test		
			Quasi-Static	Dynamic	State of Stress Loading Rate Frequency
Fig. 25, 26, 27 Table 12	Natural frequency	e		x	
	Resonant column device	e		x	
	Triaxial compression	a	x		
	Resonant column device	e		x	

(Sheet 3 of 3)

2

**Table 25**  
**Summary of Measured Extreme Values of Elastic Constants**

Material	E, psi		M <sub>R</sub> , psi		E*, psi		v, psi		G, psi		Stiffness Modulus, Psi	
	Minimum	Maximum	Minimum	Maximum	Minimum	Maximum	Minimum	Maximum	Minimum	Maximum	Minimum	Maximum
PCC Wearing Surface	800,000	6,300,000	--	--	--	--	0.08	0.21 (static)	--	--	--	--
PCC Wearing Surface	363,000†	1,290,000†	--	--	--	--	0.24 (dynamic)	--	--	--	--	--
AC Wearing Surface	28,000	2,100,000	--	--	60,000	2,000,000	0.40††	--	--	450,000	600,000	
Treated Base	8,400	1,100,000	18,000	140,000	70,000	1,600,000	0.25††	0.40††	--	--	--	--
Untreated Base	--	--	1,900	160,000	--	--	0.05	0.85	3,625	30,450	--	--
Subgrade	0	127,000	1,900	37,000	--	--	0.20 (clay)	0.60	1,000	50,000	0	0
Subgrade	--	--	--	--	--	--	0.1 (sand)	0.91	--	--	--	--

† At rupture.

†† Assumed.

The point is that values for the elastic constants cannot be randomly extracted from reports or books without qualification as can, for example, the unit weight of water at 70°F. Another point is that test procedures should not be "mixed." For example, in the computer analysis of a two-layered pavement structure, it is not good practice to choose an elastic modulus for one layer based on a wave velocity test and the modulus of the other layer based on a quasi-static triaxial compression test.

#### FACTORS THAT AFFECT VALUES OF ELASTIC CONSTANTS

The inelastic behavior of pavement materials, especially untreated base materials and subgrades, i.e., soils, is universally recognized as the basic cause of the wide variations that occur in values of elastic constants and the difficulties that arise in the measurement of the constants, their use in characterizing pavement materials, and in the ultimate use of elastic theory as a basis for the development of airport pavement design and evaluation methodology. Yet, no better approach to a solution of these problems has evidenced itself than the precalculated assumption of elastic behavior, i.e., the assumption that Hooke's law will be used, knowing that some inaccuracy is a likely consequence. As one researcher, Barkan,<sup>10</sup> puts it, "...the assumption of a relationship more complicated than Hooke's law will lead to the necessity of employing a nonlinear theory of elasticity operating with nonlinear differential equations. The solution of these equations, even in the simplest problems, leads to considerable difficulties..." He further states that the application of the nonlinear relations becomes practically impossible, and it is necessary to restrict the analysis by the assumption that the material, especially the soil, strictly follows Hooke's law. However, the problem of applying nonlinear relations can be resolved by use of finite element programs. A linear relationship can be assumed within each element, and a nonlinear relationship can be applied from element to element. Nevertheless, finite element solutions only approximate nonlinear elastic solutions, but the approximations may

be of acceptable accuracy in some cases. It must be kept in mind that the numerical values of elastic soil constants should be selected with due consideration of the influence of the simplifying assumptions.

Many specific causes of variations in values of elastic constants were cited in this literature review. These may be classified into six general categories, as follows:

- a. Frequency and duration of loading.
- b. State of stresses.
- c. Age of material.
- d. Compositions and material properties.
- e. Temperature.
- f. Strain.

Table 26 contains summary information regarding the factors that affect values of elastic constants. This table shows the elastic constant symbol (as used by the researcher); the material; the researcher or reference; the figure and table; the factor(s) affecting the elastic constant values; and the category (listed above) of the factor. A discussion, by categories, follows.

Frequency and Duration of Loading. The studies of Morgan and Scala,<sup>24</sup> Klomp and Niesman,<sup>25</sup> Witzcak,<sup>27</sup> and Pagen<sup>28</sup> showed that the elastic modulus of AC wearing surfaces is highly dependent on the frequency of loading. For example (Figure 11), at a temperature of 70°F, the AC moduli at frequencies of 1, 4, and 16 cps are 370,000, 570,000, and 770,000 psi, respectively.

Allen<sup>30</sup> reported that Seed and Chan (Table 5) indicated an effect of frequency and duration of loading on the  $M_R$  of silty sand (Table 5) but did not elucidate further. Monismith et al.<sup>35</sup> also mentioned that rate of application is an influencing factor on the  $M_R$  of untreated granular materials.

Graphs of deflection versus frequency of loading obtained from vibrator test devices on all materials, including homogenous soils, exhibit pronounced peaks and troughs (Figure 48) for rigid pavements. For test site No. N11, changing the frequency from 20 to 40 Hz reduced

Table 26  
Summary of References to Factors That Affect Values of Elastic Constants

Elastic Constant Symbol	Material	Researcher or Reference	Figure or Table	Factor Affecting Elastic Constant		Category*
				Elastic Modulus		
<u>Wearing Surface</u>						
$E_1$	PCC	Popov	Table 1	Water/cement ratio	d	
Dynamic $E$	PCC	Barkan	Fig. 5, 7	Age, composition	c, d	
$E_1$ , Dynamic $E$	PCC	Neville	Table 3	Age, E of aggregate	c, d	
$E_1$ , Dynamic $E$	PCC	WEC (Lundeen)		Confining pressure, static vs dynamic	b, a	
$E_1$	AC	Glynn & Krieger		Mix proportions, temperature	d, e	
$E_1$	AC	Morgan & Soileau		Stress level, loading rate, temperature	b, a, e	
$E_1$	AC	Kloemp & Neesman		Temperature, loading rate	e, a	
$E_1$	AC	Izatt et al.		Temperature, loading rate	e, a	
$E_1$	AC	Witczak	Fig. 10	Temperature, loading rate	e, a	
$E_1$	AC	Cook & Krieger	Fig. 11	Temperature, loading rate	e, a	
$E_1$	AC	Pagor	Fig. 12	Temperature, loading rate	e, a	
$E_1$	AC		Fig. 13	Loading rate	e, a	
<u>Treated Base</u>						
$\frac{E_1}{E_2}$	Emulsion	Cook & Krieger	Fig. 14	Temperature, curing, confining pressure	e, c, b	
$\frac{E_1}{E_2}$	Asphalt, hot-mix sand	Barker et al.	Fig. 15, 16	Temperature, density	e, d	
$\frac{E_1}{E_2}$	Cement, lime		Table 4	Cement, lime content	d	
<u>Untreated Base</u>						
$E_1$	Various	Dorman & Kloemp	Fig. 17	E of underlying layer	b, d	
$E_1$	Crushed basaltic rock	Cook & Krieger	Fig. 18	Confining pressure, water content	b, d	
$E_1$	Gravel	Glynn & Krieger	Fig. 19	Bulk stress, water content	b, d	
$E_1$	Crushed stone	Allen	Fig. 20, 21	Cell pressure, density, water content	b, d, d	
$E_1$	Various		Fig. 22	Cell pressure	b	
$E_1$			Table 5	Stress level, frequency and duration of load,	b, e	
$E_1$				Moisture content, gradation, void ratio,	d, d, d	
$E_1$				Dry density, rate of deformation	d, f	
<u>Subgrade</u>						
$E_1, E_2, E_3, E_4$	Clay, sand	Terrazzini & Peck	Fig. 26	Stress-strain	b, f	
$E_1$		Lambe & Whitman	Fig. 29	Remolding, age	d, c	
$E_1$			(Continued)	Confining pressure, clay type, drainage	b, d, d	
$E_1$				Initial principal stresses	b	

\* The six categories are (a) frequency and duration of loading, (b) state of stresses, (c) age of material, (d) compositions and material properties, (e) temperature, and (f) strain.  
(Sheet 1 of 3)

Table 26 (Continued)

Elastic Constant Symbol	Material	Researcher or Reference	Figure or Table	Factor Affecting Elastic Constant	Category
<u>Subgrade (Continued)</u>					
$E$	Lambe & Whitman	Fig. 29		Strain level Deviator stress, soil disturbance, Consolidation stress, overconsolidation ratio Aggreg, strain rate Grain size Water content Void ratio Soil type	b, d, b, b, c, f d d d d
$E$	Sand	Barkan	Table 7	Four factors above Compaction, moisture, stress history	d, d, b
	Clay		Fig. 30	Stress intensity, number of applications, age,	b, e, c
	Clay		Fig. 31	Compaction method, density, water content	d, d, d
	Various		Table 8	Confining pressure, stress level, duration, Rate of stress application, rate of deformation, aggregate type, void ratio, saturation	b, b, e, e, f,
	Sands, fine-grained soils	Nielsen (USNCEL)		Degree of saturation	d, d, d
$M_p$	Fine-grained soils	Monismith et al.	Fig. 33	Deviator stress, moisture content	d
$M_p$	Fine-grained soils		Fig. 34	Moisture content	d
	Granular		Fig. 35	Deviator stress, density	d
	Various	Poehnert & Thompson	Fig. 36	Deviator stress	b, d
			Fig. 37	Deviator stress, compaction	b, d
			Fig. 38	Deviator stress	b
			Table 9, Fig. 39	Deviator stress, stress ratio	b
			Fig. 40, 41	Deviator stress, stress ratio	b, b
			Table 13	State of stress	b
			Table 13	State of stress	b
$M_p$	Fill, mud	Cook & Kirwan		State of stress	b
$M_p$	Silt	Hicks		State of stress	b
$M_p$	X	Danley		State of stress	b
$M_p$	X	Morgan & Scala (Brown & Fell)		State of stress	b
$E_p$	X	Morgan & Scala (Seed et al.)		State of stress	b
$M_p$	X	Morgan & Scala (Holden)		State of stress	b
$E_p$	X	Nielsen (USNCEL)	Fig. 42	Lateral stress	b
$E_p$	X	Glynn & Kirwan		State of stress	b
$E_p$	X	Wang et al.		State of stress	b
$M_p$	X	Glynn & Kirwan	Fig. 43	PI, density, moisture content	d, d, d
<u>Wearing Surface</u>					
	PCC	Neville			e
	POC	Orchard			d

(Continued)

(Sheet 2 of 3)

Table 26 (Concluded)

the deflection by nearly one half (from 0.0102 to 0.0054 in.). Obviously, tests on the same material at different frequencies will not produce the same results.

State of Stresses. Work at WES<sup>8</sup> and MRD,<sup>21</sup> as well as the research of Hardin,<sup>15</sup> Cook and Krukar,<sup>11</sup> Glynn and Kirwan,<sup>13</sup> and others, showed that modulus values of materials depend on the state of the stresses or the confining pressures. Since the shape or mass of soil influenced by vibratory testing is indefinite, it is difficult to determine the pressure on the in-place soils during vibratory testing.

A dynamic theory for computations of stresses in soils beneath vibratory loading was not found; therefore, for the present, a static theory must be used as an approximation.

The variable nature of the elastic constants of soil and the variability introduced by the different test methods emphasize the desirability of in situ determinations of these constants. It has been recognized for years that the behavior of soils in the laboratory, especially clays, can be radically different from behavior in the field even when tests are performed on undisturbed specimens under carefully controlled conditions. With the knowledge being gained by contemporary researchers, it should soon be possible to design vibratory tests to exactly simulate in situ stress conditions created by aircraft and thus yield more precise results.

Of the equations relating resilient modulus and state of stress in base course materials, Barker et al.,<sup>29</sup> in his work with the structural properties of stabilized layers, found Hicks' expression

$$M_R = K_1 \sigma_3^{K_2}$$

to be most useful. The values of the constants  $K_1$  and  $K_2$  are listed for 10 categories of materials in Table 13. However, five of these categories are for gravels in five different states of crushed condition or saturation, and the other five categories of materials are classified by regional nomenclature. Therefore, the application of this equation

is limited until the list of constants is expanded.

The equations relating moduli and states of stress in soils are useful in describing the changes in moduli with change in conditions; however, application of the equations is limited because of the effect on the modulus of soils (especially clays) of the many variables, such as moisture content, porosity, and particle composition.

Age of Material. The influence of age on the elastic modulus of PCC wearing surfaces was recognized by Barker. According to his data, the aging of six concrete samples from 7 to 28 days raised the E values of five of them from about 7 to 26 percent (Table 1). The E value of one of the samples actually decreased 6 percent. No explanation of this apparent anomaly was given. The aging of concrete samples probably resulted in some dehydration, mainly in the early stages of aging, and the dehydration tended to increase the cementation forces and thus the E value. Beneficial effects of aging will continue at a reduced rate after 28 days.

Apparently, age is a significant factor in the resilient moduli of emulsion-treated base (Figure 14). Uncured test specimen A, which was tested at 80°F, exhibited significantly lower moduli values than did test specimen B, which was cured for 6 months and tested at 100°F.

Monismith et al.<sup>35</sup> stated that the age of a fine-grained soil at initial loading is a factor that influences the value of its modulus of resiliency. No attempt was made to quantify that influence. Several researchers in addition to Monismith acknowledge age effects but offer no detailed discussion. Apparently, the researchers are discussing an influence that is independent of all the factors listed in Table 26 that affects elastic constants. The only other factors that come to mind are settlement and molecular bond.

Compositions and Material Properties. The relationship, developed by Glynn and Kirwan (Figure 40), between resilient modulus, stress, PI, moisture content, and density of clays, appears promising because it considers four factors that have an important influence on the modulus value, and also because it expresses the modulus in terms of

basic soil properties that are simple to determine.

Dorman and Klomp's relationship<sup>14</sup> of CBR to subgrade E (Figure 41) is useful because it represents in situ conditions when the CBR is measured in place. However, Figure 41 shows that there is significant scatter in the data. For a CBR of 20, the E values range in the approximate limit from 15,000 to 60,000 psi. Robnett and Thompson<sup>36</sup> concluded that there is no relationship between  $E_r$  and CBR because of the scatter observed in their graph (Figure 42). Scatter in Figure 42 is comparable to that in Figure 41. The scatter evident in the CBR-E relationship does not nullify the possibility of using CBR as an estimator of E. However, the variation in E for a given CBR should be considered when this relationship is used. When modulus testing is feasible, CBR tests are not recommended as substitutes.

The relationship proposed by the Asphalt Institute<sup>12</sup> in Figure 43 ties the subgrade modulus of elasticity to plate bearing value. However, Crawford et al.<sup>49</sup> found that to approximately compute the elastic layer deformation using a Westergaard idealization, subbase k values measured in the field must be reduced by 90 percent. Crawford's findings indicate that the subgrade moduli may also require adjustment before serving as input for the layered-elastic programs.

Hardin's equations for shear moduli of soils and gravels appear to be more complete in their treatment of influencing variables than do the equations found in other references. These equations could be useful in verification and correlation work; however, it is not clear at this time if they can be adapted for the study at hand. The equations also require the determination of some index properties of soil.

Temperature. The effect of temperature on the modulus of elasticity of AC has long been recognized. An idea of how profound this effect can be may be gained by inspecting Figure 9. It can be seen that a change of 40°C (from -10 to 30°C) caused a decrease in elastic modulus of about 150,000 kg/cm<sup>2</sup> (from 160,000 to 10,000 kg/cm<sup>2</sup>). Other graphic evidence of temperature effects on the elastic modulus of AC wearing surfaces can be seen in Figures 10, 11, 12, 14, 15, and 16.

No references were examined that showed the effect of temperature on PCC wearing surfaces, base materials, or subgrade materials. It is known, however, that temperature does affect the elastic constants of these materials but to a lesser degree than it does those of AC wearing surfaces.

Strain. One has only to inspect Figure 26, a plot of stress versus strain for an unconfined clay specimen (after Terzaghi and Peck<sup>31</sup>), to recognize the extreme importance of strain on the value of an elastic constant in clay. Allen reported that Trollope, Lee, and Morris (Table 5) considered rate of deformation to be an influencing factor on the  $M_R$  of poorly graded dry sand. Lambe and Whitman<sup>33</sup> stated that  $E$  decreases and  $v$  increases as strain level increases and that  $E$  increases with an increase in strain rate. Monismith et al. listed rate of deformation as an influence on  $M_R$  of untreated granular materials. Hardin showed a logarithmically decreasing  $G$  with an increase in strain amplitude. Lysmer et al.<sup>28</sup> listed strain amplitude as one of the most significant factors affecting  $G$ .

#### SENSITIVITY OF PAVEMENT RESPONSES TO CHANGES IN ELASTIC CONSTANTS AND THICKNESS

Pichumani's studies<sup>5</sup> provide data for a summary discussion of the effect of changes in elastic constants on surface deflection. Table 27 shows the factors by which  $E$  and  $v$  may vary in flexible and rigid pavement layers to produce less than 10 percent change in the calculated surface deflections. The factors were derived by interpolation of results obtained by Pichumani with the APPAV program. Although values are only approximate, this table shows the relative importance of accurate  $E$  and  $v$  values for the pavement layers and subgrade.

#### RIGID PAVEMENTS

For rigid pavements, the  $E$  of the surface course is more critical than for flexible pavements, and accurate values for  $E$ 's of the subgrade are just as important for rigid as for flexible pavements.

Table 27  
Approximate Factor by Which Elastic Constants May Vary  
from True Value and Produce Less Than 10 Percent  
Error in Computed Surface Deflection

<u>Pavement Type</u>	<u>Course</u>	<u>Factor</u>	
		<u>E</u>	<u>v</u>
Rigid	Surface	1.43	Not studied
	Subgrade	1.03	Not studied
Flexible	Surface	2.42	10.0
	Base	3.11	10.0
	Subbase	2.16	10.0
	Subgrade	1.05	1.07

There is no data on sensitivity of calculations to variations in  $v$  for rigid pavements.

#### FLEXIBLE PAVEMENTS

In flexible pavements, calculations of surface deflection are not highly sensitive to either  $E$  values or Poisson's ratios of the surface, base, or subbase course, but both the  $E$  value and the Poisson's ratio of the subgrade must not vary more than 5 and 7 percent, respectively, from their true values, if less than 10 percent error in surface deflection is to be maintained.

Pichumani cautions that although the  $E$  values for flexible pavement base and subbase courses may not be highly significant for surface deflections, they are important in determining the state of stress in the upper layers of the pavement system.

#### RELATIONSHIPS BETWEEN VIBRATORY TEST RESULTS AND MATERIAL PARAMETERS

#### MATHEMATICAL MODELS

The method of Tschebotarioff<sup>42</sup> applies the linear spring-mass-dashpot model to one resonant peak of the frequency response spectrum. Weiss<sup>3</sup> has used a similar linear lumped-mass spring model to measured resonant peaks and has found that the linear model is inadequate to

describe the resonant peak and to determine the subgrade Young's modulus; a nonlinear dynamic theory of the frequency-response spectrum is required. Yang<sup>43</sup> uses the linear lumped-mass spring model to obtain the E modulus of a pavement from the entire measured frequency response spectrum including all resonant peaks.

Waas<sup>44</sup> and Lysmer<sup>45</sup> have developed a linear elastic half-space model for calculating the response of a foundation resting on a layered elastic half-space. Waas describes the frequency response spectrum in terms of a numerical procedure based on the finite element method. The dynamic load-deflection curves predicted by this model are always linear because of the assumption of the linear elastic half-space.

A nonlinear harmonic oscillator model has been developed by Weiss<sup>2,3</sup> to describe the measured nonlinear dynamic load-deflection curves and to extract the value of the subgrade Young's modulus from these curves. This model also describes the laboratory resilient modulus test and can obtain the value of the Young's modulus from the measured resilient modulus. The value of the Young's modulus obtained from the field and laboratory tests should agree approximately with the Shell equation,  $E = 1500 \text{ CBR}$ .

The wave propagation method of vibratory nondestructive testing of pavements has been studied recently by Lysmer et al.<sup>28</sup> Wave solutions of the basic dynamical elastic equations of motion are obtained subject to the boundary conditions at the pavement surface and at the interfaces of the pavement layers. Rayleigh wave dispersion curves giving phase velocity versus wavelength are obtained using a mechanical vibrator, and these curves exhibit discontinuous branches, which must be described theoretically by solving the secular determinant equation arising from the boundary conditions.

The wave propagation method has these disadvantages: (a) it requires a complicated theoretical description, which may not fully describe the physical situation; and (b) it predicts elastic moduli under very small stress and strain conditions, so that these elastic moduli cannot be used directly for pavement calculations that require elastic moduli under actual loading conditions.

The linear regression equation for DSM also indicates that the elastic moduli of the various pavement layers and subgrade are related to the surface deflection in a complicated fashion. In addition, in any regression equation containing several terms for each pavement layer, there is no assurance that the contribution made by each pavement layer is exactly indicated by the equation.

#### VIBRATOR WAVE PATTERNS

The utilization of deflection basin measurements in attempts to extract elastic constants from vibratory test results is not considered practical for several reasons. The first reason is that the motion of soil away from the vibrator baseplate is complicated and not understood. The fact that the ground at some distance away from the baseplate may be out of phase with the baseplate by various degrees makes the data difficult to interpret. The second reason is that there are two or more types of waves that radiate away from the baseplate during vibration. Although vibratory devices have peak detectors that produce data which plot in neat "bowl-shaped" graphs, there is no certainty that the pavement always bends to conform to the graph of the pavement surface. The third reason is that deflection rapidly decreases in magnitude as distance from the baseplate increases. In many cases, the ability of the velocity transducers to produce accurate deflection measurements will be exceeded. A fourth reason for not using deflection basins is the complication of different wavelengths created by vibrations on different pavement sections and at different frequencies. In many cases, it will not be known if in the horizontal range of the transducers, a quarter, half, full, or some unknown fraction of a wavelength is being reflected by the measurements.

The Texas Transportation Institute procedure for extracting elastic constants from vibratory test results is useful but has three shortcomings. First, it uses deflection basin measurements that are difficult to analyze. Second, it relies on the static Burmister theory to describe dynamic loading; and third, the moduli values produced

require multiplication by a judgment factor to be realistic for use in calculations involving heavy loads.

#### EXTRAPOLATION OF CONSTANTS FROM LOW TO HIGH STRESS LEVELS

The significance of stress level on modulus value is recognized, and Hardin's method<sup>18</sup> of extrapolating shear moduli at one strain level to any strain level appears to be the best available procedure. This procedure will allow the calculation of appropriate modulus values for stresses created by aircraft of any size.

#### PRELIMINARY RELATIONSHIPS ESTABLISHED BETWEEN WES 16-KIP VIBRATOR AND ELASTIC CONSTANTS

The empirical relationship between the DSM calculated for the WES 16-kip vibrator and the elastic modulus of the pavement layers apparently is valid since calculated values of DSM correlate well with measured values; however, the material properties of the layers are not known with enough precision to establish a reliable working relationship. Also, the empirical equation is not universally applicable as indicated by the fact that the minimum subgrade modulus value which can be computed is higher than values that have often been measured.

The surface pressures created by the 16-kip vibrator can be made equal to those created by aircraft by changing the baseplate size. However, the characteristics of the existing vibrator that cannot be altered to simulate aircraft loadings are: (a) one cycle of loading is not possible; (b) the static weight is fixed; and (c) it is possible to determine only the deflection created by the peak dynamic load.

## RECOMMENDATIONS

During the course of this literature review, the reviewer constantly had in mind the objective of the overall program, namely, to develop a more rational and analytical method for evaluating airport pavements based on elastic theory and using elastic constants as determined from vibratory test results. As a consequence, it was inevitable that the reviewer be prompted to certain relevant impressions and ideas. These thoughts, some from the direct results of the data examined and others largely intuitive or even obvious, are offered here in the form of "Recommendations," in the hope that they will be of value in planning and/or implementing the ongoing study and future studies to develop improved methodology. As a final recommendation, a suggested breakdown of the ongoing study into phases or work areas is offered.

### REVIEW OF ELASTIC CONSTANTS

#### MEASURING ELASTIC CONSTANTS

State of stresses for field testing should be duplicated in the laboratory. The effect of the inelastic behavior of materials on elastic modulus can be minimized by always using the same modulus ( $E_i$ ,  $E_t$ ,  $E_s$ , or  $E_h$ ) in laboratory work.

#### VARIATIONS IN ELASTIC CONSTANTS

Frequency and Duration of Loading. The nonlinear model developed by Weiss<sup>2,3</sup> allows the extraction of elastic modulus values from field vibratory test results. These modulus values are independent of frequency as well as static and dynamic loads of the vibrator. Axial stresses and confining stresses are equal to in situ conditions with no load. On a stress-strain curve for any material, the elastic modulus determined by Weiss would correspond to the initial tangent modulus,  $E_i$ . Therefore, repetitive load laboratory testing done in conjunction with the Weiss work should be performed at frequencies as low as possible to minimize any possible disparities between quasi-static and dynamic test methods.

State of Stresses. Ahlvin and Foster<sup>50</sup> developed influence diagrams for stresses imposed in semi-infinite elastic media by a uniform circular surface load, which can be used to approximate stresses induced by vibratory loading. Figures 55 and 56 are the diagrams for vertical normal stress,  $\sigma_z$ , and horizontal normal stress,  $\sigma_r$ . Because these diagrams are for a semi-infinite media, and the present concern is with stresses beneath multilayered pavements, another approximation is necessary. This involves converting the pavement layers to equivalent thicknesses of subgrade as suggested in TM 5-312.<sup>51</sup> For example, assume stresses are desired for a point in a subgrade with a unit weight of  $\gamma_s$  at a distance  $h_s$  below the top of the subgrade. The subgrade is covered with a material with a unit weight of  $\gamma_1$ , which has a thickness,  $t$ . The depth,  $z$ , to be used with the influence diagrams is computed as

$$z = h_s + \frac{\gamma_1}{\gamma_s} (t)$$

Age of Material. When age could be an important factor in modulus or vibrator test results, the effect will have to be ignored. Insufficient information exists on age effects to allow even approximate quantification of its effects on any material.

Compositions and Material Properties. Wide ranges in behavior due to compositions and properties of materials, especially soils, make the assignment of values of  $E$ ,  $v$ , and  $G$  from tabulated values nothing but guesswork. Hardin's method<sup>15</sup> for determining shear modulus of soils and gravels appears to consider all pertinent factors, and similar procedures will have to be adopted for all pavement materials; however, time will not allow the development of these procedures for the methodology presently being developed for FAA by WES. Therefore, it is recommended that methods for estimating elastic constants for the evaluation methodology be developed based on existing equations that account for in situ material properties and stress levels.

Hicks' list<sup>39</sup> of constants  $K_1$  and  $K_2$  should be expanded. His

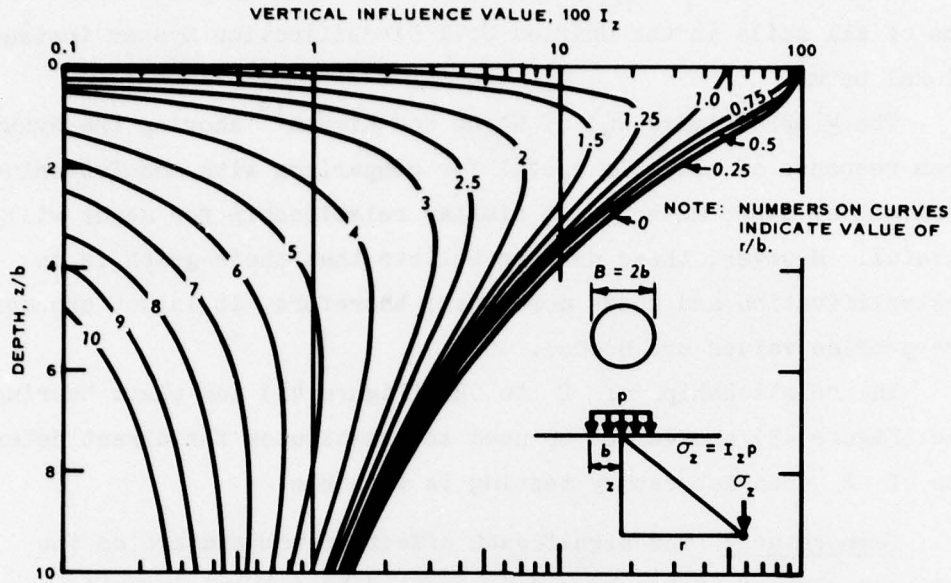


Figure 55. Influence diagram for vertical normal stress  $\sigma_z$  at various points within an elastic half-space under a uniformly loaded circular area (after Ahlvin and Foster<sup>50</sup>)

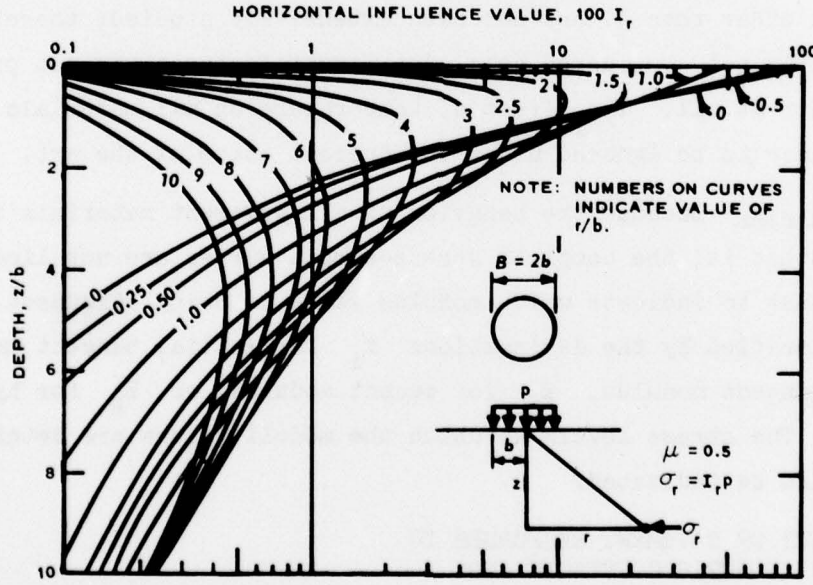


Figure 56. Influence diagram for horizontal normal stress  $\sigma_r$  at various points within an elastic half-space under a uniformly loaded circular area (after Ahlvin and Foster<sup>50</sup>)

equation could be universally applied if the constants are listed in terms of all soils in the Unified Soil Classification System instead of regional terms.

The graph (Figure 40) of Glynn and Kirwan<sup>13</sup> showing the dynamic stress response of clays is useful for comparison with modulus values determined by other methods. A similar relationship for sands will also be useful. However, these authors believe that their graph is an oversimplification and needs more work; therefore, it is not appropriate where precise values are needed.

The relationships of  $E$  to CBR (Figure 41) and plate bearing value (Figure 43) should not be used as substitutes for direct determinations of  $E$  when laboratory testing is feasible.

Temperature. The significant effect of temperature on the elastic modulus of AC has been demonstrated by several investigators. It is obvious that temperature should be accounted for in field and laboratory tests on AC. Modulus tests performed in the laboratory should duplicate field temperature conditions. The effect of temperature on materials other than AC has not been extensively studied; therefore, it is evidently not considered as a significant factor or is not practical to consider at all. The effect of temperature on all materials except AC will have to be ignored under the present state of the art.

Strain. Because the behavior of all pavement materials is inelastic, that is, the complete stress-strain curves are not linear, it is important to indicate which modulus value is being discussed. This can be clarified by the designations  $E_i$  for initial tangent modulus,  $E_t$  for tangent modulus,  $E_s$  for secant modulus, or  $E_h$  for hysteresis modulus. The stress levels at which the moduli values are determined should also be indicated.

#### SENSITIVITY OF PAVEMENT RESPONSES TO CHANGES IN ELASTIC CONSTANTS AND THICKNESS

Pichumani's study<sup>5</sup> of the sensitivity of computed pavement deflections to changes in elastic constants and thickness showed that

the E values of the layers of flexible pavement could be in error by a factor of 2 or 3 and not significantly affect the computed deflection. Also, the E value of the PCC could be in error by a factor of about 1.5 and not significantly affect the deflections computed for rigid pavements. However, he varied only one parameter at the time, but in practice, the effect of choosing erroneous values for all pavement layers, including a subbase for rigid pavement, should be considered. Consequently, it is imperative, if accurate results are to be obtained from the layered elastic method, that values of E and v be estimated with more precision than he indicates is necessary. A comprehensive sensitivity study of any proposed pavement evaluation methodology should be made.

Pichumani also showed the importance of accurate values for v of subgrade materials. However, work by several researchers indicates that v is difficult to determine even under carefully controlled laboratory conditions. Therefore, it is recommended that a procedure for estimating v be adopted.

#### RELATIONSHIPS BETWEEN VIBRATORY TEST RESULTS AND MATERIAL PARAMETERS

##### MATHEMATICAL MODELS

Weiss's nonlinear mathematical model,<sup>2,3</sup> which describes the response of a pavement structure to vibratory loading of the WES 16-kip vibrator, appears to be the most practical and accurate procedure to adopt for the determination of elastic constants. The Weiss model uses DSM graphs or frequency response curves; therefore, other forms of non-destructive test results, such as deflection basins or wave velocity measurements, need not be considered at this time.

##### VIBRATOR WAVE PATTERNS

The effect of the input wave shape on the response of a material is not known. The response of the pavement system and subgrade to sinusoidal loading of the vibrator and of test laboratory specimens to haversine loading will be assumed to approximate the response to loading by the vibrator.

EXTRAPOLATION OF CONSTANTS FROM  
LOW TO HIGH STRESS LEVELS

Hardin's method<sup>18</sup> for extrapolation of shear moduli to any stress level should be included in the proposed evaluation methodology.

PRELIMINARY RELATIONSHIP BETWEEN WES  
VIBRATOR AND ELASTIC CONSTANTS

The empirical equation that relates DSM, E, and t adds to the evidence that vibratory test results and the elastic moduli of materials are related. A better relationship could be established if pavement and subgrade constants were known with more precision. However, it is recommended that efforts be directed at developing and complementing the Weiss theory<sup>2,3</sup> rather than improving an existing empirical relationship.

BREAKDOWN OF ONGOING STUDY FOR DE-  
VELOPMENT OF EVALUATION PROCEDURE  
BASED ON LAYERED ELASTIC THEORY  
AND VIBRATORY TEST RESULTS

The ongoing study can be divided into four areas of work:

- a. Field and laboratory work that will consist of performing nondestructive testing and laboratory testing on several different types of soil in order to provide data with which to verify the theoretical procedures proposed by Weiss.
- b. Choosing the best methods to estimate the elastic moduli and Poisson's ratios of pavement layers, as substitutes for difficult testing methods.
- c. Further investigation of the procedures for:
  - (1) Extrapolating modulus values to any strain level.
  - (2) Relating pavement response characteristics to the vibrator to pavement response characteristics to the aircraft.
  - (3) Calculating stresses in soils due to vibratory loading.
  - (4) Determining relationships between quasi-static and dynamic conditions.
- d. Finally, the pertinent information contained in this report; the results of the three areas of work listed as a, b, and c above; the Weiss theory; and the reverse of a design procedure based on layered elastic theory will be formed into a pavement evaluation procedure.

#### REFERENCES

1. Green, J. L. and Hall, J. W., "Nondestructive Vibratory Testing of Airport Pavements; Experimental Test Results and Development of Evaluation Methodology and Procedure," Technical Report S-75-14, Volume I, Sep 1975, U. S. Army Engineer Waterways Experiment Station, CE, Vicksburg, Miss.
2. Weiss, R. A., "Nondestructive Vibratory Testing of Airport Pavements; Theoretical Study of the Dynamic Stiffness and Its Application to the Vibratory Nondestructive Method of Testing Pavements," Technical Report S-75-14, Volume II, Apr 1975, U. S. Army Engineer Waterways Experiment Station, CE, Vicksburg, Miss.
3. \_\_\_\_\_, "Subgrade Elastic Moduli Determined from Vibratory Testing of Pavements" (in preparation), U. S. Army Engineer Waterways Experiment Station, CE, Vicksburg, Miss.
4. Packard, R. G., "Design of Concrete Airport Pavement," Engineering Bulletin, 1973, Portland Cement Association, Skokie, Ill.
5. Pichumani, R., "Finite Element Analysis of Pavement Structures Using AFFAV Code (Linear Elastic Analysis)," Technical Report No. AFWL-TR-72-186, May 1973, Air Force Weapons Laboratory, Kirtland Air Force Base, N. Mex.
6. American Society for Testing and Materials, 1976 Annual Book of ASTM Standards, Philadelphia, 1976.
7. U. S. Army Engineer Waterways Experiment Station, CE, Handbook for Concrete and Cement, Aug 1949 (with quarterly supplements), Vicksburg, Miss.
8. Lundeen, R. L., "Dynamic and Static Tests of Plain Concrete Specimens; Phase II: Flexure and Triaxial Compression," Miscellaneous Paper 6-609, Report No. 2, Nov 1964, U. S. Army Engineer Waterways Experiment Station, CE, Vicksburg, Miss.
9. Murillo Engineering and Testing Service, Inc., "Soil Investigation and Dynaflect Testing, Runway and Taxiway Extensions, Houston Intercontinental Airport, Houston, Texas," Feb 1971, Houston, Tex.
10. Barkan, D. D., Dynamics of Bases and Foundations, McGraw-Hill, New York, 1962.
11. Cook, J. C. and Krukar, M., "Evaluation and Analysis of Results from Experimental Rings No. 1-4," Volume 5, Research Project Y-993 Supplement, Jul 1971, Washington State University, Pullman, Wash.
12. The Asphalt Institute, "Full-Depth Asphalt Pavements for Air Carrier Airports," Manual Series No. 11 (MS-11), Jan 1973, College Park, Md.

13. Glynn, T. E. and Kirwan, R. W., "Environmental Factors Involved in Analysis of Flexible Pavements," Contract No. DAJA37-70-C-1116, Sep 1971, Dublin University, Ireland.
14. Dorman, G. M. and Klomp, A. G. J., "Stress Distribution and Dynamic Testing in Relation to Road Design," Shell Bitumen Reprint No. 18, 1964, Shell Oil Company, London, England.
15. Hardin, B. O., "Shear Modulus of Gravels," Technical Report No. AFWL-TR-73-180, Nov 1973, Air Force Weapons Laboratory, Kirtland Air Force Base, N. Mex.
16. \_\_\_\_\_, "The Nature of Damping in Sands," Journal, Soil Mechanics and Foundations Division, American Society of Civil Engineers, Vol 91, No. SMI, Jan 1965, pp 63-97.
17. Brabston, W. N., Barker, W. R., and Harvey, G. G., "Development of a Structural Design Procedure for All-Bituminous Concrete Pavements for Military Roads," Technical Report S-75-10, Jul 1975, U. S. Army Engineer Waterways Experiment Station, CE, Vicksburg, Miss.
18. Hardin, B. O., "Effects of Strain Amplitude on the Shear Modulus of Soils," Technical Report No. AFWL-TR-72-201, Mar 1973, Air Force Weapons Laboratory, Kirtland Air Force Base, N. Mex.
19. Popov, E. P., Mechanics of Materials, Prentice-Hall, Englewood Cliffs, 1960.
20. Yoder, E. J., Principles of Pavement Design, Wiley, New York, 1964.
21. Materials Research and Development, "San Francisco International Airport, Pavement Evaluation and Design Study," Final Report, Project RD-310, Sep 1971, Oakland, Calif.
22. Neville, A. M., Properties of Concrete, Wiley, New York, 1963.
23. Orchard, D. F., Concrete Technology; Properties of Materials, Vol I, Wiley, New York, 1973.
24. Morgan, J. R. and Scala, A. J., "Flexible Pavement Behavior and Application of Elastic Theory - A Review," Proceedings, Fourth Conference Australian Road Research Board, Melbourne, Paper No. 509, Vol 4, Part 2, 1968, pp 1201-1243.
25. Klomp, A. J. G. and Niesman, T. W., "Observed and Calculated Strains at Various Depths in Asphalt Pavements," Proceedings, Second International Conference on the Structural Design of Asphalt Pavements, University of Michigan, Ann Arbor, Preprint Volume, 1967, pp 536-555.
26. Izatt, J. O., Lettier, J. A., and Taylor, C. A., "The Shell Group Methods for Thickness Design of Asphalt Pavements," Jan 1968, Shell Oil Company, Riverdale, Md.
27. Witczak, M. W., "Design of Full-Depth Asphalt Airfield Pavements," Research Report 72-2 (RR-72-2), Apr 1972, The Asphalt Institute, College Park, Md.

28. Lysmer, J., Monismith, C. L., and Watkins, D. J., "Nondestructive Pavement Evaluation by the Wave Propagation Method," Report No. TE-74-2, Jul 1974, Soil Mechanics and Bituminous Materials Research Laboratory, University of California, Berkeley, Calif.
29. Barker, W. R., Brabston, W. N., and Townsend, F. C., "An Investigation of the Structural Properties of Stabilized Layers in Flexible Pavement Systems," Miscellaneous Paper S-73-69, Oct 1973, U. S. Army Engineer Waterways Experiment Station, CE, Vicksburg, Miss.
30. Allen, J. J., "The Effects of Stress History on the Resilient Response of Soils," Technical Report M-49, Jun 1973, Construction Engineering Research Laboratory, Champaign, Ill.
31. Terzaghi, K. and Peck, R. B., Soil Mechanics in Engineering Practice, Wiley, New York, 1967.
32. Bowles, J. E., Foundation Analysis and Design, McGraw-Hill, New York, 1968.
33. Lambe, T. W. and Whitman, R. V., Soil Mechanics, Wiley, New York, 1969.
34. Nielsen, J. P., "Rational Pavement Evaluation - Review of Present Technology," Technical Report No. AFWL-TR-69-9, Oct 1969, Air Force Weapons Laboratory, Kirtland Air Force Base, N. Mex.
35. Monismith, C. L. et al., "Prediction of Pavement Deflections from Laboratory Tests," Proceedings, Second International Conference on the Structural Design of Asphalt Pavements, University of Michigan, Ann Arbor, Preprint Volume, 1967, pp 52-88.
36. Robnett, Q. L. and Thompson, M. R., "Resilient Properties of Subgrade Soils, Phase I - Development of Testing Procedure," Interim Report, Project IHR-603, May 1973, University of Illinois, Urbana.
37. Foster, C. R. and Heukelom, W., "Dynamic Testing of Pavements," Miscellaneous Paper No. 4-348, Jul 1959, U. S. Army Engineer Waterways Experiment Station, CE, Vicksburg, Miss.
38. Hardin, B. O., "Characterization and Use of Shear Stress-Strain Relations for Airfield Subgrade and Base Course Materials," Technical Report No. AFWL-TR-71-60, Jul 1971, Air Force Weapons Laboratory, Kirtland Air Force Base, N. Mex.
39. Hicks, R. G., Factors Influencing the Resilient Properties of Granular Materials, Ph. D. Dissertation, University of California, Berkeley, 1970.
40. Dunlap, W. A., "A Report on a Mathematical Model Describing the Deformation Characteristics of Granular Materials," Research Report No. 27-1, 1963, Texas A&M University, College Station, Tex.
41. Wang, M. C., Mitchell, J. K., and Monismith, C. L., "Behavior of Stabilized Soils Under Repeated Loading; Stresses and Deflections in Cement-Stabilized Pavements," Contract Report No. 3-145,

Report No. 4, Oct 1970, U. S. Army Engineer Waterways Experiment Station, CE, Vicksburg, Miss.; prepared by University of California under Contract No. DA-22-079-eng-414.

42. Tschebotarioff, G. P., Soil Mechanics, Foundations, and Earth Structures, McGraw-Hill, New York, 1951.
43. Yang, N. C., "Nondestructive Evaluation of Civil Airport Pavements," Report No. FAA-RD-76-83, Sep 1976, Federal Aviation Administration, Washington, D. C.
44. Waas, G., "Earth Vibration Effects and Abatement for Military Facilities; Analysis Method for Footing Vibrations Through Layered Media," Technical Report S-71-14, Report 3, Sep 1972, U. S. Army Engineer Waterways Experiment Station, CE, Vicksburg, Miss.
45. Lysmer, J., "Vertical Motion of Rigid Footings," Contract Report No. 3-115, Jun 1965, U. S. Army Engineer Waterways Experiment Station, CE, Vicksburg, Miss.; prepared by University of Michigan, under Contract No. DA-22-079-eng-340.
46. Transportation Research Board, "Pavement Rehabilitation," Report No. DOT-OS-40022, Task Order 1, Jul 1974, Washington, D. C.
47. Scala, A. J., comments on "The Utilization of the Results of the Measurements of Surface Deflection Profiles as a Means of Estimating the Stiffness of Pavement Materials," by W. H. Cogill, Proceedings, Sixth Conference, Australian Road Research Board, Canberra, Paper No. 818, Vol 6, Part 4, 1972, pp 154-156.
48. Michalak, C. H., Moore, W. M., and Scrivner, F. H., "Calculation of the Elastic Moduli of a Two Layer Pavement System from Measured Surface Deflections," Research Report No. 123-6, Mar 1971, Texas A&M University, College Station, Tex.
49. Crawford, J. E., Hopkins, J. S., and Smith, J., "Theoretical Relationships Between Moduli for Soil Layers Beneath Concrete Pavements," Report No. FAA-RD-75-140, May 1976, Federal Aviation Administration, Washington, D. C.
50. Ahlvin, R. G. and Foster, C. R., "Stresses and Deflections Induced by a Uniform Circular Load," Proceedings, Highway Research Board, Vol 33, 1954, pp 467-470.
51. Office, Chief of Engineers, Department of the Army, "Military Fixed Bridges," Technical Manual TM 5-312, Dec 1968, Washington, D. C.

#### APPENDIX A: ABBREVIATIONS AND SYMBOLS

Recurring abbreviations and symbols are listed below. Symbols used only once or repeatedly in close proximity, and defined in that proximity, are not shown in the list. Symbols of this type appear in some tables and figures. To be certain of the significance of symbols in tables and figures, the reader should refer to the pertinent text.

AC	Asphaltic concrete
AI	Asphalt Institute
DSM	Dynamic stiffness modulus
E	Young's modulus; elastic modulus
$E_h$	Hysteresis modulus
$E_i$	Initial tangent modulus
$E_r$	Resilient modulus
$E_s$	Secant modulus
$E_t$	Tangent modulus
$E^*$	Complex modulus
$ E^* $	Magnitude of complex modulus
FAA	Federal Aviation Administration
G	Shear modulus
h	Thickness of a pavement layer
MIT	Massachusetts Institute of Technology
$M_R$	Resilient modulus
MRD	Materials Research and Development
PCC	Portland cement concrete
USNCEL	USN Civil Engineering Laboratory
WES	U. S. Army Engineer Waterways Experiment Station
$\gamma$	Shear strain
$\epsilon$	Strain
$\epsilon_x, \epsilon_y, \epsilon_z$	Strains along the axes, x, y, and z
$\lambda$	Wavelength
$\nu$	Poisson's ratio
$\sigma$	Normal stress

$\sigma_x, \sigma_y, \sigma_z$

Normal stresses acting along the axes, x, y, and z

$\sigma_1, \sigma_2, \sigma_3$

Normal stresses acting along the axes, 1, 2, and 3 of  
an orthogonal coordinate system

$\tau$

Shear stress